NASA CR-145239

(NASA-CR-145239) DETERMINATION OF SCATTERING FUNCTIONS AND THEIR EFFECTS ON REMOTE SENSING OF TURBIDITY IN NATURAL WATERS (Mitre Corp.) 148 p HC A07/MF A01 CSCL 08H G3/43

N78-15551

Unclas
58011

Determination of Scattering Functions and Their Effects on Remote Sensing of Turbidity in Natural Waters

by
Ali H. Ghovanlou
Jai N. Gupta
Robert G. Henderson

July 1977

Prepared under Contract No F19628-77-C-0001

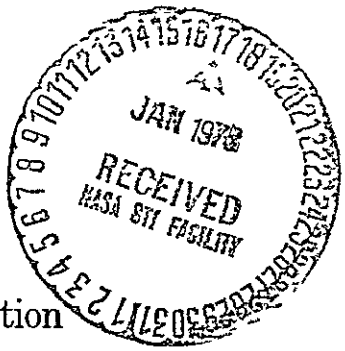

by
The METREK Division of The MITRE Corporation

for

National Aeronautics and Space Administration

Langley Research Center
Hampton, Virginia 23665
AC 804 827-3966

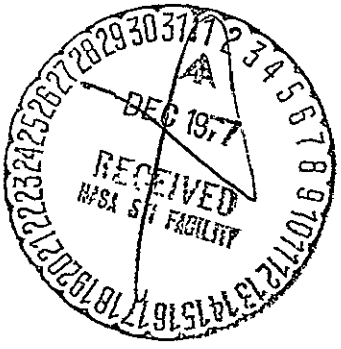

NASA CR-145239

Determination of Scattering Functions and Their Effects on Remote Sensing of Turbidity in Natural Waters

by
Ali H. Ghovanlou
Jai N. Gupta
Robert G. Henderson

July 1977

Contract Sponsor· NASA/Langley Research Center
Contract Number F19628-77-C-0001
Project Number 819S
Department W-52

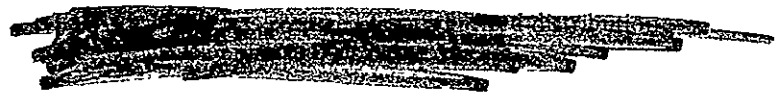

by
The METREK Division of The MITRE Corporation
McLean, Virginia

ABSTRACT

Development of quantitative analytical procedures for relating the water quality parameter to the characteristics of the back-scattered signals, measured by a remote sensor, necessitates further physical insight in the area of radiative transfer processes in turbid media. The present report discusses the applications of a Monte Carlo simulation model for radiative transfer in turbid water. The model is designed to calculate the characteristics of the back-scattered signal from an illuminated body of water as a function of the turbidity level, and the spectral properties of the suspended particulates. The optical properties of the environmental waters, necessary for model applications, have been derived from available experimental data and/or calculated from Mie formalism. Results of applications of the model, which have been implemented in support of a laboratory program at NASA/Langley Research Center, are presented.

TABLE OF CONTENTS

LIST OF ILLUSTRATIONS

LIST OF TABLES

1.0 INTRODUCTION AND CONCLUSIONS

The importance of continuous monitoring of environmental water quality has long been recognized. The recent emphases placed on such operations are due to newly gained insights (1) in the limitations of the cleansing capability of the natural waters, (2) a better understanding of ecological consequences of water pollutants, and (3) availability of better information for assessing economic impacts of various stresses imposed on the water systems. Considering the dynamic character of the environmental waters the monitoring procedures for measuring water quality parameters should be based on timely data collection systems, such as can be provided by applications of remote sensing technology.

Hypothetically, in a remote sensing experiment the optical sensor measures the radiance signal which contains information on spectral and spatial variation of the source of radiation and the intervening media. The received radiance is then "processed" according to an established scheme, which is a quantitative analytical procedure, and the radiance characteristics are ultimately related to the desired parameters.

The data interpretation techniques for remote measurement of water quality parameters are presently in preliminary stages. Although some attempts have been made to develop analytical procedures for data processing, a generally accepted processing scheme has not emerged.

Among the quantities that effect the radiance characteristics measured by a remote sensing instrument are:

- Atmospheric path radiances and signal transmission effects
- Spatial and spectral variability of atmospheric constituents such as particulates and molecular species
- Sun angle
- Characteristics of air-water interface
- Vertical non-homogenity of water bodies and bottom reflection properties

Considering these effects and the fact that aquatic environments change continuously with the complex interactions between wind, water and land masses; the development of data interpretation schemes, in support of remote sensing, necessitates field experiments and controlled laboratory experiments as well as radiative transfer modeling approaches. A variety of field experiments from low and high flying aircraft and from satellite platforms have been conducted, or planned for the immediate future.

A laboratory program is presently being pursued at the NASA-Langley Research Center (LaRC). The purpose of this program is to investigate the remote sensing of water quality parameters under controlled conditions. During the first phase of this program, remote sensing applications of suspended particulates (various types of clays) have been investigated. A schematic diagram of LaRC's experimental set-up is shown in Figure 1-1. In this experiment, the beam of a solar simulator is deflected to illuminate a large water

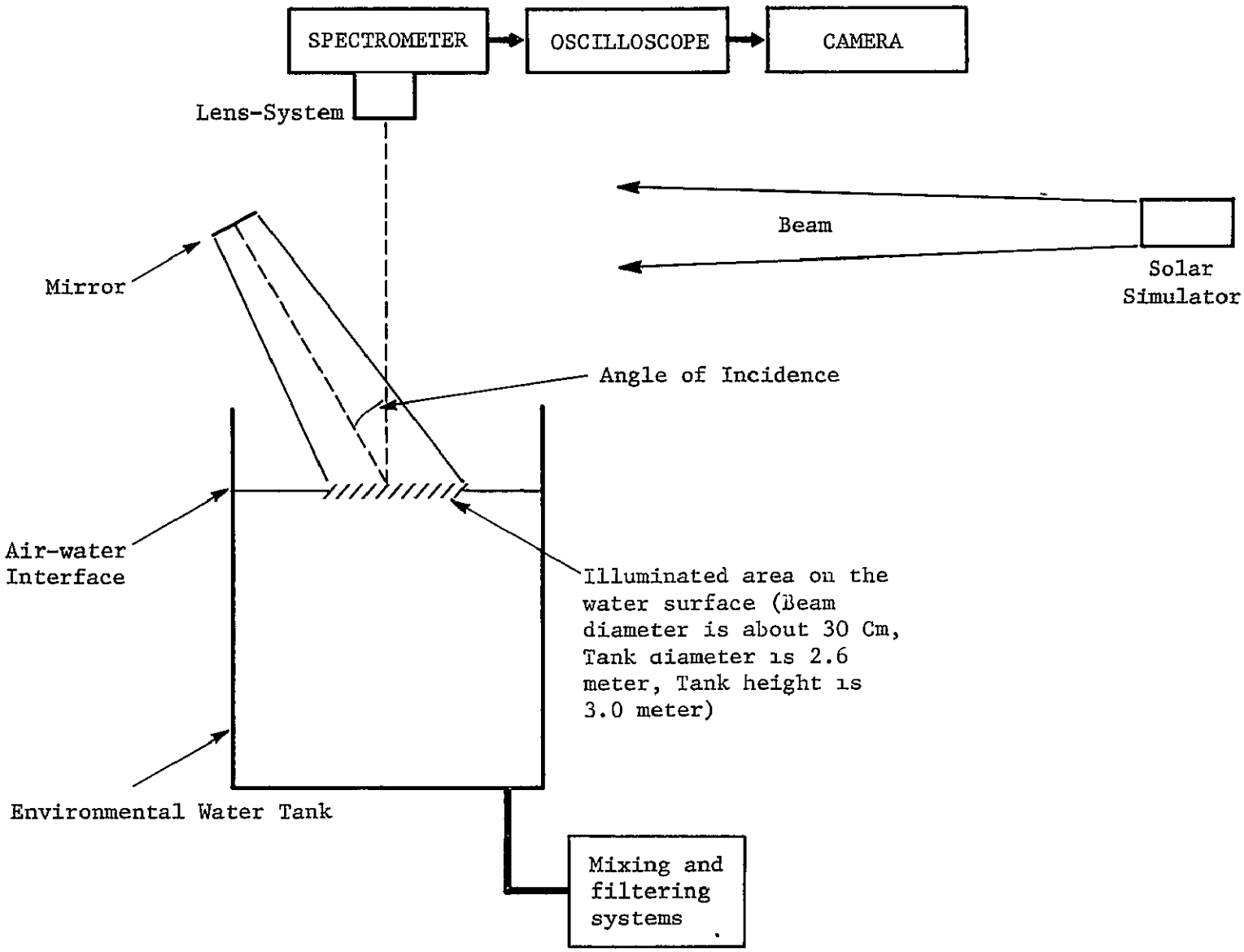

FIGURE 1-1
SCHEMATIC DIAGRAM OF LaRC's EXPERIMENTAL SET-UP

tank filled with turbid water; the water turbidity in the tank is caused by the stepwise introduction of specific amounts of particulates. An overhead detector system including a spectrometer, electronics, and a camera, measures the strengths and the characteristics of the upwelling radiance signal.

In order to analyze the experimental results and to optimize the experimental conditions a radiative transfer model has been developed for the LaRC's experimental arrangement at The METREK Division of The MITRE Corporation. The description of the modeling approach and the results of a sensitivity study concerning the optimized spot size to be illuminated by the solar simulator have been reported in two earlier documents.[1,2]

The present report deals with variations in the characteristics of the backscattered radiance as a result of changes in the scattering function, for various waters. The scattering function represents one of the important optical parameters of the turbid water and various scattering functions may represent various types of turbid waters. In Section 1.3 specific goals of the present report are described in more detail. Before this is done however, it is necessary to summarize some background material on (1) optical parameters of turbid waters, and (2) on our radiative transfer modeling procedure. These background materials are treated in Sections 1.1, and 1.2 respectively.

1.1 Optical Parameters of Turbid Water

In the absence of polarization the following parameters are necessary for optical characterization of turbid water medium:

- total absorption coefficient, a.
- total scattering coefficient, s.

These coefficients have the dimension of $meter^{-1}$. The attenuation coefficient, α, is the sum of absorption and scattering coefficients. The last parameter of interest is the scattering function, $\sigma(\theta)$. This function specifies the angular pattern of the scattering of a collimated beam from an infinitesimal volume of turbid water. The scattering probability function for polar angle, $F(\theta)$, may be defined in terms of the scattering function by the ratio:

$$F(\theta) = \int_0^{\theta} \sigma(\theta) \, \mathrm{Sin}\, \theta \; d\theta \Bigg/ \int_0^{\pi} \sigma(\theta) \, \mathrm{Sin}\, \theta \; d\theta \qquad (1\text{-}1)$$

More information on these parameters may be found in Appendix A of Reference 1.

1.2 Radiative Transfer Model

The development of METREK's radiative transfer model is based on a two step process which is described in this section. The adopted modeling procedure is geared toward handling turbid type waters, and toward saving the computer time necessary for model execution. The model development includes the following steps:

Step 1. The outgoing radiance distribution just above the air-water interface, due to a narrow beam transmission in the turbid water media is calculated using Monte Carlo simulation techniques.

Step 2. The outgoing radiance emerging from the area within the detector's field-of-view, and traveling in a direction coincident with the range of the detector's acceptance angle is calculated using the interface radiance distribution (Step 1) and integrating over the incident beam area.

The advantage of this approach as compared to conventional Monte Carlo simulation approaches is that the narrow beam consideration allows the production of a better set of statistics within reasonable computer resources.

1.2.1 Monte Carlo Simulation for Narrow Beam Transmission

The advances in laser technology in the last decade have led to a variety of theoretical considerations of the narrow beam transmission in the water media. In general, the theoretical approaches may be sub-divided in two categories, (1) analytical solution of the equation of radiative transfer and (2) Monte Carlo simulation methods.

The Monte Carlo simulation methods avoid many of the mathematical complexities involved in the analytical solution approach, and for this reason are more appropriate for calculating the narrow beam transmission. This is even more true in calculations simulating laboratory experiments where the experimental conditions, such as the tank geometry, significantly complicate the boundary conditions for the solution of the radiative transfer equation. Thus, the Monte Carlo simulation method has been used in the development of

the analytical model for LaRC's experiment. A description of the Monte Carlo simulation approach, which is geared toward decreasing computer time and handling turbid rather than oceanic type waters is given in References 1 and 2. The procedure leading to the calculation of radiance is based on making use of the distribution of the emerging photons generated by the Monte Carlo program, and the geometry of LaRC's experimental arrangement.[1,2]

The listing of the complete computer program, description of the input data, output data, and instructions for analysis of the output data to arrive at the upwelling radiance, are given in Appendix A.

1.3 Conclusions and Organization of This Report

In our previous reports,[1,2] we have documented the results of our modeling effort concerning the relationship between the spot size of the incident beam and the upwelling radiance, in the LaRC's laboratory experiment. These results, however, were based on the usage of only Morrison's scattering probability function.[3] In the present work we report on the effects of various inputs of both measured and calculated scattering probability functions.

In Sections 2 and 3 we have (1) summarized the available information on the measurements of the scattering function, and (2) have utilized the Mie formalism to calculate the scattering function for polydispersed suspensions on the basis of size distribution measurements provided through the LaRC laboratory program, and

reasonable inputs for the index of refraction including its imaginary part. The compiled measured scattering probability functions for natural water, cover a wide range of turbid waters and show considerable variations. The upper and lower bounding measured for the scattering probability functions correspond to San Diego Harbor, and sea water filtered thoroughly.[4-10] The scattering probability function measured by Morrison[3], used in Reference (1,2) lies between these limits, closer to the upper bound. Due to the lack of sufficient observations no conclusions could be drawn regarding the changes of the measured scattering functions with wavelength.

The calculated results of the scattering probability functions have been obtained for the following cases and their combinations:

- Size distributions including large particle sizes (~100 μ)
- Size distributions including a cutoff at 10 μ
- Zero or 0.004 for the imaginary part of the index of refraction
- Two wavelengths values at 500 and 600 nm

The conclusions derived from these results are:

1) Size distributions including large particles sizes (~100 μ) lead to an extremely large forward scattering peak, which shows up as a fast rise in the scattering probability function. The scattering probability function calculated for this situation is higher than the upper bound of the measured functions as may be seen by comparing Figures 3-15 and 2-8.

2) Size distributions including a cutoff at 10 μ results in the scattering probability functions which lie between the upper and lower bounding of the measured probability functions shown in Figure 2-8.

3) The effect of non-zero imaginary part for the index of refraction is to decrease the fast rise of the scattering probability function at small angles, and to put these functions within the bounds of the measured data.

4) The functions calculated for wavelengths of 500 nm and 600 nm do not show significant differences.

Based on the results and the conclusion described above three functions were selected for the investigation of the dependence of the upwelling radiance on the scattering function. These functions, which have been used in the Monte Carlo simulations radiative transfer code of Appendix A are:

- The lower bound of the measured scattering probability function
- The upper bound of the measured scattering probability function, and
- The upper bound of the calculated scattering probability functions. This function has been calculated for Feldspar soil, a zero value for the imaginary part of the index of ($\sim$100 μ). This function is higher than the upper bound of the measured scattering functions.

The turbidity levels treated in section 4.0 correspond to scattering coefficients s = 6.0 and s = 12 meter^{-1}; the wavelength of interest is 500 nm. The maximum number of incident photons traced in most computer runs is 10,000. The values calculated with the input of calculated upper bound scattering function is in good agreement with the measured upper bound scattering function for larger range of exit angle. However, for small range of exit angle ($\leq 25^{o}$ degrees for s = 6.0 meter^{-1} and $\leq 35^{o}$ for s = 12 meter^{-1}) no statistically significant result could be drived for this function,

from the ensemble of backscattered events for 10,000 incident photons. For this reason only the results derived from the use of measured upper and lower scattering functions were processed further, and form the basis of our conclusions.

The results generated for s = 6.0 and s = 12.0 meter^{-1} are in very good agreement as shown in Figure 4-3 (the figure-of-merit), where the ratio of the backscattered radiances (radiance due to the lower limit measured scattering probability function, divided by the radiance due to the upper limit measured scattering probability function) have been displayed as a function of the upper limit of the exit angle. As can be seen from Figure 4-3, the influence of the scattering probability function is quite significant, but decreases with decreasing exit angle. We expect that this trend will continue to be true for smaller angular ranges (such as 0 to 0.5^{o} which represent the acceptance angle of the LaRC's overhead detector) and, therefore, conclude that the effect of various scattering probability functions is not significant in the LaRC's experimental set-up.

The reason the smaller angular ranges were not examined specifically in this report has been due to the constraint on computer resources. It is recommended, therefore, that the computer program developed in this report be executed for a larger number of photons (larger than 10,000 photons considered in this study) to strengthen our conclusions.

2.0 MEASURED SCATTERING FUNCTIONS

In order to measure the complete scattering function, the scatterance must be observed at a number of angles between 0^{o} and 180^{o}. Two types of scattering meters have been used in the past for the measurements of the scattering functions. These are: (1) general angle scattering meters, and (2) low angle scattering meters. The mathematical definition of scattering function and an overview of the scattering meters are given in Appendix B.

The instrumentation required for in-situ measurements of the scattering functions are very sophisticated, hence only a small number of such measurements have been performed.

Figures 2-1 and 2-2 show several in-situ measured scattering functions covering turbid to clear water conditions. Figure 2-1 represents the observations made in lake water,[4] coastal waters,[5] Atlantic surface water,[6] Pacific near-coastal water,[7] Mediterranean,[8] and Saragasso Sea water.[9] Most of these observations are taken between $\theta = 10^{o}$ and $\theta = 155^{o}$. Figure 2-2 illustrates the measurements taken by the Scripps Institution of Oceanography[10] in deep clear oceanic water (tongue of the ocean), near shore ocean water (off shore of Southern California), and very turbid harbor water (San Diego Harbor). The measurements shown in Figure 2-2 are carried out over the entire range $0^{o} \leq \theta \leq 180^{o}$. The scattering

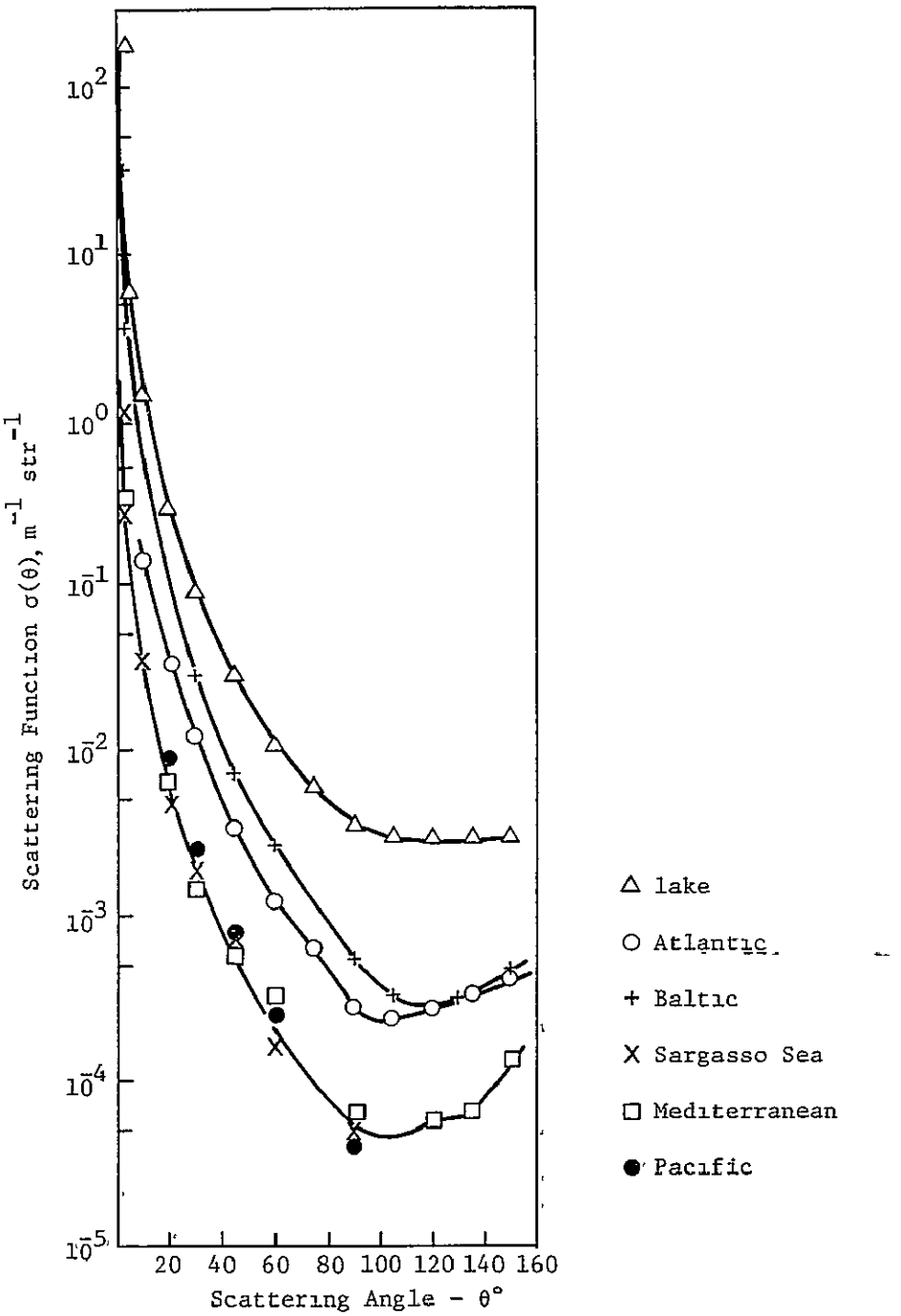

FIGURE 2-1
SCATTERING FUNCTIONS OBSERVED IN-SITU

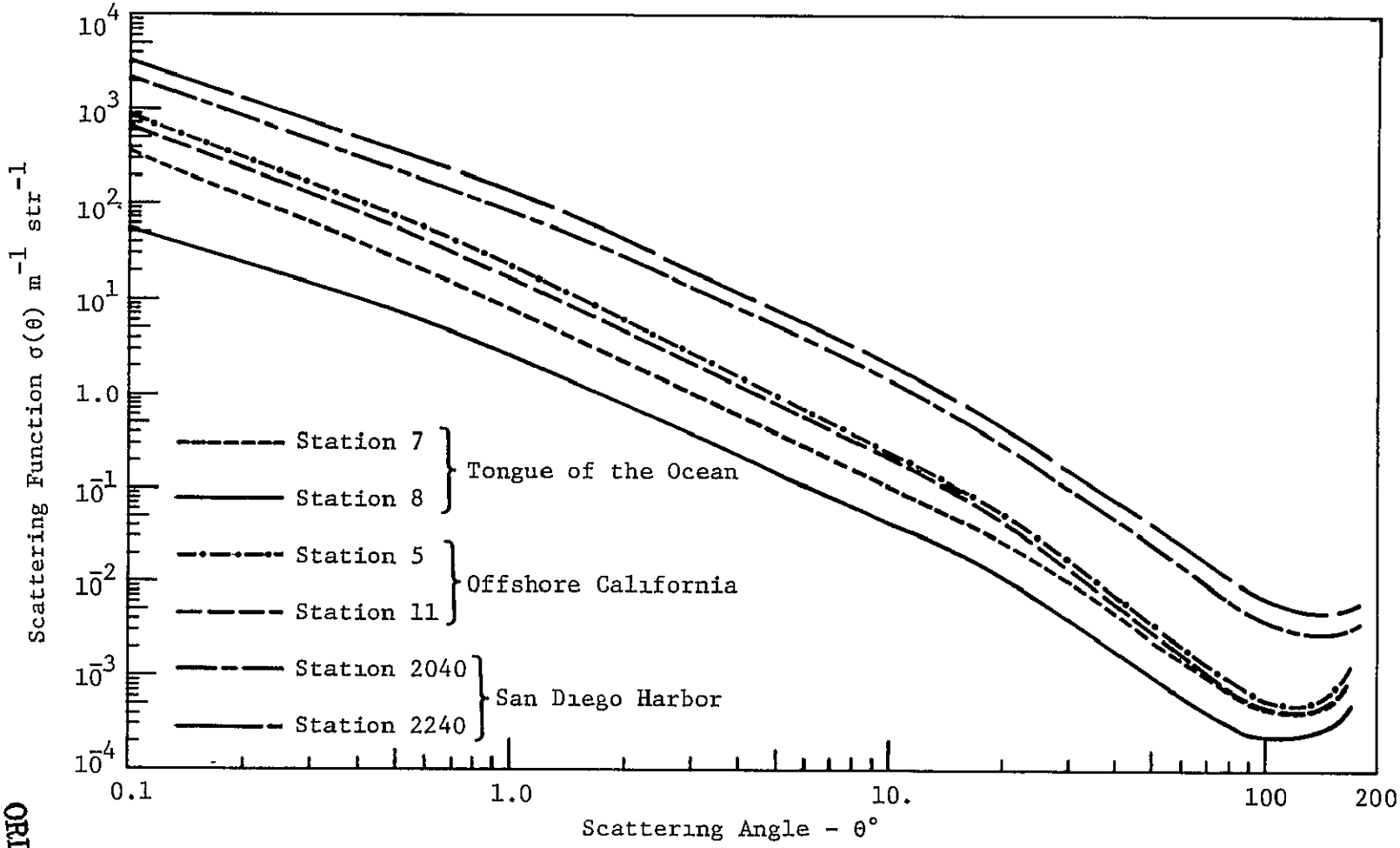

FIGURE 2-2
SCATTERING FUNCTIONS OBSERVED IN DEEP CLEAR OCEANIC WATER AND VERY TURBID HARBOR WATER

functions shown in both these figures are similar in general form. The differences between the scattering functions are most pronounced in the backward region above 90^{o}, and in the forward region below 10^{o}. Although the differences do reflect real variations in the scattering functions for various areas, they may reflect the inherent experimental difficulties as well.

The experimental difficulties become more striking when the scattering functions are measured in-vitro. The observations taken in-vitro by Petzold[10] are probably the most reliable ones. The measurements were taken to determine the effect of adding scattering and absorbing materials in the water. For this, scattering materials (compounds of aluminum hydroxide and magnesium hydroxide), and absorbing materials (black dye nigrosin), were introduced into fresh water pumped through a filter containing diatomaceous earth. The resultant change in scattering functions as observed with the scattering meters are presented in Figure 2-3. It is clear from Figure 2-3 that the scattering functions are insensitive to the absorption properties of the water.

2.1 Variation of Scattering Function with Wavelength λ

Not many of the experiments either in-situ or in-vitro so far have been performed for different wavelengths. Most of the observations are in $460 \leq \lambda \leq 655$ nm wavelength region. The scattering functions presented in Figures 2-2 and 2-3 were measured at $\lambda = 530$ nm. Due to a lack of observations at other wavelengths for

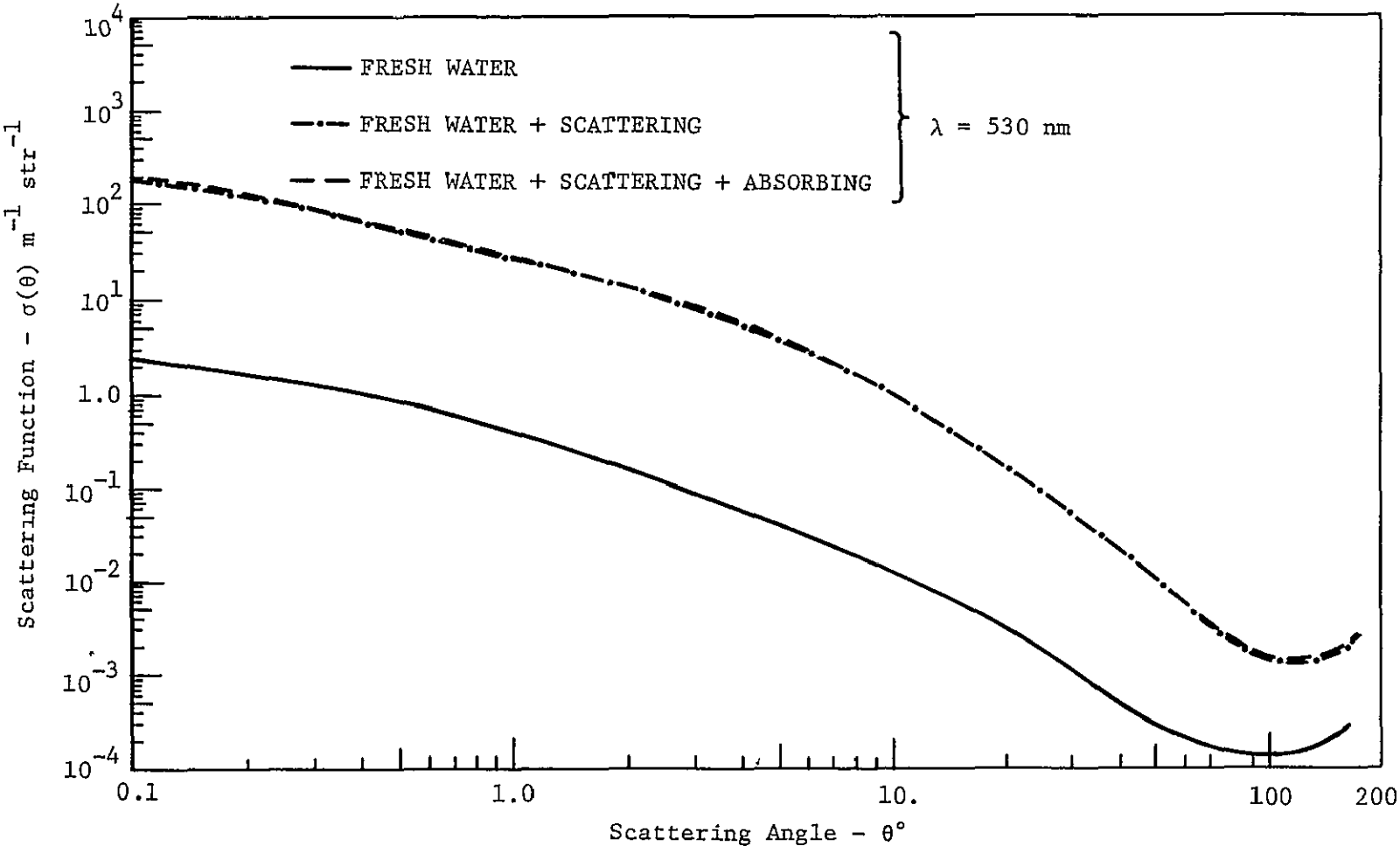

FIGURE 2-3
SCATTERING FUNCTIONS OBSERVED IN-VITRO

the same meters and under similar conditions (Figures 2-2 and 2-3), it is difficult to draw any conclusions regarding the changes in scattering functions with wavelength. However, Kullenberg has measured $\sigma(\theta)$ at 655 nm and 460 nm in the Sargasso Sea.[11] These measurements are shown in Figure 2-4. The scattering function is evidently the same at both these wavelengths, in the forward scattering region of $0 \leq \theta \leq 35^{o}$.

2.2 Scattering Probability Function $F(\theta)$

The scattering probability function, $F(\theta)$, has been defined by equation (1-1). $F(\theta)$ is the ratio of power scattered into angles less than θ relative to the total power scattered in all directions. $F(\theta)$ is an important parameter and is a measure of forward as well as backward scattering in natural environment waters. $F(\theta)$ is the function used in the Monte Carlo simulation model, as mentioned in the introduction.

Figure 2-5 shows the scattering probability function obtained by integrating the function represented in Figure 2-2, while Figure 2-6 illustrates $F(\theta)$ obtained from Figure 2-3. The probability scattering functions presented in Figure 2-6 show the effect of adding scattering and absorbing materials in the waters. Clearly, the addition of scattering material increases the backscattering whereas addition of absorbing material contributes insignificant changes to the scattering probability function.

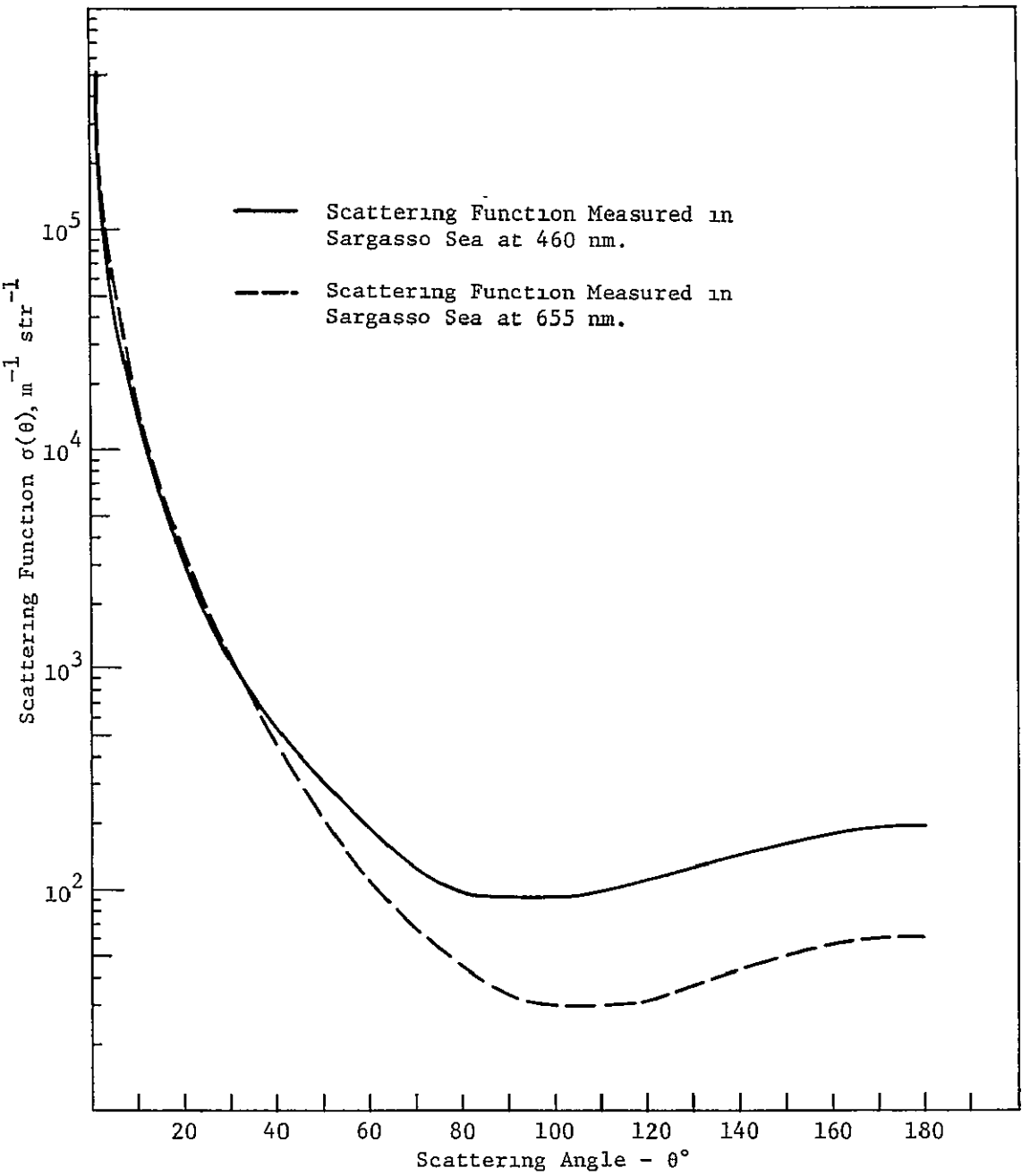

FIGURE 2-4
SCATTERING FUNCTIONS AT DIFFERENT WAVELENGTHS

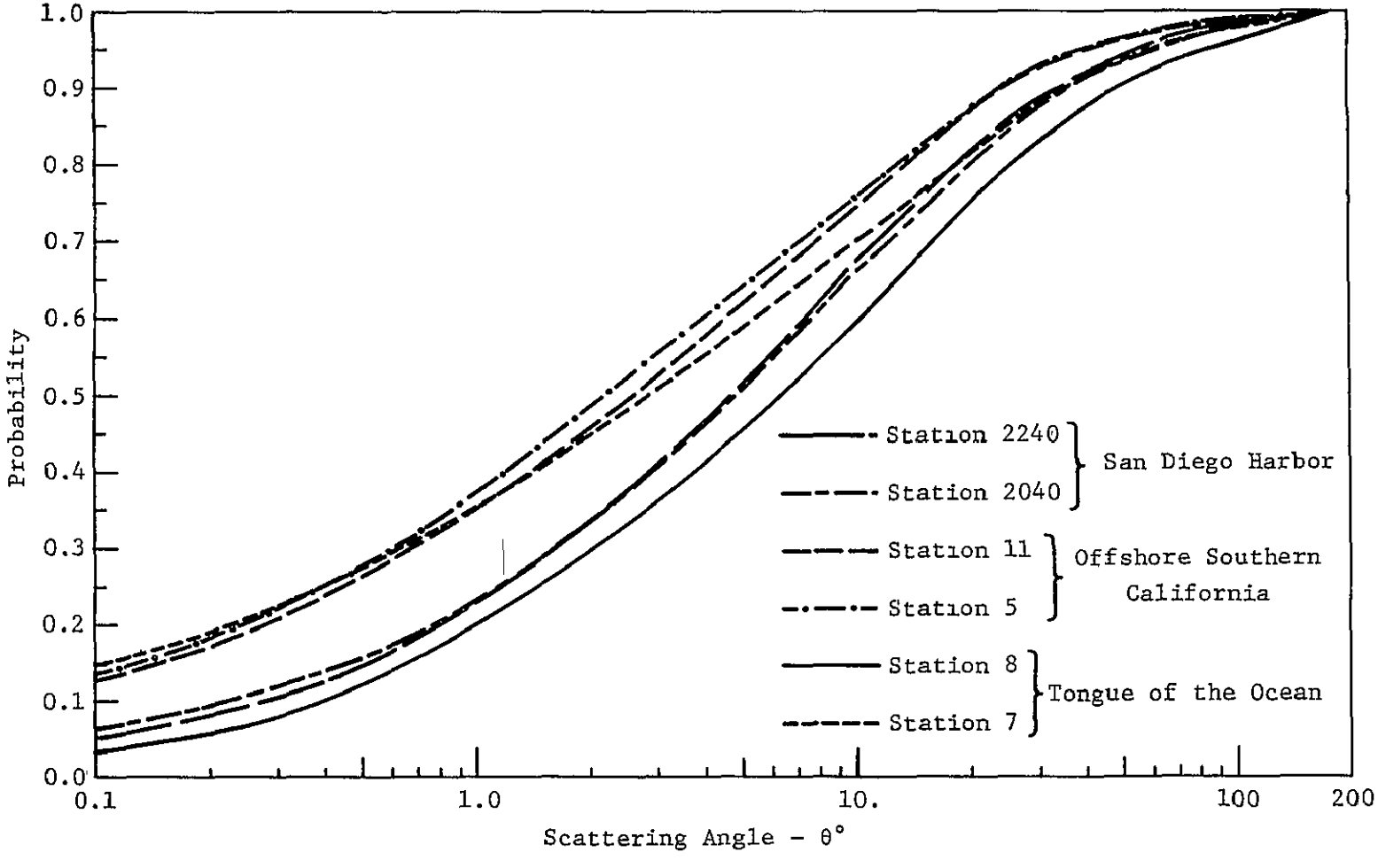

FIGURE 2-5
SCATTERING PROBABILITY FUNCTIONS OBTAINED IN DEEP CLEAR OCEANIC WATER AND VERY TURBID HARBOR WATERS

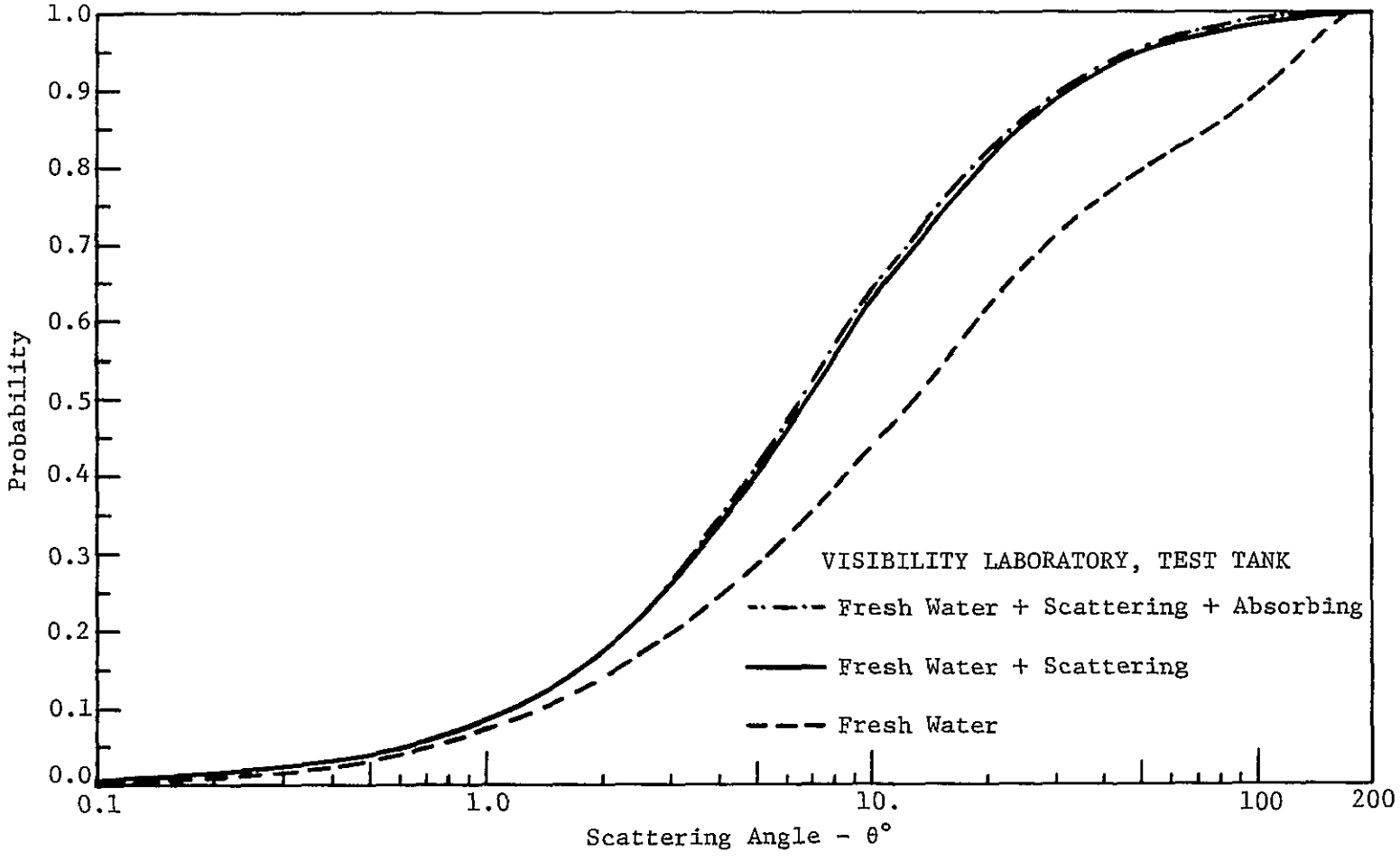

FIGURE 2-6
THE EFFECT OF SCATTERING AND ABSORBING MATERIALS IN FRESH WATER ON SCATTERING PROBABILITY FUNCTION

To illustrate the effect of varying wavelength on the scattering probability function, the functions presented in Figure 2-4 were filled in the angular range larger than 1^{o} degree, were extrapolated into the angular range smaller than 1^{o} degree, and were integrated to obtain $F(\theta)$ at 655 nm and 540 nm, as shown in Figure 2-7.

Since one of the objectives of this paper is to record experimentally determined upper and lower bounding scattering probability functions, the information from Figures 2-5, 2-6, and 2-7 are shown collectively in Figure 2-8. The lowest bound on the scattering probability function is given by the pure water, where particulate scattering is insignificant. Natural environmental waters are not usually free of particulates and, therefore, experiments have been performed to define their characteristics. An experiment conducted at Scripps Institution of Oceanography[10] examined sea water pumped into the laboratory and measured scattering probability functions for the water as delivered, and after several steps of filtration. After 18 hours of filtering, low-angle foward scattering signals have been found too low to be measurable. The results obtained from this experiment, in addition to the scattering probability functions obtained by Morrison at Long Island Sound stations,[3] are included in Figure 2-8.

The work presented in this section indicates that the San Diego Harbor water, the most turbid water, gives the upper bound to the experimentally determined scattering probability functions. The

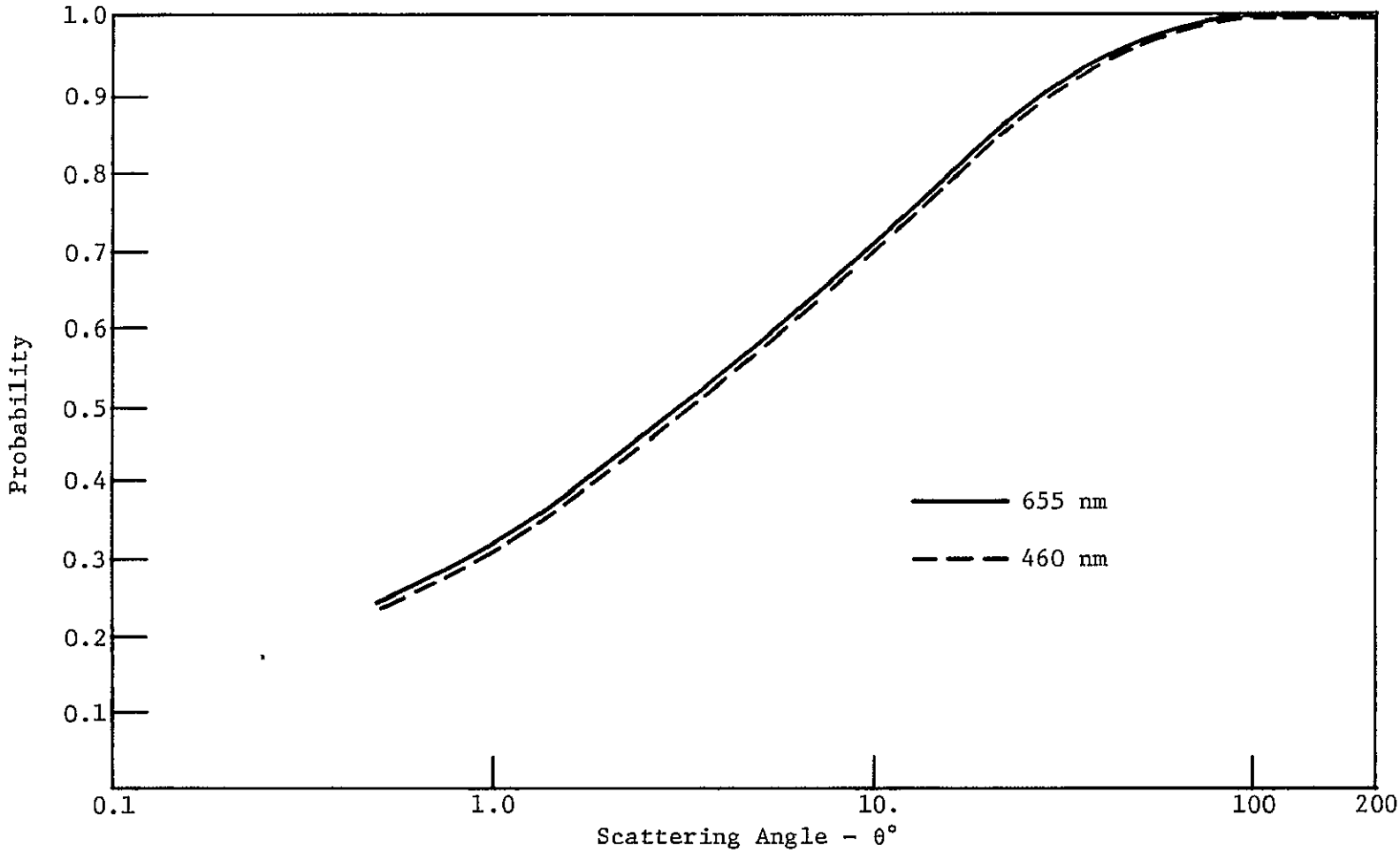

FIGURE 2-7
SCATTERING PROBABILITY FUNCTION MEASURED IN SARGASSO SEA AT 2 WAVELENGTHS

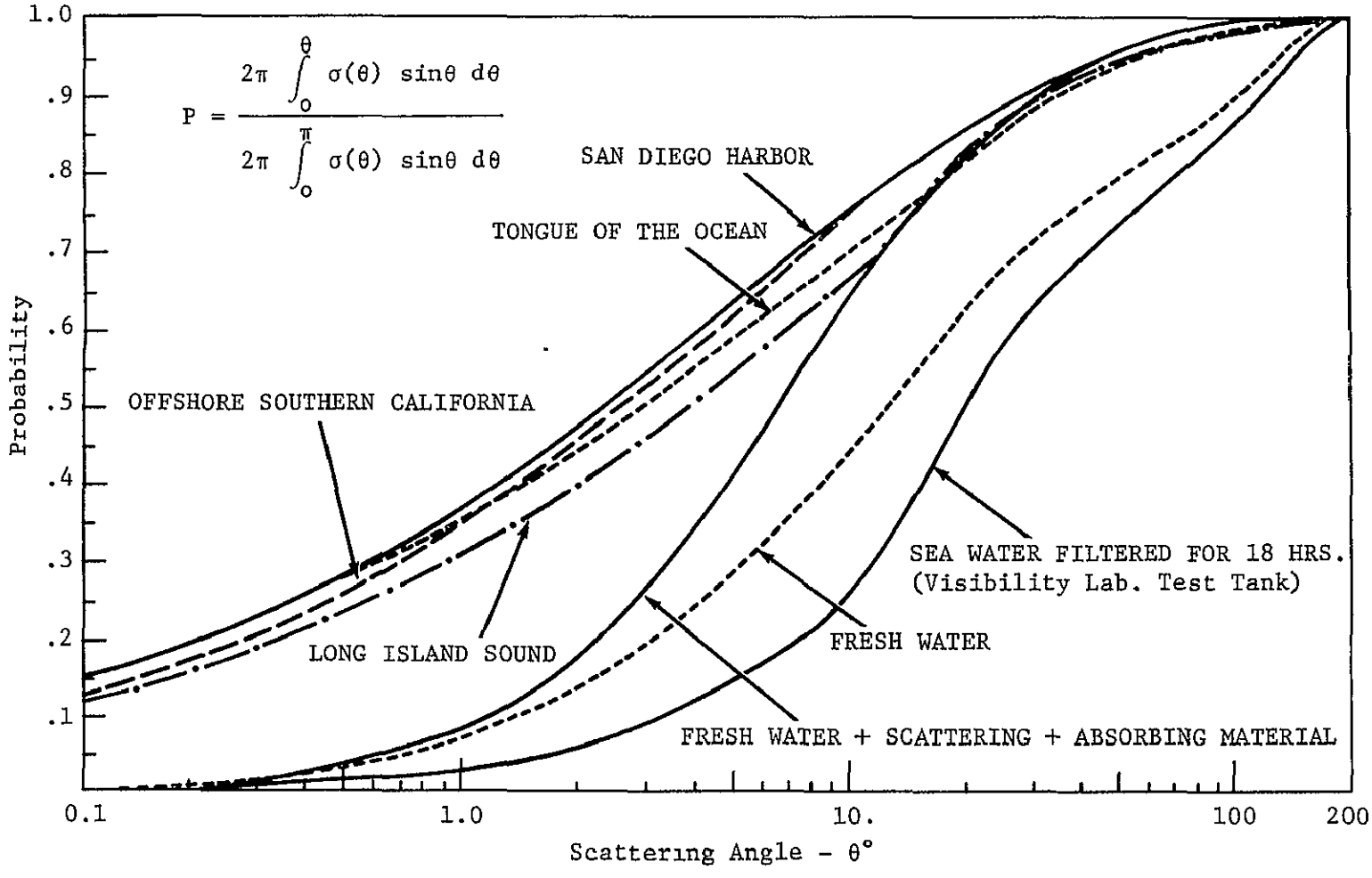

FIGURE 2-8
SCATTERING PROBABILITY FUNCTIONS FOR NATURAL OCEAN WATERS AND FOR FRESH WATER THAT HAS BEEN FILTERED AND ARTIFICIALLY MODIFIED

lower bound is given by the sea water thoroughly filtered. The scatterance characteristics of various waters considered are quite different. Very turbid waters show very high forward scatterance. At 1^{o} scattering angle, the forward scattering measured in San Diego Harbor water is almost 15 times of that measured in filtered water. This ratio reduces to three at 10^{o} scattering angle.

The implications of these results on remote detection of water turbidity will be discussed in Section 4.0.

3.0 CALCULATED SCATTERING FUNCTIONS

This section is devoted to the theoretical treatment of scattering and absorption from suspended particulates. The Mie theory of light scattering from a single particule is treated in Sub-section 3.1. The extension of Mie theory to the case of polydispersed suspensions is then discussed along with the computational methods used to calculate the scattering function, in Subsections 3.2 and 3.3 (Appendix E discusses the relationships between the Mie parameters and the extiction, scattering and absorption coefficients). Sub-section 3.4 includes a discussion of the size distributions and optical properties of the clay sediments considered in the calculations. Finally, in Section 3.5 the results of the calculation of the scattering function are presented along with a discussion of their implications for the NASA/Langley tank experiment.

The following discussion of the Mie theory of scattering and the computational methods is a brief summary. For more detailed discussions of Mie theory for single scattering, the reader is referred to References 13, 14, and 15. Reference 16 contains a good discussion of Mie scattering from polydispersions and reference 17 contains the details of the computational procedures and requirements.

3.1 Mie Theory for Single Particle Scattering

When light is incident on a particle, it undergoes both scattering and absorption (we will ignore inelastic scattering processes which result in a change in frequency). The characteristics of the scattered radiation depend on the wavelength, λ, of the incident light, the generally complex index of refraction, m, of the particle, and the size, r, and shape of the particle. In this report we will restrict the discussion to spherical particles; for the treatment of inorganic sediments in water this is probably not a serious restriction.

If a monochromatic beam of light of intensity I_o is incident on a spherical particle at an angle $\theta = 0$, then the scattered intensity is given by

$$I(x,m,\theta) = \frac{\lambda^2}{4\pi^2} \sigma(x,m,\theta) I_o \qquad (3\text{-}1)$$

Where $\sigma(x,m,\theta)$ is the single particle scattering function, $\sigma(x,m,\theta)$ depends in general, on the size parameter,

$$x = \frac{2\pi r}{\lambda} \qquad (3\text{-}2)$$

and the complex index of refraction, m. The calculation of $\sigma(x,m,\theta)$ requires the solution of Maxwell's equation in spherical coordinates with a discontinuous change in the index of refraction across the

spherical surface. This solution was originally derived by G. Mie[18] and independently by P. Debye[19].

The scattering function can be written as:

$$\sigma(x,m,\theta) = \left[\frac{\sigma_1(x,m,\theta) + \sigma_2(x,m,\theta)}{2}\right] \tag{3-3}$$

and the Mie solution is

$$\begin{aligned} \sigma_1(x,m,\theta) &= S_1(x,m,\theta)\, S_1^*(x,m,\theta) \\ \sigma_2(x,m,\theta) &= S_2(x,m,\theta)\, S_2^*(x,m,\theta) \end{aligned} \tag{3-4}$$

Where $S_1(x,m,\theta)$ and $S_2(x,m,\theta)$ are the complex amplitudes for the scattered radiation,

$$\begin{aligned} S_1(x,m,\theta) &= \sum_{n=1}^{\infty} \frac{(2n+1)}{n(n+1)} \left\{a_n(x,m)\pi_n(\mu)+b_n(x,m)\tau_n(\mu)\right\} \\ S_2(x,m,\theta) &= \sum_{n=1}^{\infty} \frac{(2n+1)}{n(n+1)} \left\{b_n(x,m)\pi_n(\mu)+a_n(x,m)\tau_n(\mu)\right\} \end{aligned} \tag{3-5}$$

In these expressions $\pi_n(\mu)$ and $\tau_n(\mu)$ are derivatives of the Legendre polynomials:

$$\begin{aligned} \pi_n(\mu) &= \frac{dP_n(\mu)}{d\mu}, \\ \tau_n(\mu) &= \mu\pi_n(\mu) - (1-\mu^2)\frac{d\pi_n(\mu)}{d\mu} \end{aligned} \tag{3-6}$$

(where $\mu = \cos\theta$). Also

$$a_n(x,m) = \frac{\psi_n'(mx)\psi_n(x) - m\psi_n(mx)\psi_n'(x)}{\psi_n'(mx)\xi_n(x) - m\psi_n(mx)\xi_n'(x)}$$

$$b_n(x,m) = \frac{m\psi_n'(mx)\psi_n(x) - \psi_n(mx)\psi_n'(x)}{m\psi_n'(mx)\xi_n(x) - \psi_n(mx)\xi_n'(x)} \qquad (3\text{-}7)$$

and the ψ's and ξ's are related to the spherical Bessel functions of the first and second kinds (j_n and y_n respectively):

$$\begin{aligned}
\psi_n(z) &= z j_n(z) \\
\xi_n(x) &= x j_n(x) - i y_n(x) \\
\psi_n'(z) &= z j_{n-1}(z) - n j_n(z) \\
\xi_n'(x) &= x j_{n-1}(x) - i y_{n-1}(x) - n\, j_n(x) - i y_n(x)
\end{aligned} \qquad (3\text{-}8)$$

3.2 Mie Theory for Scattering from Polydispersions

A polydispersion is a suspension of scattering particles of uniform physical characteristics but of varying number concentration depending on particle size. Because of the existence of different particle sizes it makes little sense to talk of scattering from a single particle. Instead, it is useful to consider the scattering properties of a small volume element containing a number of particles. The size of this volume element is of some, at least theoretical, importance. Clearly, if it is to be used to represent the scattering

properties of all similar volume elements then it must contain a representative set of particle sizes - this requires that the volume element not be too small. On the other hand, since we are considering only single scattering from the volume element, it must not be too large. An additional condition that must be imposed is that the inter-particle separation be large compared to the wavelength. The reason for this is that the interaction of light with a particle will be assumed independent of the interactions with all other particles. This condition requires that the particle density in the volume element not be too large. For our purposes, it will be assumed that all of the above conditions are satisfied.

The polydispersion can be completely specified, for our purposes, by an index of refraction m and a probability density function n(r). The density function gives the relative concentration of each size contained in a volume element.

The characteristics of the scattered radiation due to the volume element can then be represented by a volume scattering function $\sigma(m,\theta)$ in a manner analogous to Equation (3-1):

$$I(m,\theta) = \frac{\lambda^2}{4\pi^2} \sigma(m,\theta) I_o \qquad (3\text{-}9)$$

The scattering function can be calculated from the set of particle scattering functions:

$$\sigma(m,\theta) = \int_0^\infty \sigma(x,m,\theta)\, n(r) dr \qquad (3\text{-}10)$$

where

$$\int_0^\infty n(r)dr = N \tag{3-11}$$

and N is the total number of particles per unit volume. In what follows, N will be assumed to be unity since $\sigma(m,\theta)$ scales with N. The ability to represent $\sigma(m,\theta)$ as a linear superposition of the $\sigma(s,m,\theta)$s is a direct consequence of our assumption that the inter-particle separation is much greater than λ.

The calculation of $\sigma(m,\theta)$ thus reduces to calculations of the individual $\sigma(s,m,\theta)$ and then integration over all sizes with the proper weighting given by n(r).

3.3 Computational Methods

The calculation of the scattering functions and the averaging over size distributions was carried out on an IBM 370/148. The program listings are reproduced in Appendix C.

In computing the sums in Equation (3-5), the major difficulty arises in the evaluation of the $a_n(x,m)$ and $b_n(x,m)$. Using the definitions of ψ_n, ψ_n', ξ_n, and ξ_n', and the standard recurrence relations for the Bessel functions, Equation (3-7) can be rewritten:

$$a_m(x,m) = \frac{\left\{\frac{A_n(mx)}{m} + n/x\right\} \mathrm{Re}\left[\xi_n(x)\right] - \mathrm{Re}\left[\xi_{n-1}(x)\right]}{\left\{\frac{A_n(mx)}{m} + n/x\right\} \xi_n(x) - \xi_{n-1}(x)}$$

$$b_n(x,m) = \frac{\left\{mA_n(mx)+n/x\right\} \mathrm{Re}\left[\xi_n(x)\right] - \mathrm{Re}\left[\xi_{n-1}(x)\right]}{\left\{mA_n(mx)+n/x\right\} \xi_n(x) - \xi_{n-1}(x)} \tag{3-12}$$

Where

$$A_n(mx) = \frac{\psi_n'(mx)}{\psi_n(mx)} \tag{3-13}$$

the logarithmic derivative of $\psi_n(mx)$, and Re denotes the real part. The natural approach to the evaluation of Equation (3-12) is to employ a standard upward recurrence procedure. Unfortunately, if the imaginary part of m, Im(m), is not zero and n is larger then the upward recurrence procedure results in larger instabilities in the calculation of $A_n(mx)$. For this reason, the DBMIE subroutine employs a downward recurrence procedure to calculate the $A_n(mx)$s. These values are then stored for use in the evaluation of Equation (3-12). Because of the large storage requirements resulting from this procedure ($n \sim 7000$), and the fact that double precision is employed in all of the calculations, a virtual machine with 512 K bytes of storage is required for the implementation of the DBMIE and POLYMIE routines.

While the scattering functions are computed in the DBMIE subroutine, the average, Equation (3-10), is computed in the calling routine POLYMIE. While analytic functions have been used for the size distributions, n(r), the integral has been approximated by a summation over a discrete set of radii. Tests to determine the effect of using a summing procedure have shown that this results in no loss of accuracy. In addition, test runs were made to compare the results when $\Delta r = 0.1\mu$ (0.1 micron) and $\Delta r = 1\mu$ were used in the

summing procedure. The use of $\Delta r = 1\mu$ resulted in no significant change in the results from those obtained using $\Delta r = 0.1\mu$ over the range $0 < r < 100\mu$. Calculations were made using $r_{max} = 100\mu$ ($\Delta r = 1\mu$) and $r_{max} = 10\mu$ ($\Delta r = 0.1\mu$). A discussion of the proper upper limit for r is given in Section 3.4.

The amount of virtual CPU time required for these calculations is significant and has been a major factor in determining r_{max} and Δr. As an example, the calculation of the volume scattering function for a polydispersion with $m = 1.144 - 0.0i$, $\lambda = 0.5\mu$, $r_{max} = 100\mu$ and $\Delta r = 1\mu$ requires approximately 26 minutes of virtual CPU time.

3.4 Properties of Clay Samples

Data on four different clay samples were provided by NASA/LaRC. This data consisted of empirical size distribution curves as well as brief descriptions of chemical composition. The physical characteristics of the clay are discussed in Section 3.4.1 while the size distributions are presented in Section 3.4.2.

3.4.1 Physical Characteristics of Clay Samples

Four types of clay were selected by NASA/LaRC. These were: Feldspar, Calvert, Ball and Jordan. According to the analysis of these clays performed by NASA/LaRC[20] the compositions are:

- Feldspar - Feldspar and Quartz minerals
- Calvert and Jordan - Kaolinite and Illite
- Ball - Montmorilloite, Kaolinite and Illite

The real refractive index and chemical components of these minerals is shown in Table 3.1.[21] For reasons which will be discussed in Section 3.4.2, Feldspar and Ball clay were chosen to be included in this study.

To estimate the index of refraction of the clay samples, we take a simple average of the indices of refraction of the components. Thus, for both Feldspar and Ball clay, the real part of the index of refraction is estimated as

$$RE\ (m_{Air}) = 1.53$$

This, of course, is the index of refraction with respect to air and we require the index of refraction with respect to water which can be obtained by dividing $Re(m_{Air})$ by the index of refraction of water 1.337 (for wavelengths of approximately 500 nm).

Thus

$$Re(m_{water}) = 1.144$$

Estimating the imaginary part of the index of refraction is not so straightforward, since direct measurements of Im(m) have not been made. Since these minerals have very low conductivity, it is expected that the imaginary part of m will be quite small. The imaginary part of m has been measured for soil aerosols and has been found to be about .005 (with respect to air).[22] For this study two values for Im(m) will be used:

$$Im(m_{water}) = \begin{cases} 0 & \text{,Non-absorbing} \\ \frac{0.005}{1.337} = 0.004, & \text{Weakly-absorbing} \end{cases}$$

TABLE 3.1

CHEMICAL COMPOSITION AND INDEX OF REFRACTION
OF CLAY CONSTITUENTS

NAME	CHEMICAL COMPOSITION	INDEX OF REFRACTION
Kaolinite	$Al_2O_3.2SiO_2.2H_2O$	1.56
Illite	$K_{1-1.5}Al_4Si_{7-6.5}Al_{1-1.5}O_2(OH)_4$	1.54
Montmorillonite	$(.5Ca,Na)_{.7})Al,Mn,Fe)_4(si,Al)_8)_{20}(HO)_4nH_2O$	1.48
Feldspars:		
Microcline	$K_2O.Al_2O_3.6SiO_2$	1.52
Andesine	$(CaO_1Na_2O)Al_2O_3.4SiO_2$	1.55
Anthoclase	$(Na,K)_2O.Al_2O_3.6SiO_2$	1.53

3.4.2 Particle Size Distributions

Emperical cumulative size distributions for the four samples were provided by NASA/LaRC and are shown in Figures 3-1, 3-2, 3-3 and 3-4. It is apparent from these figures that the size distributions for Ball, Jordan, and Calvert differ significantly from the size distribution for Feldspar. Since it was planned that two distributions would be employed, Feldspar and Ball clay were chosen. This choice allows the investigation of the effect of radically different size distributions.

To utilize the size distribution information, it is necessary to determine size distribution density functions, n(r), which specify the relative number of particles with radius r per unit volume. If we denote the cumulative size distribution as provided by NASA/LaRC as $N(r_o)$ then the relationship between $N(r_o)$ and n(r) is given by:

$$N(r_o) = 1 - \int_0^{r_o} n(r)\, dr, \tag{3-14}$$

or

$$n(r) = \frac{dN(r_o)}{dr_o} \Bigg|_{r_o = r} \tag{3-15}$$

A general curve fitting routine (See Appendix D) was used to determine the best distribution for both the Ball clay and Feldspar.

For the Feldspar sample, it was found that the data was well represented by a modified Gamma distribution:

$$n(r) = a_1 r^{a_2} \exp\left(-a_3 r^{a_4}\right) \tag{3-16}$$

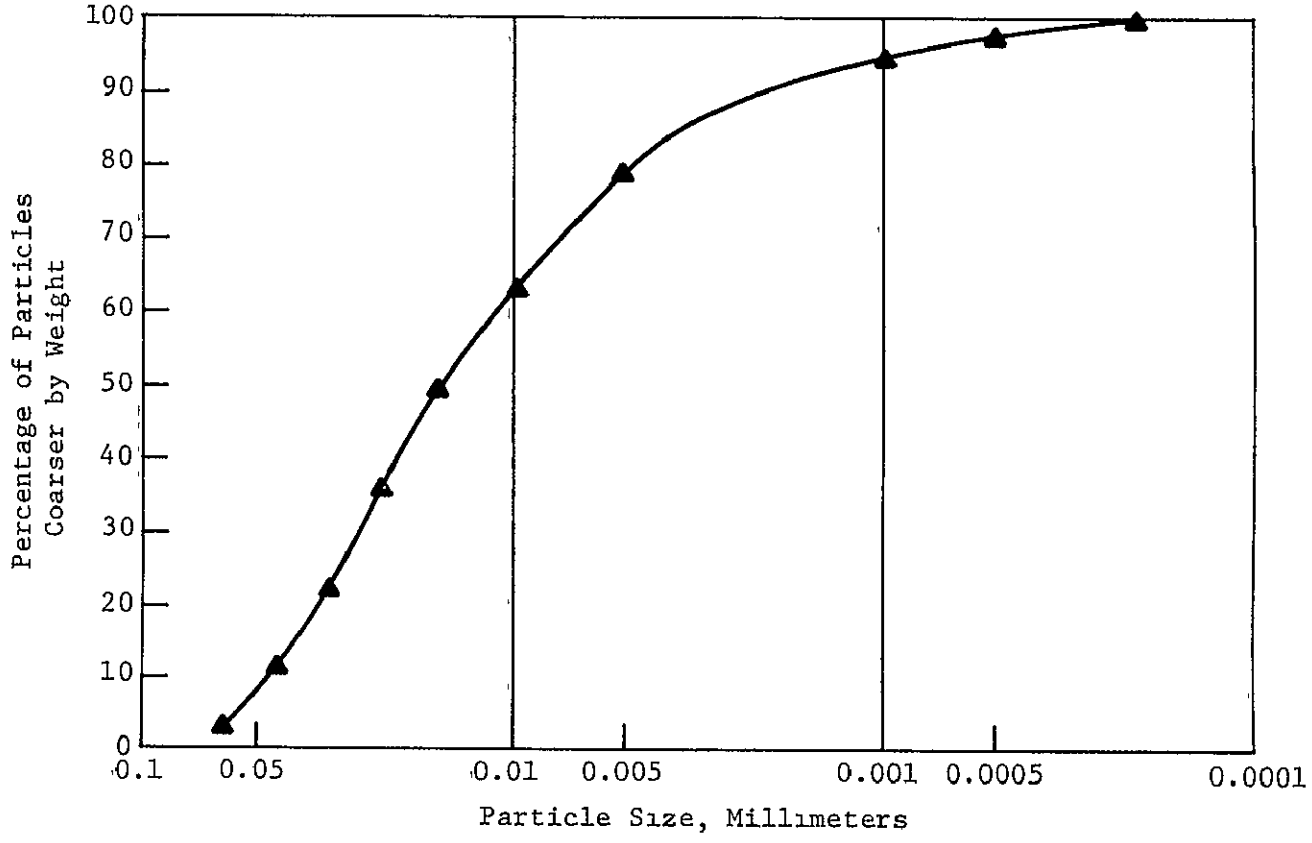

FIGURE 3-1
CUMULATIVE SIZE DISTRIBUTION OF FELDSPAR SAMPLE

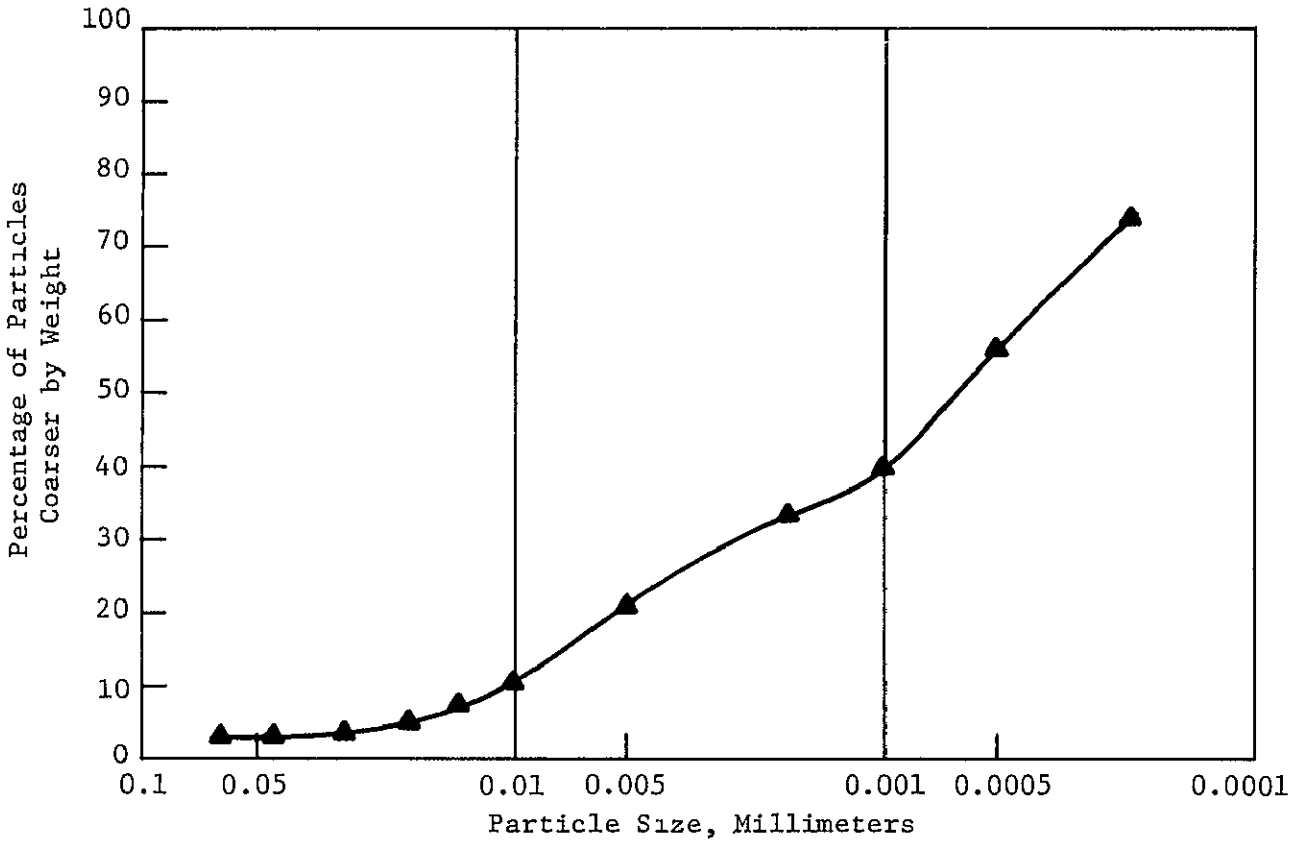

FIGURE 3-2
CUMULATIVE SIZE DISTRIBUTION OF CALVERT SAMPLE

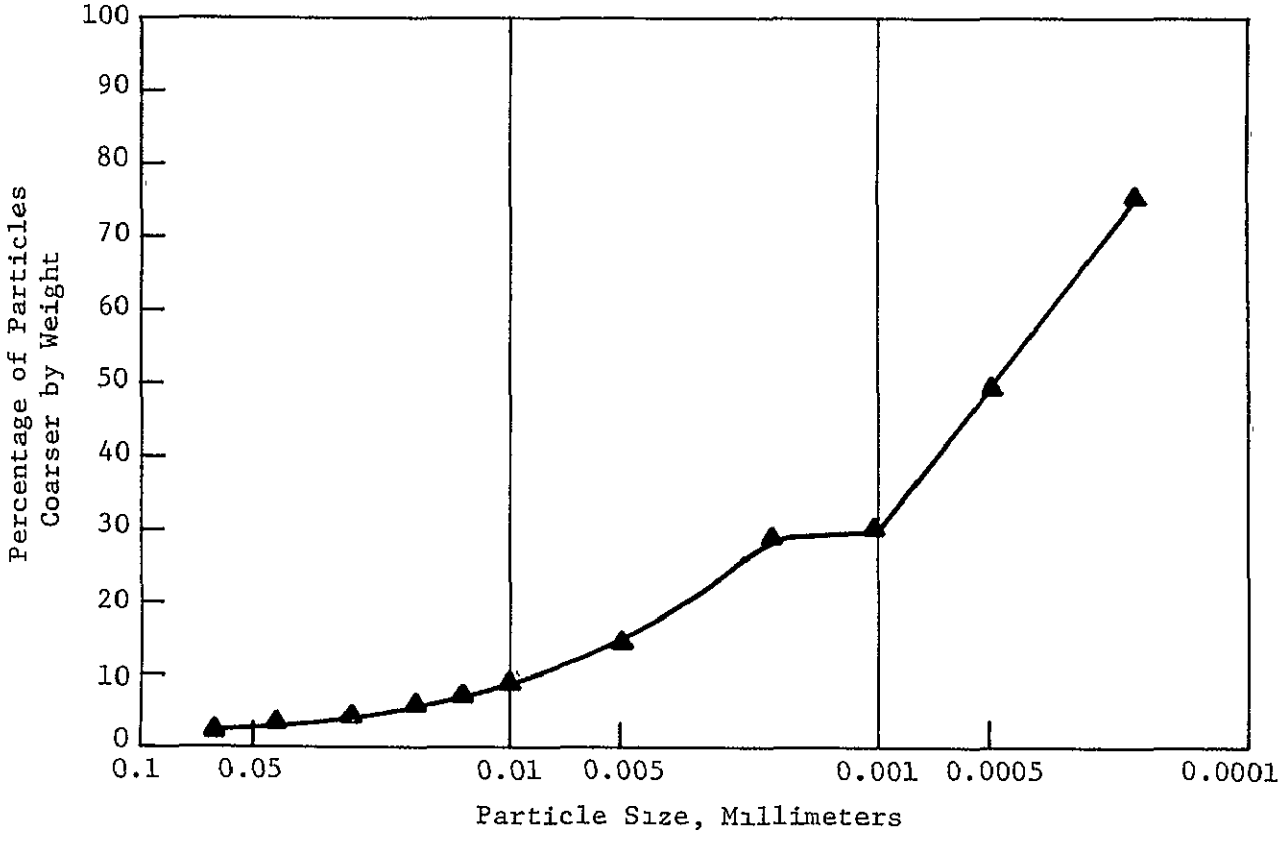

FIGURE 3-3
CUMULATIVE SIZE DISTRIBUTION OF BALL SAMPLE

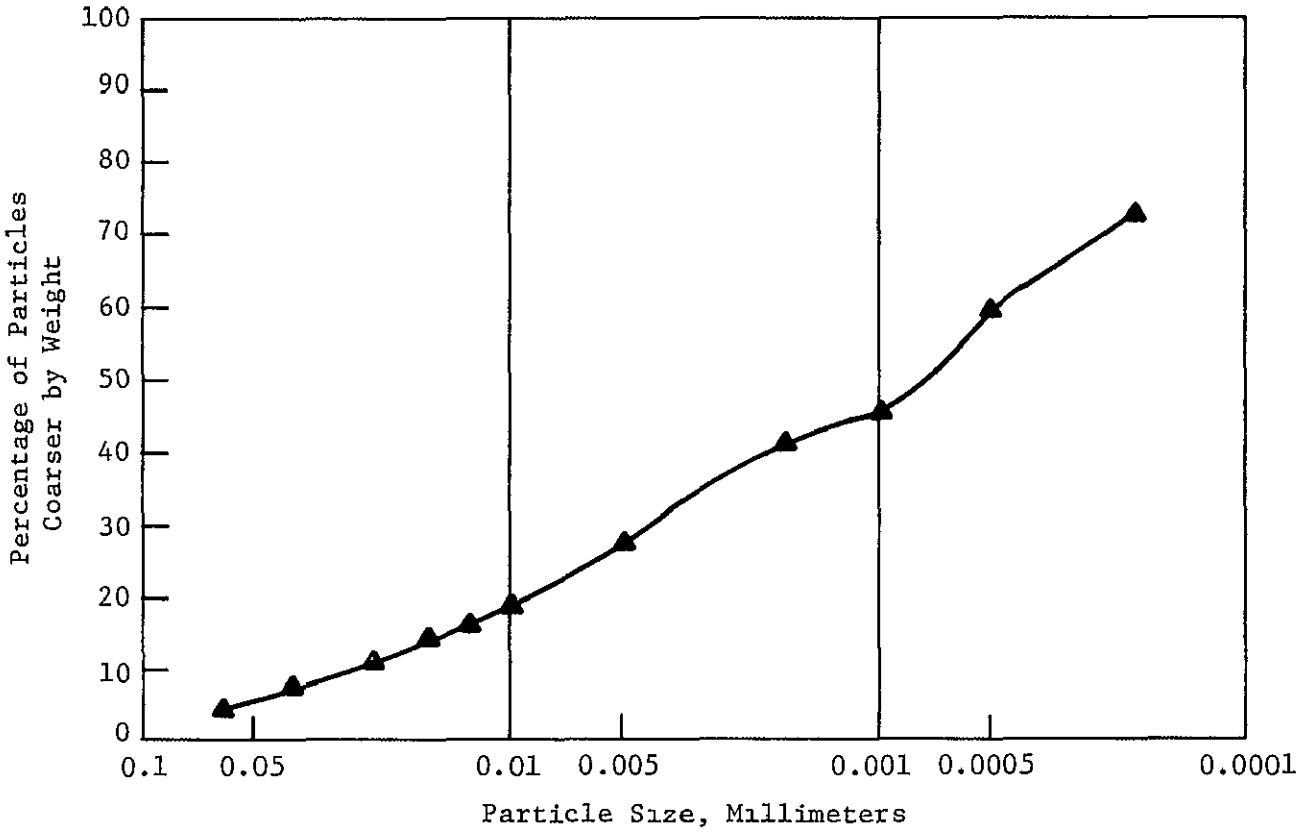

FIGURE 3-4
CUMULATIVE SIZE DISTRIBUTION OF JORDAN SAMPLE

The parameters were determined, using a minimum mean square error criterion, to be

$$a_1 = 2.05089$$

$$a_2 = 0.671066$$

$$a_3 = 3.58393$$

$$a_4 = 0.218499$$

A plot of this size distribution density function is shown in Figure 3-5, while a plot of the corresponding cumulative size distribution function (as obtained from Equation 3-16) is shown in Figure 3-6. As can be seen in Figure 3-6, the modified Gamma distribution gives a good fit to the data points obtained in the NASA/LaRC analysis.

To fit the size distribution of the Ball clay sample, Junge's distribution model was chosen:

$$n(r) = a_1 \, r^{-a_2} \tag{3-17}$$

with the parameters,

$$a_1 = .2006$$

$$a_2 = 1.624746$$

determined using the same curve fitting routine employed for Feldspar. The size distribution density function and the cumulative size distribution function for Ball clay using Junge's distribution are shown in Figures 3-7 and 3-8. It is apparent from Figure 3-7 that Junge's distribution function is not, strictly speaking, a probability distribution since the integral (Equation 3-11),

$$\int_0^\infty n(r) \, dr = N$$

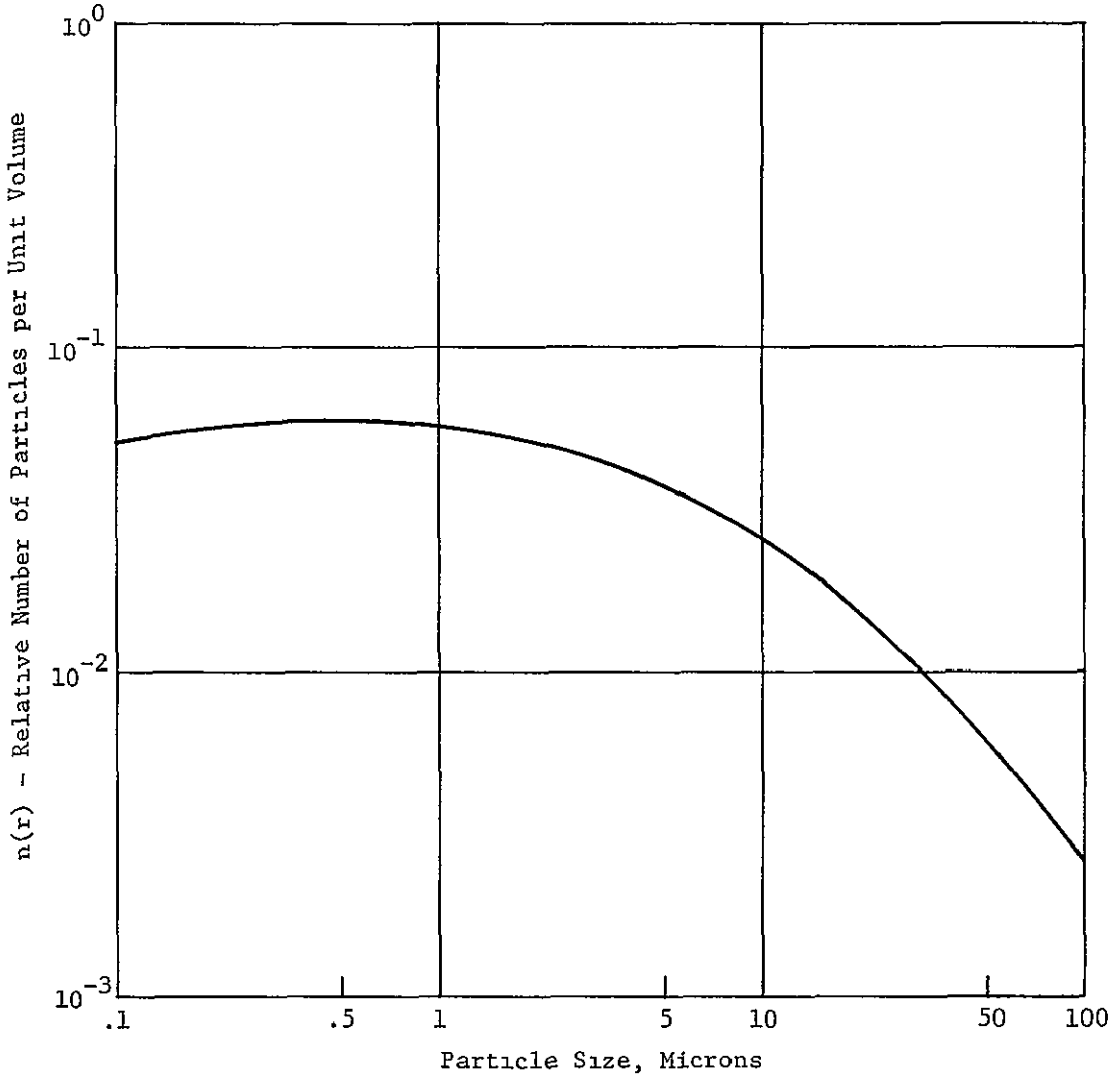

FIGURE 3-5
PARTICLE SIZE DENSITY FUNCTION FOR FELDSPAR (MODIFIED GAMMA DISTRIBUTION)

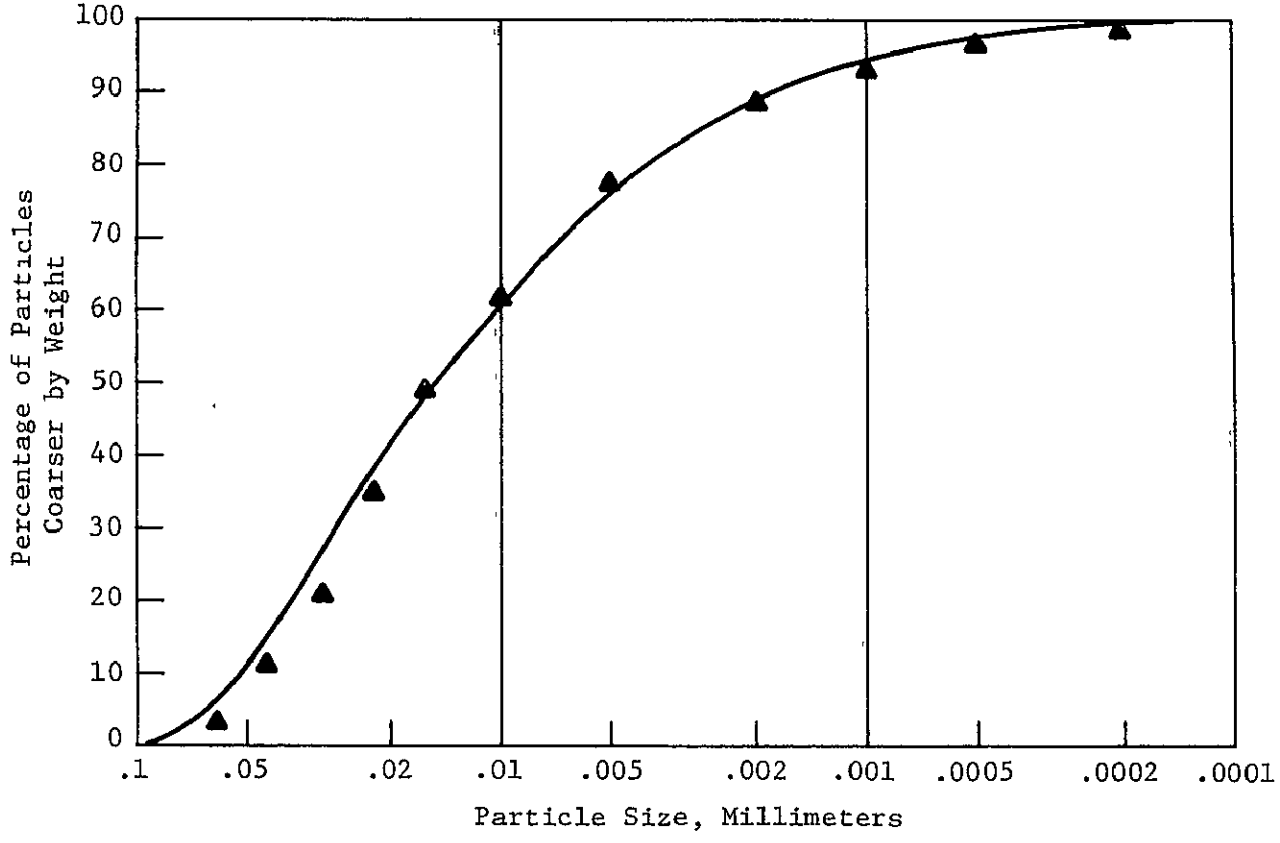

FIGURE 3-6
CUMULATIVE SIZE DISTRIBUTION FIT OF FELDSPAR SAMPLE USING MODIFIED GAMMA DISTRIBUTION

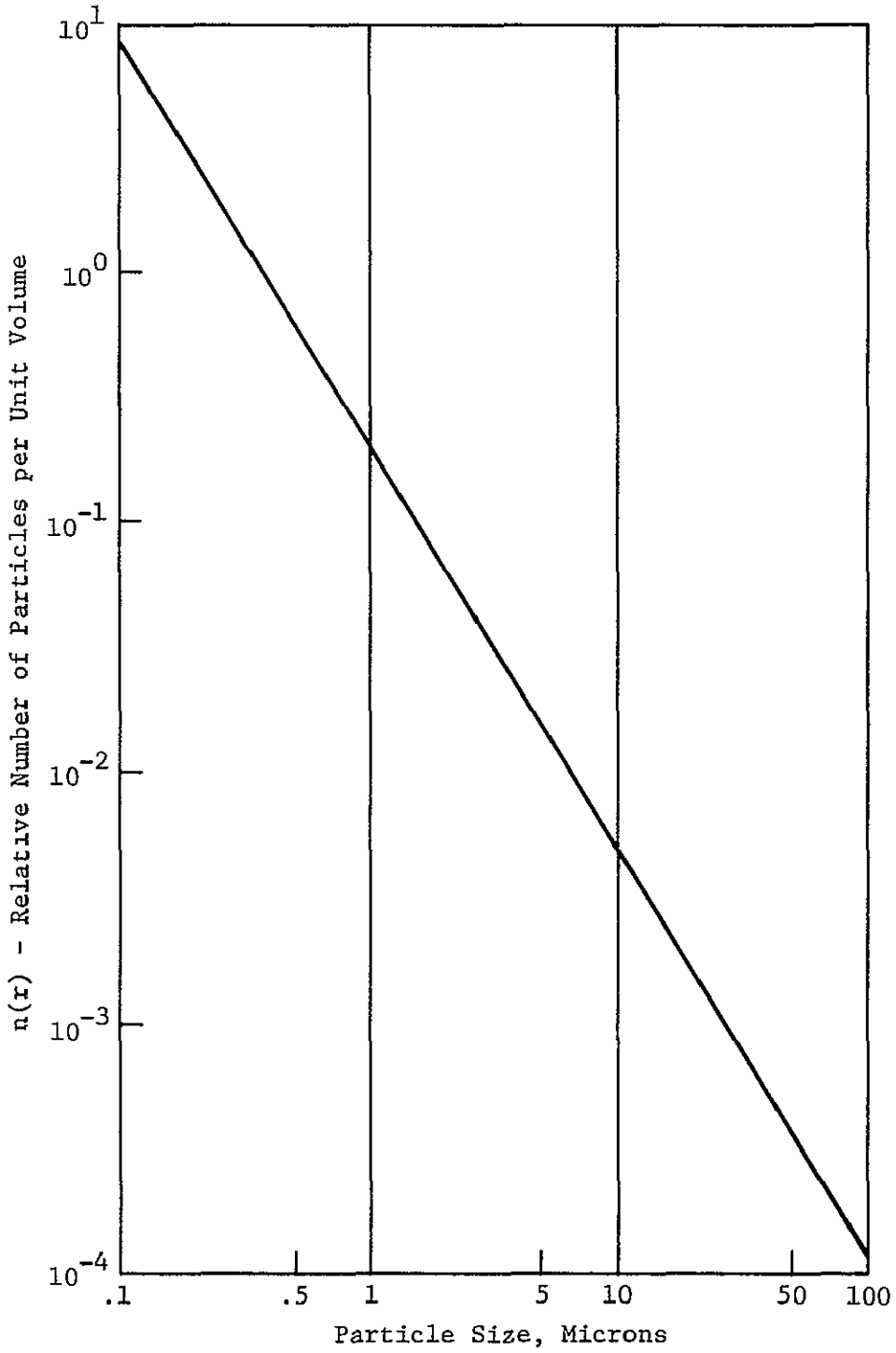

FIGURE 3-7
PARTICLE SIZE DENSITY FUNCTION FOR BALL CLAY (JUNGES DISTRIBUTION)

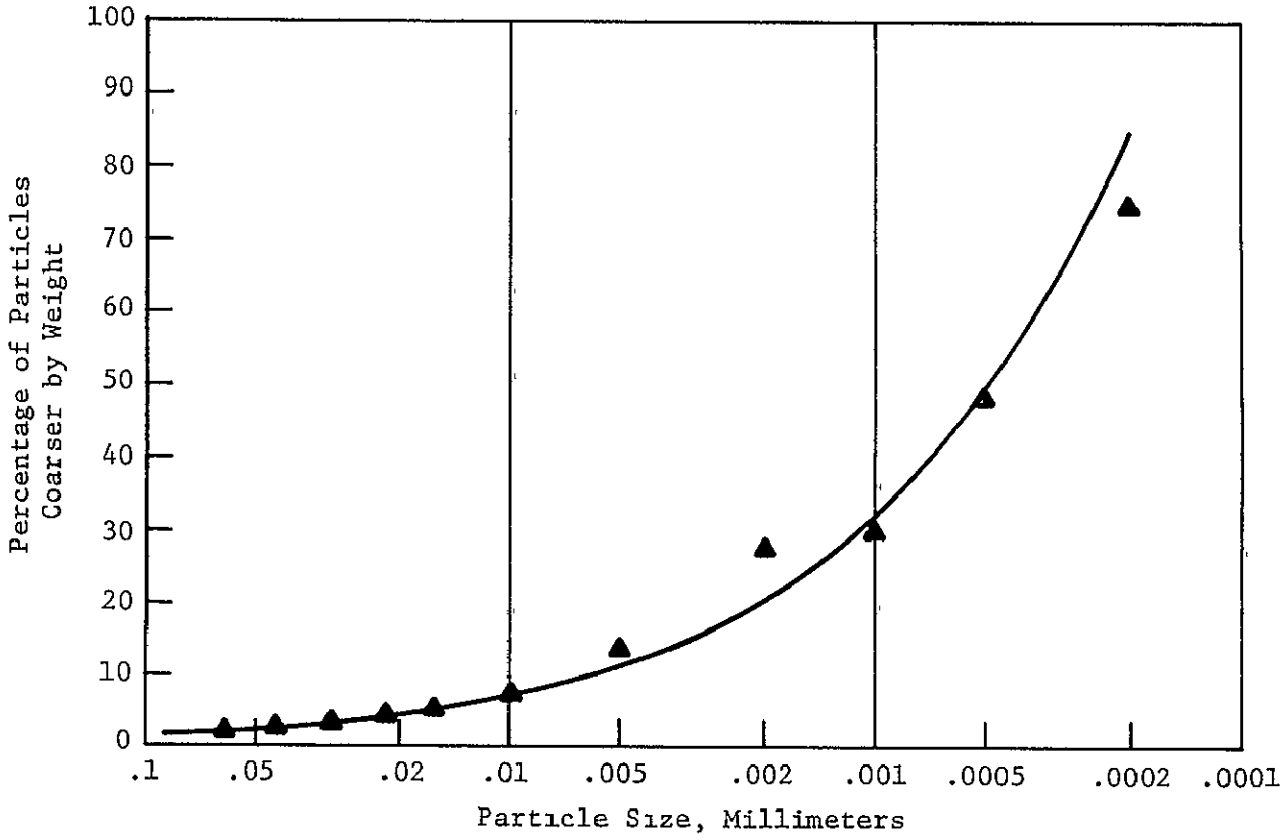

FIGURE 3-8
CUMULATIVE SIZE DISTRIBUTION FIT OF BALL CLAY SAMPLE USING JUNGE DISTRIBUTION

can not be normalized, i.e., N is infinite. However, Junge's distribution has been found to accurately represent particle sizes of ocean sediments.[23] In addition, the lower and upper limits of integration in Equations (3-11) and (3-10) are not set equal to zero and infinity, in practice, allowing Equation (3-11) to be normalized.

The question of the proper upper limit for Equation (3-10) and Equation (3-11) is of more than theoretical interest. From the empirical size distributions provided by NASA/LaRC, it appears that an upper limit in Equation (3-10) should be chosen as 100 microns (μm). However, as can be seen in Table 3.2[24] the settling rate for 100 μm particles is on the order of forty seconds. Thus, the history of the particulates in the body of water is important. If the particulates have been allowed to settle, then the size distributions determined before the particles are introduced into the water are inappropriate. In the NASA/LaRC water tank experiment the water is continuously mixed, thus forcing the large particles to remain in suspension. In order to investigate the effect of settling, two upper limits, 100 μm and 10 μm, were chosen for the integrals of Equations (3-10) and (3-11). Equation (3-11) was used to properly normalize Equation (3-10) with respect to the choice of upper limit.

3.5 Results of Computations

The results of the computation of the volume scattering functions (3.5.1) and the volume scattering distribution functions (3.5.2), using the size distributions of Section 3.4, are presented

TABLE 3.2

SETTLING VELOCITIES OF SAND AND SILT IN STILL WATER

(Source: Amer Water Works Assoc.)

[Temperature 50°F, all particles assumed to have a specific gravity of 2 65]

Diameter of particle	Order of Size	Settling Velocity	Time Required to Settle 1 Foot
mm.		*mm /sec*	
10 0	Gravel	1,000	0 3 seconds
1.0	Coarse Sand	100	3 0 seconds
0 8		83	
0 6		63	
0 5		53	
0 4		42	
0 3		32	
0 2		21	
0.15	Fine Sand	15	
0 10		8	38 0 seconds
0 08		6	
0 06		3 8	
0 05		2 9	
0 04		2 1	
0 03		1 3	
0 02		0 62	
0 015	Silt	0 35	
0 010		0 154	33 0 minutes
0 008		0 098	
0 006		0 065	
0 005		0 0385	
0 004		0 0247	
0 003		0 0138	
0 002		0 0062	
0 0015		0 0035	
0 001	Bacteria	0 00154	55 0 hours
0 0001	Clay Particles	0 0000154	230 0 days
0 00001	Colloidal Particles	0 000000154	63 0 years

in this section. In addition to examining the effect of settling on the calculations, the wavelength dependence of the scattering functions are also investigated.

3.5.1 Volume Scattering Functions

The computed volume scattering functions are shown in Figures 3.9 through 3.14.

Figures 3.9 and 3.14 display the extremely large forward scattering peak which is primarily the result of including the large ($\sim$100 μm) particulates in the size distributions. Both the Feldspar and Ball clay phase functions show considerable difference between the non-absorbing and absorbing cases at large angle. While it is not evident in the figures, the forward scattering peak is larger for the absorbing case at small but non-zero angles ($\theta \sim 0.5^{o}$).

Figures 3-11 and 3-12 demonstrate the effect of cutting the size distributions off at 10 μm instead of 100 μm. The relative size of the forward peak is reduced and the difference between the absorbing and non-absorbing cases at large angles is reduced. It is interesting to note that, although the shape of the Feldspar and Ball clay size distributions are very different, the upper limit on the size appears to be much more important in terms of the difference in phase functions.

Figures 3-13 and 3-14 show the scattering functions computed for λ = 600 nm (with a 10 μm cutoff) instead of λ = 500 nm as in Figures 3-11 and 3-12. It can be seen that the phase functions are not heavily

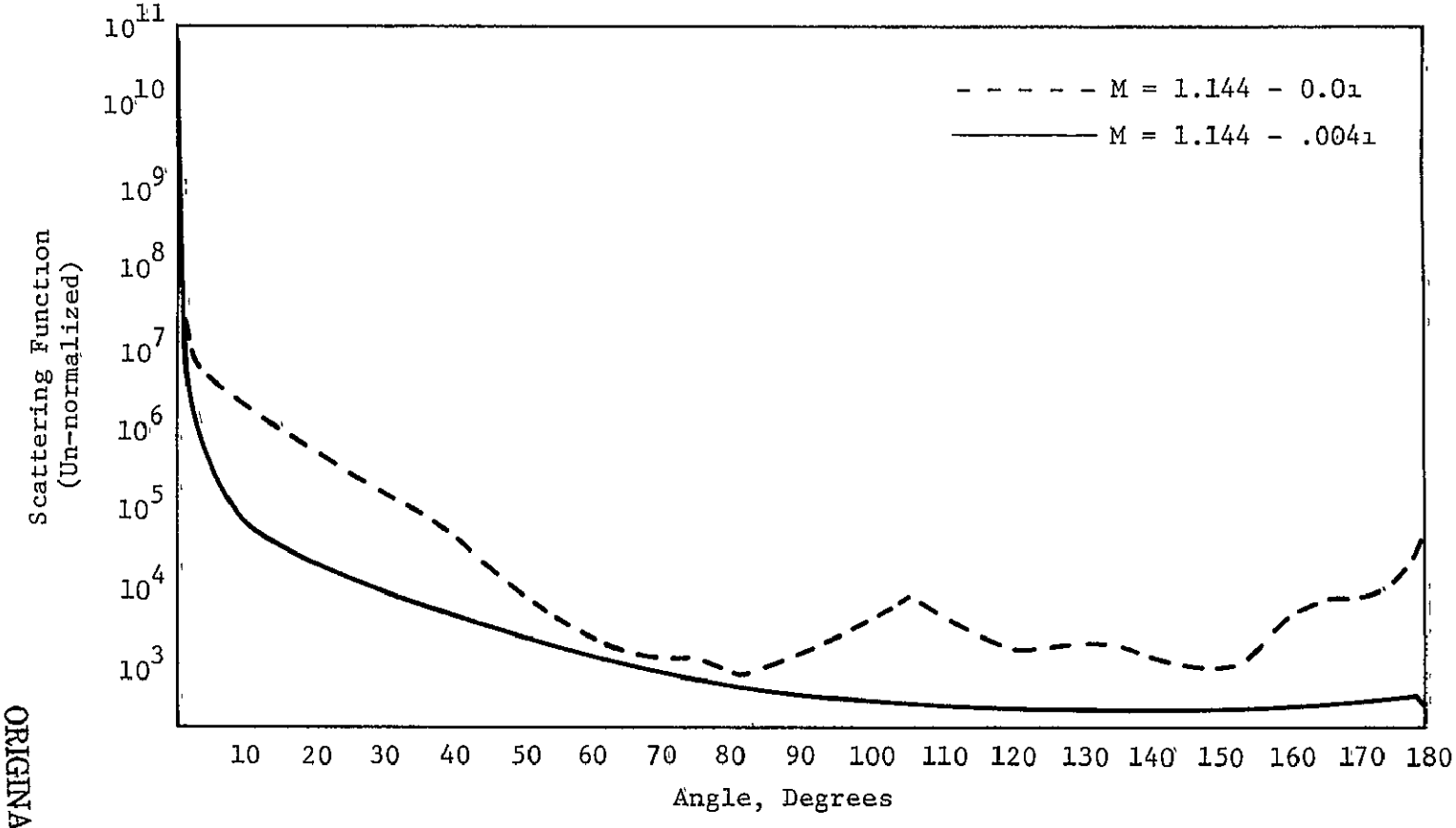

FIGURE 3-9
VOLUME SCATTERING FUNCTIONS FOR FELDSPAR (λ = 500NM)

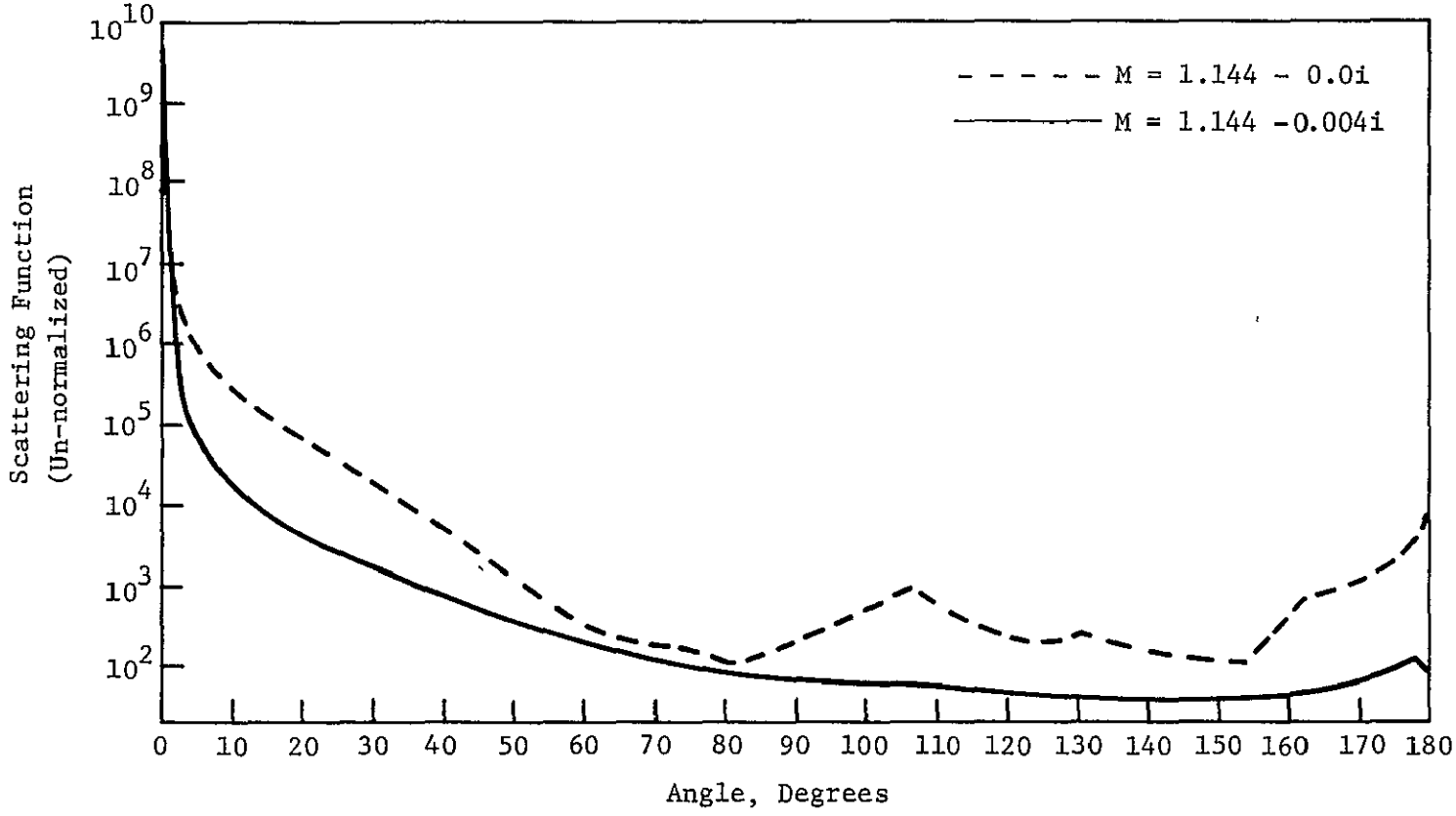

FIGURE 3-10
VOLUME SCATTERING FUNCTIONS FOR BALL CLAY (λ = 500NM)

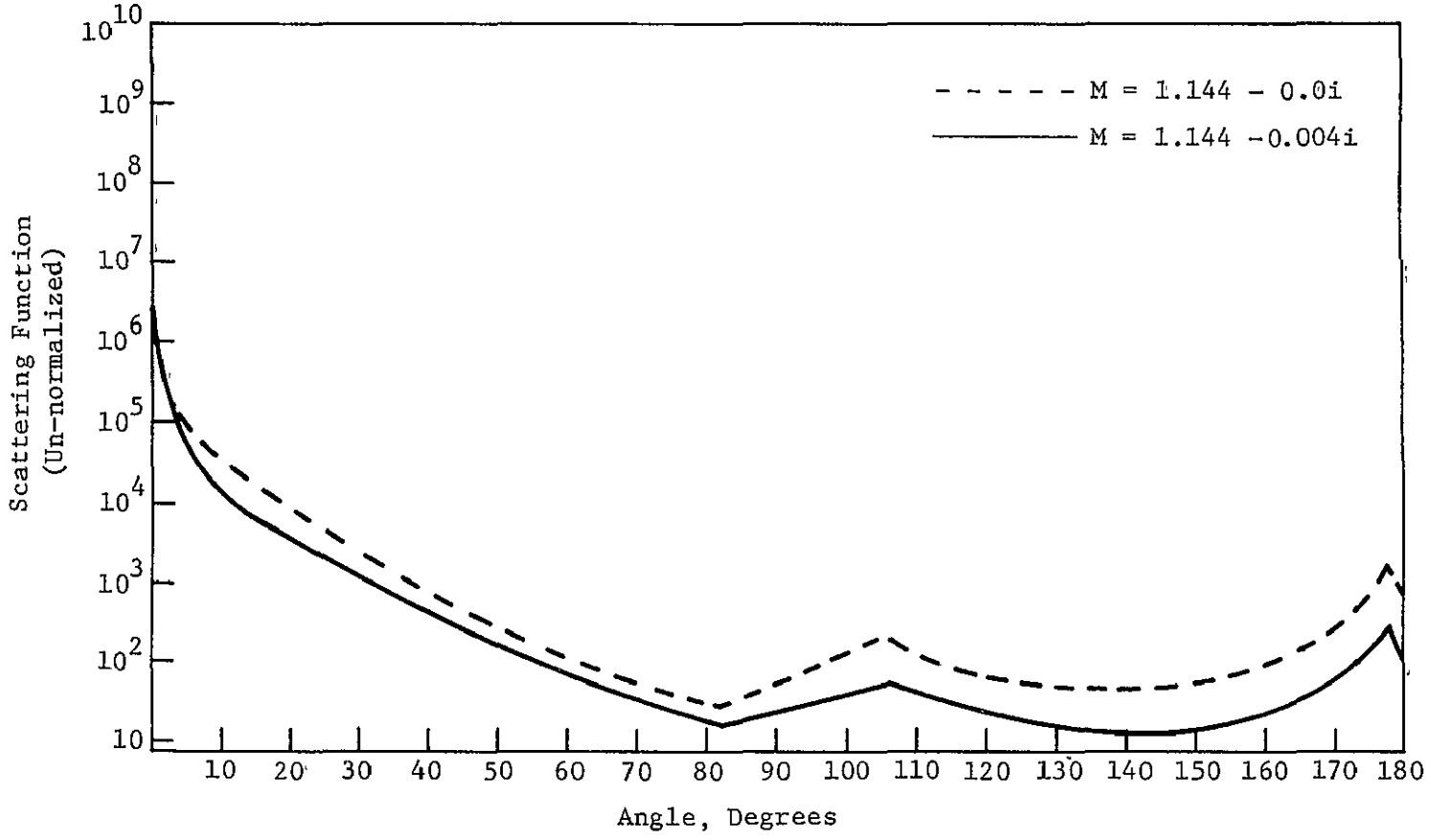

FIGURE 3-11
VOLUME SCATTERING FUNCTIONS FOR FELDSPAR (10μM CUTOFF λ = 500NM)

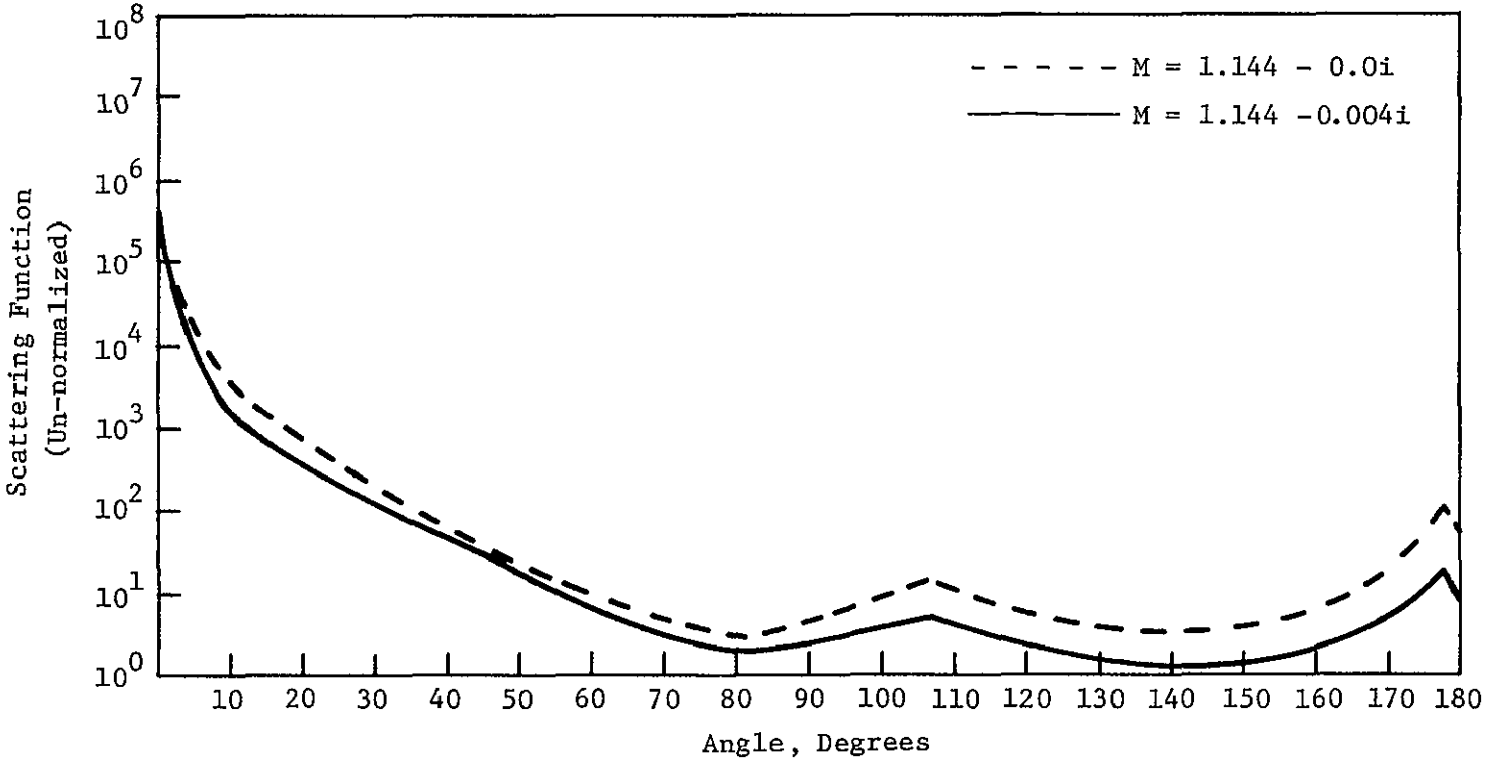

FIGURE 3-12
VOLUME SCATTERING FUNCTIONS FOR BALL CLAY (10μM CUTOFF λ = 500NM)

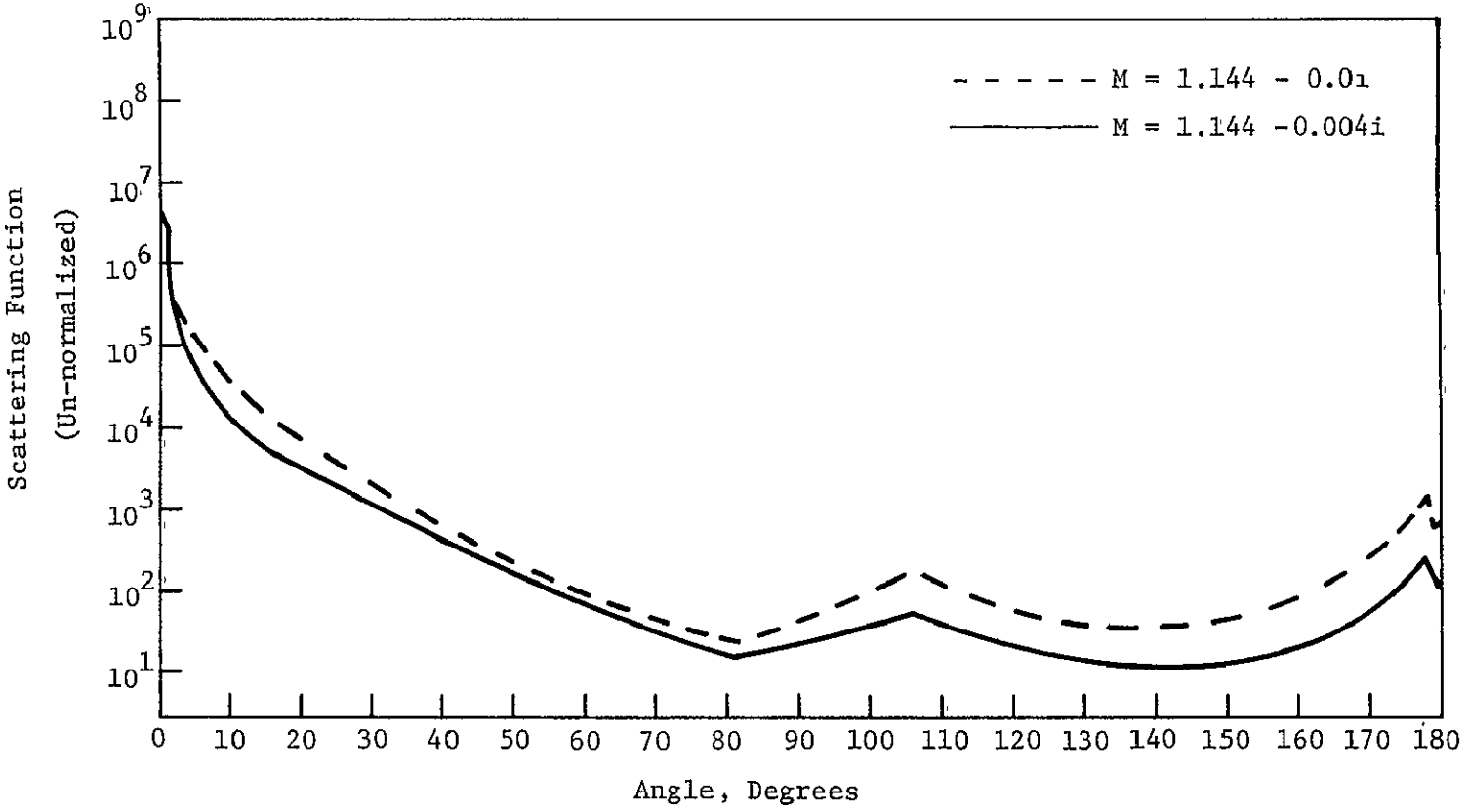

FIGURE 3-13
VOLUME SCATTERING FUNCTIONS FOR FELDSPAR (10μM CUTOFF λ = 600NM)

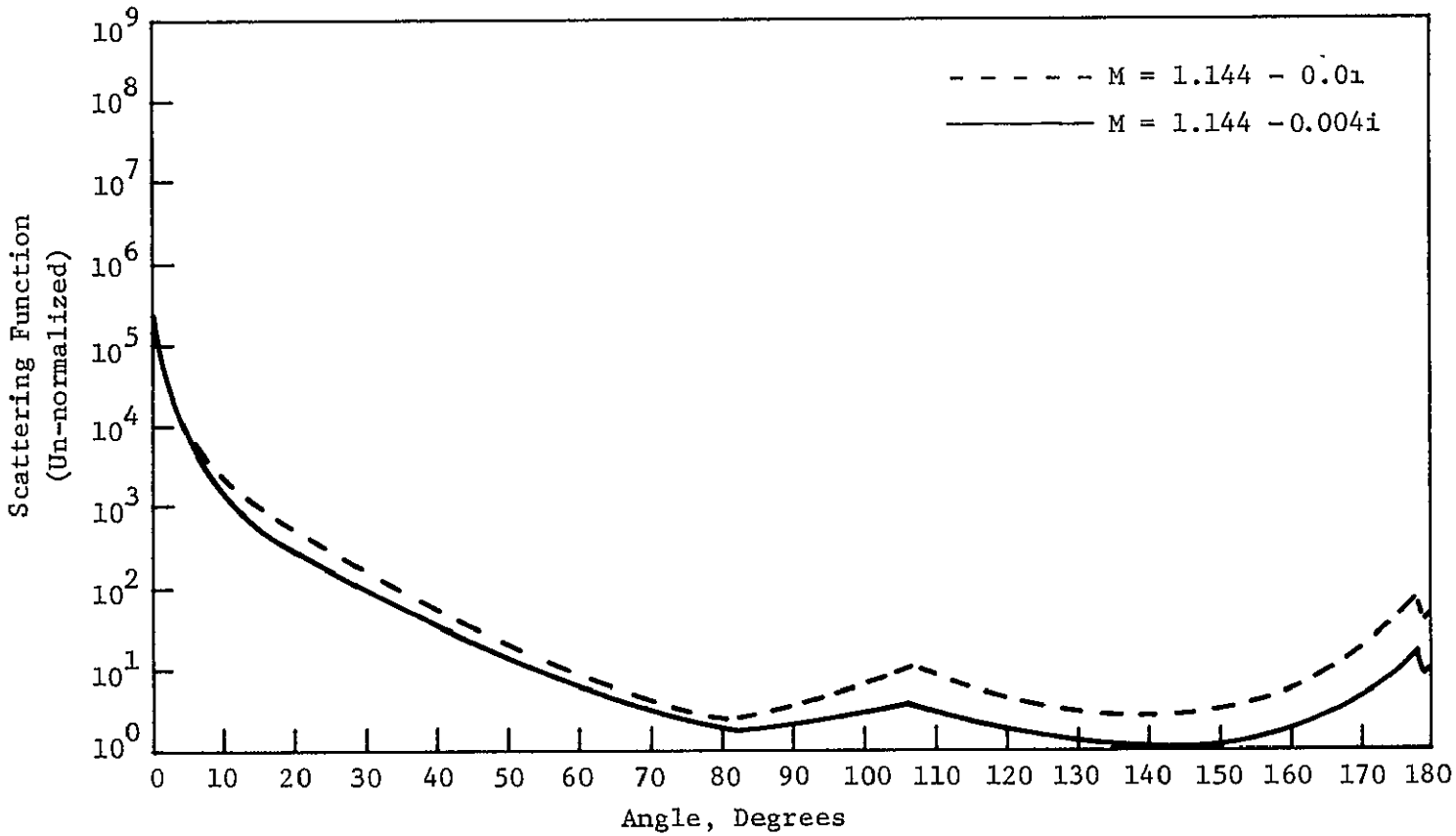

FIGURE 3-14
VOLUME SCATTERING FUNCTIONS FOR BALL CLAY (10μM CUTOFF λ = 600NM)

wavelength dependent. In fact, it can be shown that for a uniform size distribution and upper and lower limits of zero and infinity in Equation (3-10), the volume scattering function will be strictly independent of wavelength.

3.5.2 Volume Scattering Distribution Functions

While the volume scattering function describes the angular dependence of scattered radiation, a more important function for use with the Monte Carlo simulation is the volume scattering distribution function, $F(\theta)$, defined by equation (1-1). The distribution function gives the normalized probability that a photon is scattered in the range 0 to θ degrees. The volume scattering distribution functions for the cases considered in Section 3.5 are shown in Figures 3-15 through 3-20.

It is again apparent in Figures 3-15 and 3-16 that there is a considerable difference between the absorbing and non-absorbing case. The difference due to the Feldspar and Ball clay size distributions is small.

As with the scattering functions, the use of a 10 μm cutoff decreases the difference between the absorbing and non-absorbing cases. In addition, the volume scattering distribution functions are changed consdierably when the 10 μm cutoff is imposed.

Figures 3-19 and 3-20 demonstrate the small change in the volume scattering distribution functions when the wavelength is changed.

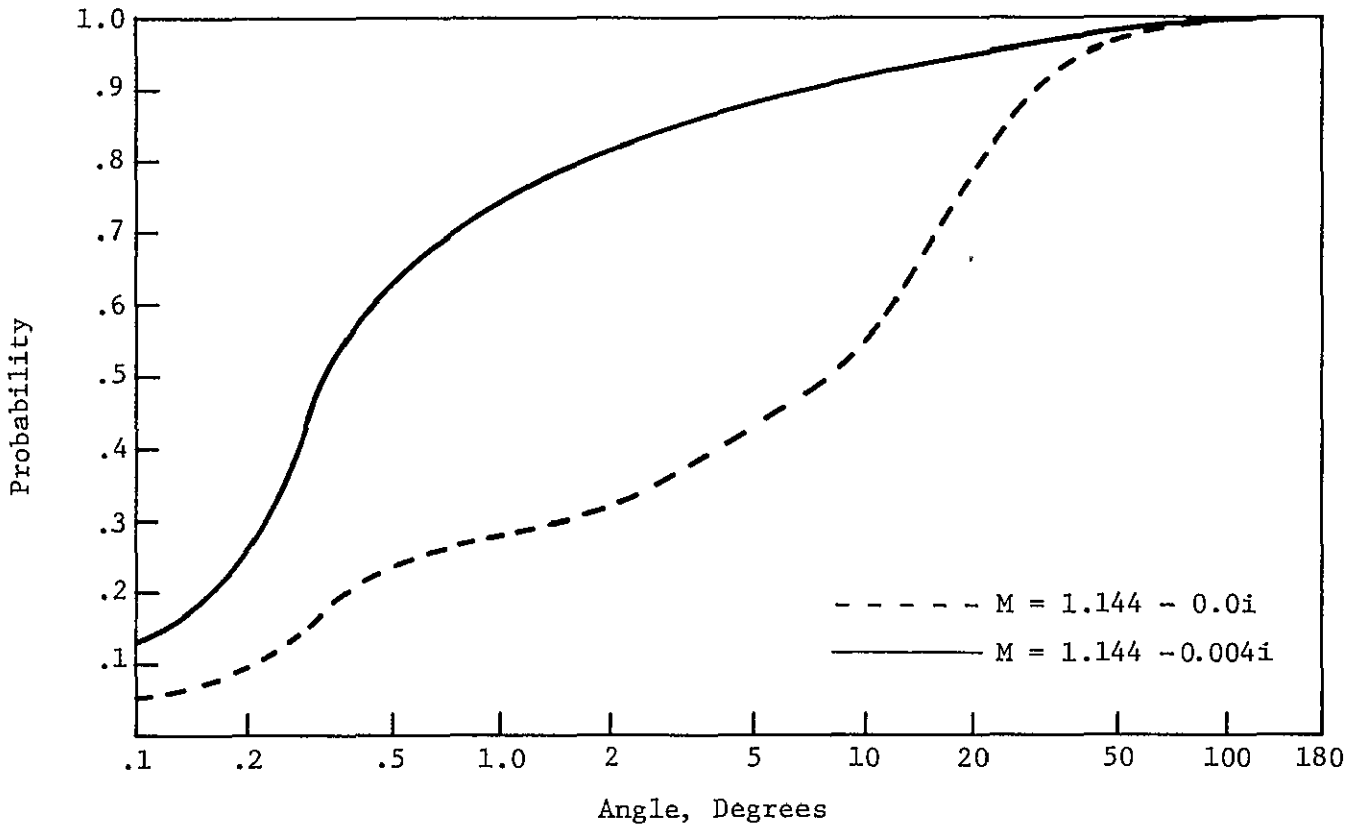

FIGURE 3-15
VOLUME SCATTERING DISTRIBUTION FUNCTIONS FOR FELDSPAR (λ = 500NM)

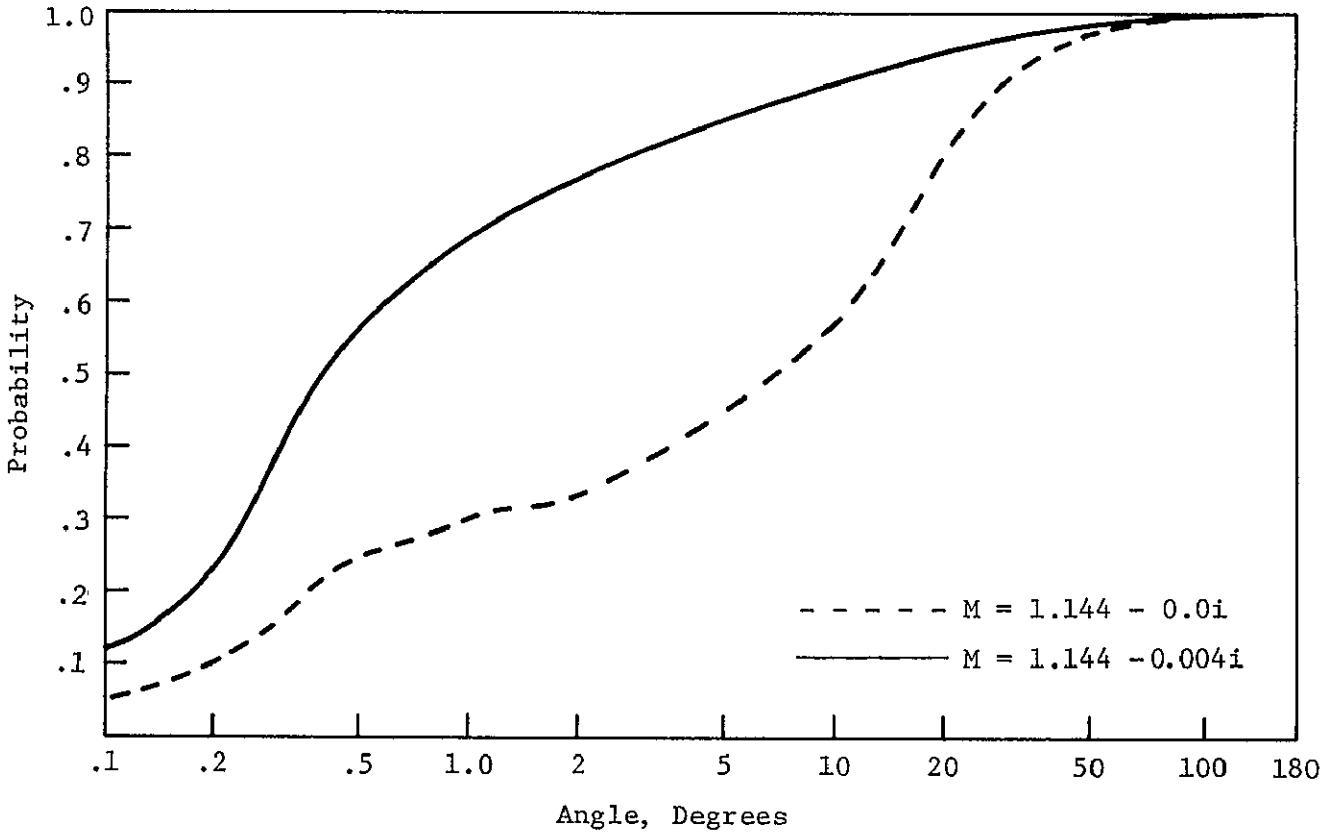

FIGURE 3-16
VOLUME SCATTERING DISTRIBUTION FUNCTIONS FOR BALL CLAY (λ = 500NM)

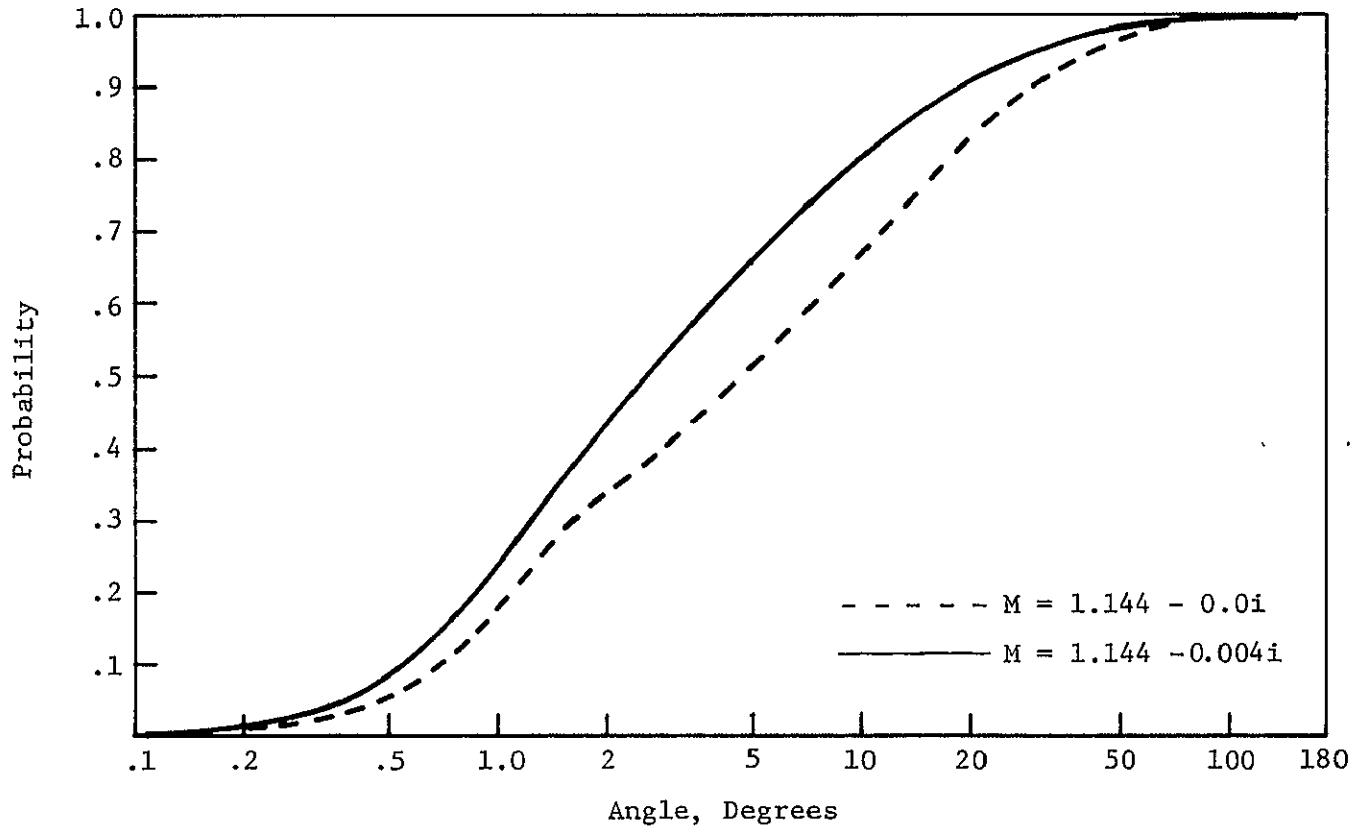

FIGURE 3-17
VOLUME SCATTERING DISTRIBUTION FUNCTIONS FOR FELDSPAR (10μM CUTOFF λ = 500NM)

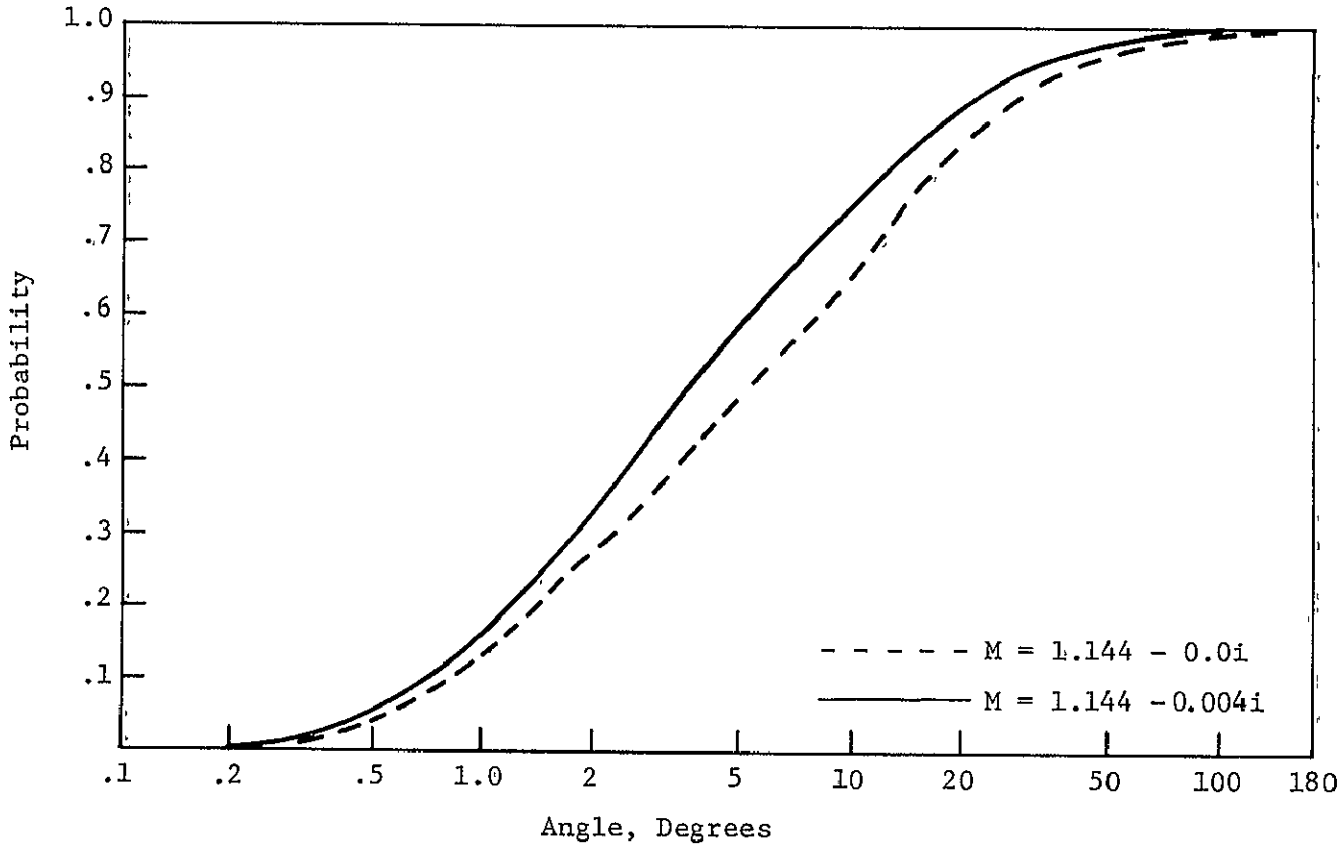

FIGURE 3-18
VOLUME SCATTERING DISTRIBUTION FUNCTIONS FOR BALL CLAY (10μM CUTOFF λ = 500NM)

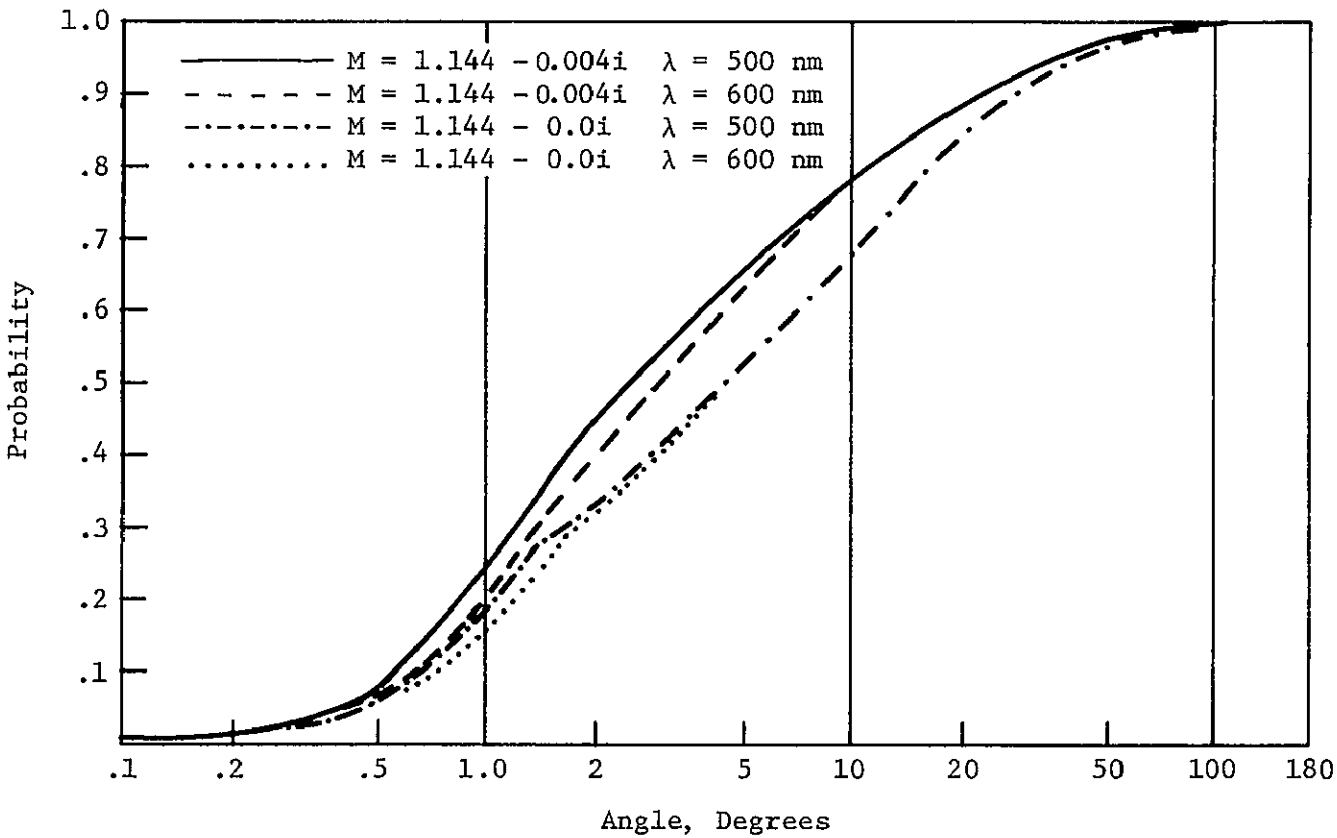

FIGURE 3-19
WAVELENGTH DEPENDENCE OF VOLUME SCATTERING DISTRIBUTION FUNCTIONS FOR FELDSPAR (10μM CUTOFF)

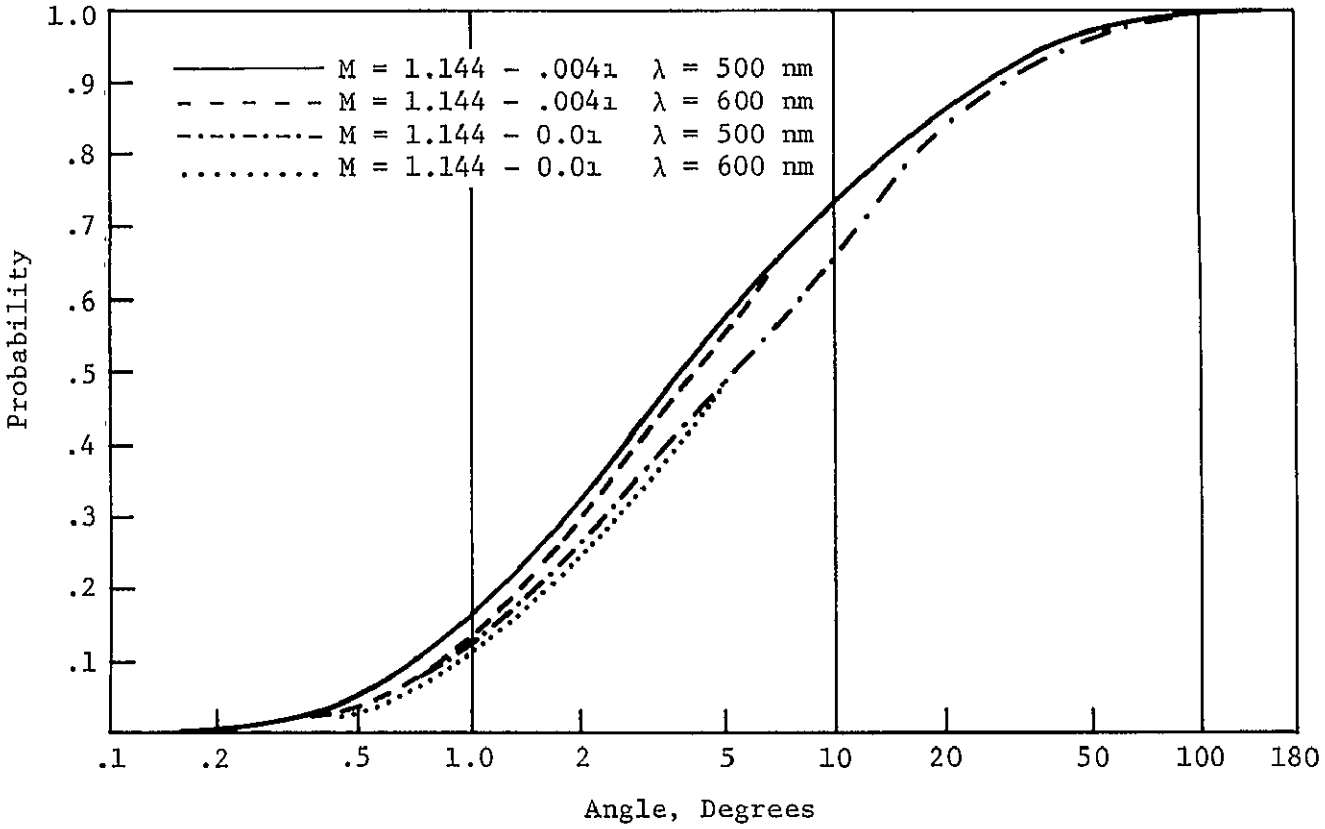

FIGURE 3-20
WAVELENGTH DEPENDENCE OF VOLUME SCATTERING FUNCTIONS FOR BALL CLAY (10μM CUTOFF)

4.0 DEPENDENCE OF UPWELLING RADIANCE ON SCATTERING FUNCTION

In this section we describe our results on the dependence of the upwelling radiance as it relates to the variations of the scattering function, or equivalently to its integrated form the scattering probability function. Before this is done, however, we will summarize the information on the scattering probability functions derived earlier.

In the previous two sections, we have (1) summarized the available information on the measurements of the scattering function, and (2) have utilized the Mie formalism to calculate the scattering function for polydispersed suspensions on the basis of size distribution measurements provided through the LaRC laboratory program. The compiled measured scattering probability functions for natural water, Figure 2-8, cover a wide range of turbid waters and show considerable variations. The upper and lower bounding measured for the scattering probability functions correspond to San Diego Harbor, sea water filtered thoroughly. The scattering probability function measured by Morrison[3], used in Reference (1,2) lies between these limits, closer to the upper bound. Due to the lack of sufficient observations no conclusions could be drawn regarding the changes of the measured scattering functions with wavelenth. The calculated results of the scattering probability functions have been obtained for the following cases and their combinations:

- Size distributions including large particle sizes (~100 μm)
- Size distributions including a cutoff at 10 μm

- Zero or 0.004 for the imaginary part of the index of refraction
- Two wavelengths values at 500 and 600 nm

The conclusions which may be derived from these results are:

1) Size distributions including large particles sizes (~100 μ) lead to an extremely large forward scattering peak, which shows up as a fast rise in the scattering probability function. The scattering probability function calculated for this situation is higher than the upper bound of the measured functions as may be seen by comparing Figures 3-15 and 2-8.

2) Size distributions including a cutoff at 10 μ results in the scattering probability functions which lie between the upper and lower bounding of the measured probability functions shown in Figure 2-8.

3) The effect of non-zero imaginary part for the index of refraction is to decrease the fast rise of the scattering probability function at small angles, and to put these functions within the bounds of the measured data.

4) The functions calculated for wavelengths of 500 nm and 600 nm do not show significant differences.

Based on the results and the conclusion described above three functions were selected for the investigation of the dependence of the upwelling radiance on the scattering function. These functions, which were input to the Monte Carlo simulations radiative transfer code of Appendix A, have been designated by SCATR 1, SCATR 2, and SCATR 3. SCATR 2 is the lower bound of the measured scattering probability function shown in Figure 2-8. SCATR 1 is the upper bound of the measured scattering probability function shown in Figure 2-8. SCATR 3 is the upper bound of the calculated scattering probability functions, and is shown in Figure 3-15. This function has been calculated for Felspar soil, a zero value for the imaginary part of

index of refraction, a size distribution including large particles (~100 μ) at 500 nm wavelength.

4.1 Results

Besides the parameters characterizing the cross sectional radius (1.2 meters) and the height (2.6 meters) of the LaRC cylindrical water tank, and the reflectivity of the tank walls (3.0 percent) the following input parameters are required for the model:

(1) Total scattering coefficient s,

(2) Total absorption coefficient a,

(3) Scattering probability function.

A fourth model input concerns the maximum number of photons to be traced in each computer run.

The results presented in the remainder of this section refer to two turbidity levels which have been simulated in the model. These turbidity levels correspond to s = 6 meter^{-1}, and s = 12 meter^{-1} respectively. The wavelength considered is 500 nm. From the functional relationship between a/s ratio and the wavelength, reported in Reference 1, the value of a/s for particles at 500 nm is 0.27. Based on this value, absorption coefficients of 1.6 and 3.2 meter^{-1} have been calculated for s = 6 and s = 12 meter^{-1} respectively, and are shown in Table 4.1.

On making use of the computer code documented in Appendix A the radiances emerging from the area within the field of view of the over-

TABLE 4.I

OPTICAL PARAMETERS USED IN THE BACKSCATTERED RADIANCE CALCULATIONS

WAVELENGTH (nm)	TOTAL SCATTERING COEFFICIENT ($meter^{-1}$) s	TOTAL ABSORPTION COEFFICIENT ($meter^{-1}$) a	TOTAL ATTENUATION COEFFICIENT ($meter^{-1}$) α
500	6 0	1.6	7.6
	12.0	3.2	15.2

head detector in the LaRC's experimental arrangement,* and into the exit angles in the range 0-10 degrees, 0-20 degrees, 0-30 degrees, have been calculated. The results of these calculations in terms of the backscattered radiance vs, the upper limit of the exit angle is shown in Figures 4-1 and 4-2 for s = 6.0 and s = 12.0 meter^{-1}. Three scattering probability functions, namely the measured upper and lower bounding functions have been used. The model has been executed for 10,000 photons in each case. The values calculated with the input of calculated upper bounding scattering function is in good agreement (the shape of the respective curves) with the measured upper bounding scattering function for the large range of the exit angles. For the small range of the exit angles, ($\leq 25^{o}$ degrees for s = 6 meter^{-1} and $\leq 35^{o}$ for s = 12 meter^{-1}) no statistically significant result could be derived from the ensemble of backscattered photons for 10,000 incident photons. For this reason the reminder of this report will discuss the results concerning the upper two curves in Figure 4-1 and 4-2.

The presented results indicate that the upwelling radiance has a strong dependence on the scattering function used. This dependence seems to get less important with decreasing range of the exit angle. If the same trend continues to be true for smaller than 10^{o} angles

*An area 2.5 cm in radius in the middle of the incident spot which is about 30 cm in diameter (see Figure 1-1 for reference). The incident beam impinges upon the water surface at an angle of 13.5 degrees in the air (9.0 degrees in the water).

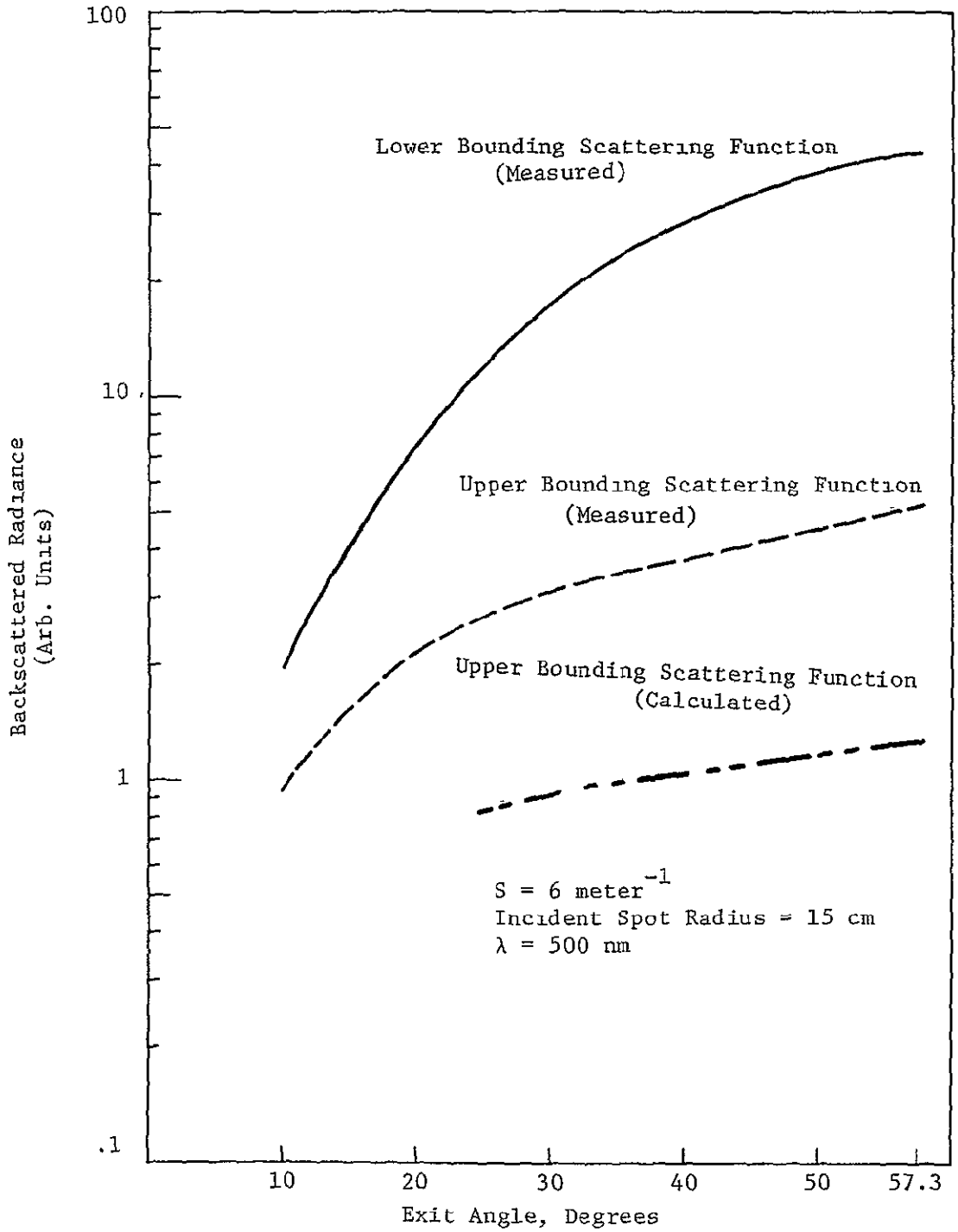

FIGURE 4-1
BACKSCATTERED RADIANCE VS. UPPER LIMIT OF THE EXIT ANGLE FOR s = 6 METER^{-1}

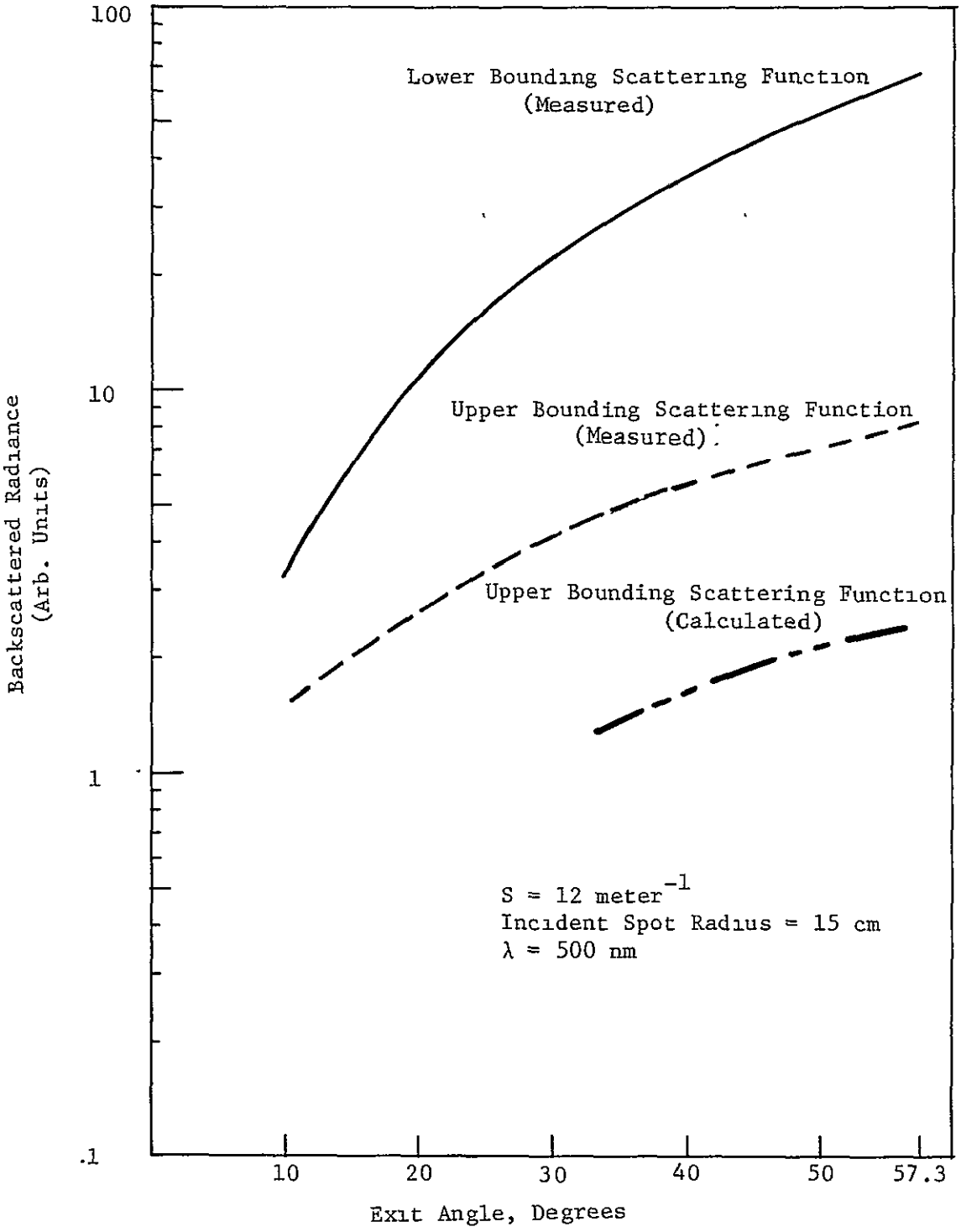

FIGURE 4-2
BACKSCATTERED RADIANCE VS. UPPER LIMIT OF THE EXIT ANGLE FOR s = 12 METER^{-1}

than 10° angles (for which no significant statistic could be derived for 10,000 photons)* then, at 0.5° angle which is the actual acceptance angle of the LaRC's detector, the effect of various scattering functions will not be significant. This is displayed graphically by the results presented in Figure 4-3, where the ratio of the backscattered radiances for the upper and lower bounding of the scattering function is shown as a function of the upper limit of the exit angle. These results will be discussed in more detail in section 1.4.

*20,000 photons were traced to produce the results shown in the lower curve in Figure 4-2.

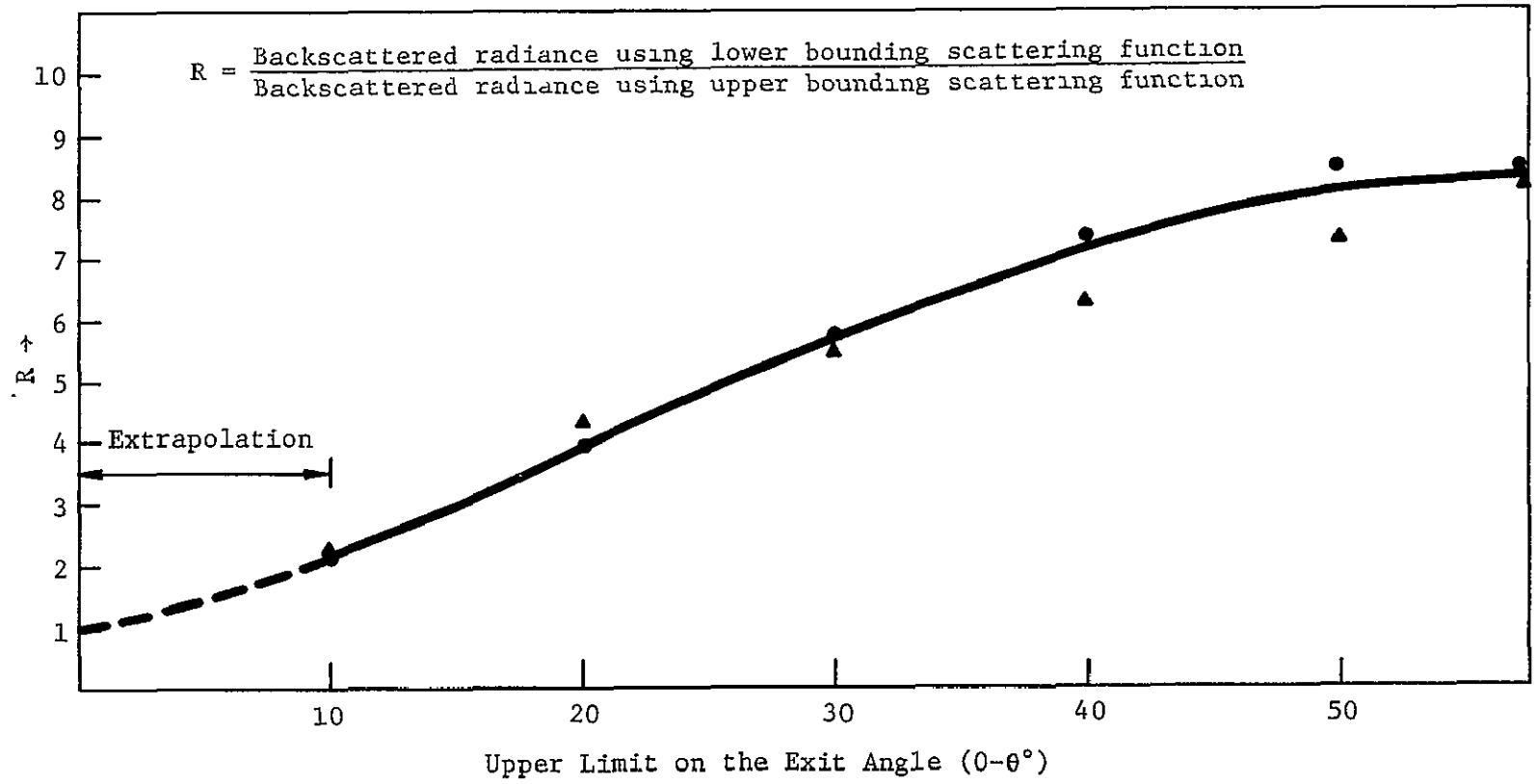

FIGURE 4-3
RATIO OF THE BACKSCATTERED RADIANCE FOR UPPER AND LOWER BOUNDING SCATTERING FUNCTIONS

PAGE INTENTIONALLY BLANK

APPENDIX A

RADIATIVE TRANSFER COMPUTER PROGRAM

In this appendix we have included two versions of our radiative transfer code. These programs are appropriately modified versions of the program listed in Reference 2. The modified computer codes make it easier to incorporate any desired scattering probability function in the model. The functions included in Code 1 of this appendix are, the upper and the lower bounding, measured scattering probability functions shown in Figure 2-8. These functions are represented in the code by SCATER 1, and SCATER 2 respectively. Code 2 of this appendix is designed to handle the calculated scattering functions, specifically, the code includes the upper bound of the calculated functions shown in Figure 3-15. SCATER 3 represents this function. The out-puts of both codes are (1) the probability weights of each emerging photon, and (2) the angles of emergence. The sum of the probability weights for each angular range, normalized to the number of incident photons represents the upwelling radiances shown in Figures 4-1 and 4-2.

RADIATIVE TRANSFER COMPUTER PROGRAM

Code 1

```
C
C      MONTECARLO PROGRAM WITH DOCUMENTATION.
C      TANK BOUNDARIES AND TOTAL REFLECTION ARE INCLUDED.
C
       COMMON/BLOCK1/XMAX,YMAX,ZMAX,X,Y,Z,T,GAMA,TETA,FI.PI,DTRC,S,IS.ZP
C
C      READ DATA FROM THE DATA FILE.
C
       READ(5,25)MAXNPH,NMAX,IS
   25  FORMAT(3(2X.I12))
       READ(5,30)TETAI,FII
   30  FORMAT(2(5X,F8.3))
       READ(5,35)XMAX,YMAX,ZMAX
   35  FORMAT(3(5X,F8.3))
       READ(5,37)S
   37  FORMAT(F8.3)
       READ(5,24)A400,A500,A600
   24  FORMAT(3(5X,F8.3))
       WRITE(6,26)MAXNPH
   26  FORMAT('0','MAXIMUM NO. OF PHOTONS TO BE TRACED= ',I9)
       WRITE(6,27)NMAX
   27  FORMAT('0','MAXIMUM NO. OF EVENTS FOR EACH PHOTON= ',I12)
       WRITE(6,29)IS
   29  FORMAT('0','INITIAL SEED FOR RANDOM NO. GENERATOR= ',I12)
       WRITE(6,31)TETAI,FII
   31  FORMAT('0','INITIAL TETA IN DEGREES= ',F8.3,'   INITIAL FI IN DEGR
      1EES= ',F8.3)
       WRITE(6,36)XMAX,YMAX,ZMAX
   36  FORMAT('0','TANK DIMENSIONS IN METERS:','  XMAX=',F8.3,
      1'  YMAX=',F8.3,'  ZMAX=',F8.3)
       WRITE(6,38)S
   38  FORMAT('0','SCATTERING COEFFICIENT IN INVERSED METERS= ',F8.3)
       WRITE(6,23)A400,A500,A600
   23  FORMAT('0','ABSORPTION COEFFICIENTS AT 400, 500, 600 NM IN INVERSE
      1METERS:','  A400=',F8.3,'  A500=',F8.3,'  A600=',F8.3,//////)
       RNW=1.334
C
C      RNW IS THE REFRACTION INDEX OF WATER.
C
       PI=3.141592654
       DTRC=PI/180.
       XMAX=XMAX*S
       YMAX=YMAX*S
       ZMAX=ZMAX*S
       TETAI=TETAI*DTRC
       FII=FII*DTRC
       NPH=1
   10  IF(NPH .GT. MAXNPH)GO TO 2000
```

```
C
C      NPH IS  THE NO. OF PHOTONS AT A GIVEN TIME.
C      RECORD NO. OF PHOTONS TRACED AND TEST FOR END OF COMPUTATIONS.
C      INITIALIZE THE COORDINATES OF THE PHOTON ENTERING THE MEDIUM.
C
       TETA=TETAI
       FI=FII
       X=0.
       Y=0.
       Z=0.000001
C
C      DECIDE HOW FAR PHOTON TRAVELS BEFORE AN EVENT OCCURS.
C
       CALL RANDNO(IS,RHOD)
       T=-ALOG(RHOD)
       GAMA=T
C
C      T IS THE DISTANCE IN SCATTERING LENGTH UNITS PHOTON TRAVELS TO THE
C      EVENT PHOTON IS AT.
C
       X=X+T*SIN(TETA)*COS(FI)
       Y=Y+T*SIN(TETA)*SIN(FI)
       Z=Z+T*COS(TETA)
       GO TO 150
  100  NPH=NPH+1
C
C      EITHER ABSORPTION HAS OCCURED,OR PHOTON HAS COME OUT OF WATER. THE
C      FORE,START A NEW PHOTON.
C
       GO TO 10
  150  CONTINUE
       KMIN=2
       IF (Z) 400,500,500
  400  XINT=X-Z*TAN(TETA)*COS(FI)
       YINT=Y-Z*TAN(TETA)*SIN(FI)
       DINT=SQRT(XINT**2+YINT**2)
       DDINT=DINT/S
       IF(DDINT .GT. 0.20)GO TO 100
       IF (RNW*SIN(TETA) .GT. 1.0) GO TO 604
       TETAAR=ARSIN(RNW*SIN(TETA))
       IF(TETAAR .GT. 1.0)GO TO 100
       XINT=XINT/S
       YINT=YINT/S
       DINT=DDINT
       ACT=ABS(COS(TETA))
       TCUT=(ABS(ZR)-ABS(Z))/ACT
       GAMA=GAMA+TCUT
       GAMA=GAMA/S
```

```
      WRITE (6,410) DINT,TETAAR
  410 FORMAT(///,2X,'DISTANCE FROM AXIS= ',F8.5,5X,'POLAR ANGLE= ',F8.5)
      WRITE (6,420) FI,XINT,YINT
  420 FORMAT (' ','AZIM ANGLE= ',F8.5,5X,'XINT= ',F8.5,5X,'YINT= ',F8.5)
      WRITE(6,109) GAMA
  109 FORMAT('0','GAMA = ',E12.3)
      WRITE(6,888)J
  888 FORMAT(' ','NO OF EVENTS=',I8)
      WRITE(6,101)NPH
  101 FORMAT('0','NO. OF PHOTONS TRACED = ',I8)
C
C      CALCULATE PHOTON PROBABILITY WEIGHT.
C
      CALL PHPW(PI,GAMA,DINT,A400,A500,A600)
      WRITE(6,5999)IS
 5999 FORMAT('  RANDOM NUMBER USED  ',I12)
      GO TO 100
  604 KMIN=J+1
      ACT=ABS(COS(TETA))
      TCUT=(ABS(ZR)-ABS(Z))/ACT
      GAMA=GAMA+TCUT
      TETA=PI-TETA
      FI=FI+PI
      IF(FI .GE. 2.*PI)FI=FI-2.*PI
      X=XINT
      Y=YINT
      Z=0.000001
      CALL RANDNO(IS,RHOD)
      T=-ALOG(RHOD)
      X=X+T*SIN(TETA)*COS(FI)
      Y=Y+T*SIN(TETA)*SIN(FI)
      Z=Z+T*COS(TETA)
  500 CALL PSIW(KMIN,NMAX,J,IRTCOD)
      IF(IRTCOD .EQ. 1)GO TO 100
      IF(IRTCOD .EQ. 2)GO TO 400
      GO TO 100
 2000 WRITE (6,5000) IS
 5000 FORMAT (' ','LAST RANDUM NUMBER USED=',I12)
      STOP
      END
```

```
      SUBROUTINE PSIW(KMIN,NMAX,J,IRTCOD)
C
C     THIS SUBROUTINE WILL BE CALLED ONLY WHEN PHOTON IS STILL IN WATER
C     (WHEN Z>0).
C     IT DETERMINES THE COORDINATES OF THE END POINT IN THE NON-ROTATED
C     SYSTEM BY FIRST ROTATING THE SYSTEM USING ANGLES TETA AND FI.
C     IT GENETATES THE ROTATION MATRIX,WITH THE CONSTRAINT THAT YSTAR-
C     AXIS LIES IN A PLANE PARALLEL TO THE YZ-PLANE.
C     THE TOTATION MATRIX IS DESIGNATED AS AIJ(I=1,3,J=1,3).
C
      COMMON/BLOCK1/XMAX,YMAX,ZMAX,X,Y,Z,T,GAMA,TETA,FI,PI,DTRC,S,IS,ZR
      IRTCOD=0
      DO 1290 J=KMIN,NMAX
      CT=COS(TETA)
      CF=COS(FI)
      CT2=CT*CT
      CF2=CF*CF
      ST=SIN(TETA)
      SF=SIN(FI)
      ST2=ST*ST
      SF2=SF*SF
      SS1=CT2+SF2*ST2
      SS=SQRT(SS1)
      SSD=1./SS
      A11=SQRT(1.-CF2*ST2)
      A12=-SF*CF*ST2*SSD
      A13=-CT*ST*CF*SSD
      A22=CT*SSD
      A23=-SF*ST*SSD
      A31=CF*ST
      A33=CT
      A32=SF*ST
C
C     ROTATION MATRIX HAS BEEN GENERATED.
C     SCATTERING HAS OCCURED.
C     CALL ANGELS FIP,TETAP TO DISTINGUISH FROM FI,TETA
C     FIP,TETAP ARE DETERMINED IN SYSTEM WITH Z-AXIS PARALLEL TO THE
C     INCIDENT DIRECTION.
C
      CALL RANDNO(IS,RHOF)
      FIP=2.*PI*RHOF
      CALL RANDNO(IS,RHOT)
      CALL SCATP1(RHOT,TETA)
      TETA=TETA*DTRC
      TETAP=TETA
C
C     DETERMINE HOW FAR BEFORE AN EVENT OCCURS,IN THE ROTATED SYSTEM.
C
```

```
      CALL RANDNO(IS,RHOD)
      T=-ALOG(RHOD)
C
C     CALCULATE COORDINATES OF END POINT IN THE ROTATED SYSTEM.
C
      XSTAR=T*SIN(TETAP)*COS(FIP)
      YSTAR=T*SIN(TETAP)*SIN(FIP)
      ZSTAR=T*COS(TETAP)
C
C     APPLY ROTATION MATRIX TO DETERMINE THE COORDINATES OF THE END
C     POINT IN A SYSTEM PARALLEL TO THE ORIGINAL ONE BUT DISPLACED.
C
      XR=A11*XSTAR+A31*ZSTAR
      YR=A12*XSTAR+A22*YSTAR+A32*ZSTAR
      ZR=A13*XSTAR+A23*YSTAR+A33*ZSTAR
C
C     CALCULATE TETA,AND FI IN THE PRESENT SYSTEM,WHICH IS PARALLEL TO
C     THE ORIGINAL ONE.
C
      FI=ATAN(ABS(YR)/ABS(XR))
      IF (XR .LT. 0.0)GO TO 133
      IF (YR)  333,333,633
333   FI=2.*PI-FI
      GO TO 533
633   FI=FI
      GO TO 533
133   IF (YR)  233,233,433
233   FI=FI+PI
      GO TO 533
433   FI=PI-FI
533   CONTINUE
      XR2=XR*XR
      YR2=YR*YR
      ZR2=ZR*ZR
      DT=XR2+YR2+ZR2
      SQDT=SQRT(DT)
      TETA=ARCOS(ZR/SQDT)
C
C     CALCULATE X,Y,Z OF THE END POINT OF THE PHOTON WITH RESPECT TO
C     THE ORIGINAL AXIS.
C
      X=X+XR
      Y=Y+YR
      X2=X*X
      Y2=Y*Y
      DIS2=X2+Y2
      XMAX2=XMAX*XMAX
      YMAX2=YMAX*YMAX
```

```
      DIMAX2=XMAX2+YMAX2
      IF(DIS2 .GE. DIMAX2)GO TO 100
      Z=Z+ZR
      IF (Z) 400,400,700
  700 IF(ZMAX-Z)702,702,701
  702 X=X-(Z-ZMAX)*TAN(TETA)*COS(FI)
      Y=Y-(Z-ZMAX)*TAN(TETA)*SIN(FI)
      ACT=ABS(COS(TETA))
      TT=T-(Z-ZMAX)/ACT
      Z=ZMAX
      CALL RANDNO(IS,RHOB)
      IF(RHOB-0.03)704,704,100
C
C     CHECK THREE PERCENT REFLECTION WITH UNIFORM ANGULAR PROBABILITY.
C
  704 CALL RANDNO(IS,RHOBT)
      TETA=0.5*PI*RHOBT+0.5*PI
      CALL RANDNO(IS,RHOBF)
      FI=2.*PI*RHOBF
      CALL RANDNO(IS,RHOD)
      T=-ALOG(RHOD)
      X=X+T*SIN(TETA)*COS(FI)
      Y=Y+T*SIN(TETA)*SIN(FI)
      Z=ZMAX+T*COS(TETA)
      T=T+TT
  701 GAMA=GAMA+T
 1290 CONTINUE
  100 IRTCOD=1
      GO TO 500
  400 IRTCOD=2
  500 RETURN
      END
```

```
      SUBROUTINE PHPW(PI,GAMA,DINT,A400,A500,A600)
C
C     THIS SUBROUTINE CALCULATES THE PHOTON PROBABILITY WEIGHT FOR GIVEN
C     WAVELENGTHS.
C
      TIR=0.0254
      TIR2=TIR*TIR
      CK=PI*TIR2
      R=0.15
      WRITE(6,860)R
  860 FORMAT('0','BEAM RADIUS IN METERS= ',F8.3)
      R2=R*R
      DINT2=DINT*DINT
      XINT=(R2-TIR2+DINT2)/(2.*DINT)
      XINT2=XINT*XINT
      YINT=SQRT(ABS(R2-XINT2))
      GC1=ATAN(YINT/XINT)
      GC2=ATAN(YINT/(DINT-XINT))
      GC3=PI-ATAN(YINT/(ABS(XINT-DINT)))
      AAA=GC1*R2+GC2*TIR2-DINT*YINT
      BBB=GC1*R2+GC3*TIR2-DINT*YINT
      BIR=R+TIR
      CIR=R-TIR
      IF(DINT .GE. 0.0  .AND.  DINT .LT. CIR)AREA=CK
      IF(DINT .GE. CIR  .AND.  DINT .LT. R)AREA=BBB
      IF(DINT .GE. R  .AND.  DINT .LT. BIR)AREA=AAA
      IF(DINT .GE. BIR)AREA=0.
      E500=EXP(-GAMA*A500)
C
C     PHOTON PROBABILITY WEIGHTS FOR 500 NM.
C
      PPW500=AREA*E500
      WRITE(6,861)PPW500
  861 FORMAT('0','PHOTON PROB. WT. FOR 500 NM= ',F10.6)
      RETURN
      END
```

```
      SUBROUTINE RANDNC(IX,RNUM)
C
C
C      THIS SUBROUTINE GENERATES UNIFORM RANDOM NUMBERS BETWEEN 0 AND 1.
C
C
      IY=IX*65539
      IF(IY) 5,6,6
    5 IY=IY+2147483647+1
    6 RNUM=IY
      RNUM=RNUM*.4656613E-9
      IX=IY
      RETURN
      END
```

```
      SUBROUTINE SCATR1(RHOT,TETA)
C
C
C     THIS SUBROUTINE DETERMINES ANGLE 'THETA' FROM A GIVEN SCATTERING
C     FUNCTION (UPPER BOUND).
C
C
      IF(RHOT .LE. .150)GO TO 1
      IF(RHOT .LE. .200)GO TO 2
      IF(RHOT .LE. .225)GO TO 3
      IF(RHOT .LE. .250)GO TO 4
      IF(RHOT .LE. .275)GO TO 5
      IF(RHOT .LE. .300)GO TO 6
      IF(RHOT .LE. .320)GO TO 7
      IF(RHOT .LE. .345)GO TO 8
      IF(RHOT .LE. .360)GO TO 9
      IF(RHOT .LE. .385)GO TO 10
      IF(RHOT .LE. .480)GO TO 11
      IF(RHOT .LE. .550)GO TO 12
      IF(RHOT .LE. .600)GO TO 13
      IF(RHOT .LE. .655)GO TO 14
      IF(RHOT .LE. .685)GO TO 15
      IF(RHOT .LE. .715)GO TO 16
      IF(RHOT .LE. .730)GO TO 17
      IF(RHOT .LE. .755)GO TO 18
      IF(RHOT .LE. .800)GO TO 19
      IF(RHOT .LE. .830)GO TO 20
      IF(RHOT .LE. .890)GO TO 21
      IF(RHOT .LE. .918)GO TO 22
      IF(RHOT .LE. .935)GO TO 23
      IF(RHOT .LE. .945)GO TO 24
      IF(RHOT .LE. .960)GO TO 25
      IF(RHOT .LE. .967)GO TO 26
      IF(RHOT .LE. .974)GO TO 27
      IF(RHOT .LE. .981)GO TO 28
      IF(RHOT .LE. .988)GO TO 29
      IF(RHOT .LE. .994)GO TO 30
      IF(RHOT .LE. 1.00)GO TO 31
    1 TETA=0.1
      GO TO 50
    2 TETA=.10+(RHOT-.15)*(.20-.10)/(0.20-.15)
      GO TO 50
    3 TETA=.20+(RHOT-.20)*(.30-.20)/(.225-.20)
      GO TO 50
    4 TETA=.30+(RHOT-.225)*(.40-.30)/(.250-.225)
      GO TO 50
    5 TETA=.40+(RHOT-.250)*(.50-.40)/(.275-.250)
      GO TO 50
```

```
 6  TETA=.50+(RHOT-.275)*(.60-.50)/(.300-.275)
    GO TO 50
 7  TETA=.60+(RHOT-.300)*(.70-.60)/(.320-.300)
    GO TO 50
 8  TETA=.70+(RHOT-.320)*(.80-.70)/(.345-.320)
    GO TO 50
 9  TETA=.80+(RHOT-.345)*(.90-.80)/(.360-.345)
    GO TO 50
10  TETA=.90+(RHOT-.360)*(1.0-.90)/(.385-.360)
    GO TO 50
11  TETA=1.0+(RHOT-.385)*(2.-1.)/(.480-.385)
    GO TO 50
12  TETA=2.0+(RHOT-.480)*(3.-2.)/(.550-.480)
    GO TO 50
13  TETA=3.0+(RHOT-.550)*(4.-3.)/(.600-.550)
    GO TO 50
14  TETA=4.0+(RHOT-.600)*(5.-4.)/(.655-.600)
    GO TO 50
15  TETA=5.0+(RHOT-.655)*(6.-5.)/(.685-.655)
    GO TO 50
16  TETA=6.0+(RHOT-.685)*(7.-6.)/(.715-.685)
    GO TO 50
17  TETA=7.0+(RHOT-.715)*(8.-7.)/(.730-.715)
    GO TO 50
18  TETA=8.0+(RHOT-.730)*(9.-8.)/(.755-.730)
    GO TO 50
19  TETA=9.0+(RHOT-.755)*(10.-9.)/(.800-.755)
    GO TO 50
20  TETA=10.0+(RHOT-.800)*(15.-10.)/(.830-.800)
    GO TO 50
21  TETA=15.0+(RHOT-.830)*(20.-15.)/(.890-.830)
    GO TO 50
22  TETA=20.0+(RHOT-.890)*(25.-20.)/(.918-.890)
    GO TO 50
23  TETA=25.0+(RHOT-.918)*(30.-25.)/(.935-.918)
    GO TO 50
24  TETA=30.0+(RHOT-.935)*(35.-30.)/(.945-.935)
    GO TO 50
25  TETA=35.0+(RHOT-.945)*(40.-35.)/(.960-.945)
    GO TO 50
26  TETA=40.0+(RHOT-.960)*(45.-40.)/(.967-.960)
    GO TO 50
27  TETA=45.0+(RHOT-.967)*(50.-45.)/(.974-.967)
    GO TO 50
28  TETA=50.0+(RHOT-.974)*(60.-50.)/(.981-.974)
    GO TO 50
29  TETA=60.0+(RHOT-.981)*(70.-60.)/(.988-.981)
    GO TO 50
```

```
30   TETA=70.0+(RHOT-.988)*(80.-70.)/(.994-.988)
     GO TO 50
31   TETA=80.0+(RHOT-.994)*(180.-80.)/(1.00-.994)
50   RETURN
     END
```

```
      SUBROUTINE SCATR2(RHOT,TETA)
C
C
C     THIS SUBROUTINE DETERMINES ANGLE 'THETA' FROM A GIVEN SCATTERING
C     FUNCTION (LOWER BOUND).
C
C
      IF(RHOT .LE. .000)GO TO 1
      IF(RHOT .LE. .010)GO TO 2
      IF(RHOT .LE. .014)GO TO 3
      IF(RHOT .LE. .018)GO TO 4
      IF(RHOT .LE. .022)GO TO 5
      IF(RHOT .LE. .026)GO TO 6
      IF(RHOT .LE. .031)GO TO 7
      IF(RHOT .LE. .034)GO TO 8
      IF(RHOT .LE. .040)GO TO 9
      IF(RHOT .LE. .060)GO TO 10
      IF(RHOT .LE. .090)GO TO 11
      IF(RHOT .LE. .120)GO TO 12
      IF(RHOT .LE. .150)GO TO 13
      IF(RHOT .LE. .175)GO TO 14
      IF(RHOT .LE. .200)GO TO 15
      IF(RHOT .LE. .220)GO TO 16
      IF(RHOT .LE. .250)GO TO 17
      IF(RHOT .LE. .280)GO TO 18
      IF(RHOT .LE. .380)GO TO 19
      IF(RHOT .LE. .530)GO TO 20
      IF(RHOT .LE. .580)GO TO 21
      IF(RHOT .LE. .635)GO TO 22
      IF(RHOT .LE. .665)GO TO 23
      IF(RHOT .LE. .700)GO TO 24
      IF(RHOT .LE. .740)GO TO 25
      IF(RHOT .LE. .750)GO TO 26
      IF(RHOT .LE. .770)GO TO 27
      IF(RHOT .LE. .780)GO TO 28
      IF(RHOT .LE. .800)GO TO 29
      IF(RHOT .LE. .833)GO TO 30
      IF(RHOT .LE. .860)GO TO 31
      IF(RHOT .LE. .885)GO TO 32
      IF(RHOT .LE. .950)GO TO 33
      IF(RHOT .LE. .970)GO TO 34
      IF(RHOT .LE. .980)GO TO 35
      IF(RHOT .LE. .990)GO TO 36
      IF(RHOT .LE. .995)GO TO 37
      IF(RHOT .LE. 1.000)GO TO 38
    1 TETA=0.2
      GO TO 50
    2 TETA=.20+(RHOT-.000)*(.30-.20)/(.010-.000)
```

```
      GO TO 50
    3 TETA=.30+(RHOT-.010)*(.40-.30)/(.014-.010)
      GO TO 50
    4 TETA=.40+(RHOT-.014)*(.50-.40)/(.018-.014)
      GO TO 50
    5 TETA=.50+(RHOT-.018)*(.60-.50)/(.022-.018)
      GO TO 50
    6 TETA=.60+(RHOT-.022)*(.70-.60)/(.026-.022)
      GO TO 50
    7 TETA=.70+(RHOT-.026)*(.80-.70)/(.031-.026)
      GO TO 50
    8 TETA=.80+(RHOT-.031)*(.90-.80)/(.034-.031)
      GO TO 50
    9 TETA=.90+(RHOT-.034)*(1.0-.90)/(.040-.034)
      GO TO 50
   10 TETA=1.0+(RHOT-.040)/(.060-.040)
      GO TO 50
   11 TETA=2.0+(RHOT-.060)/(.090-.060)
      GO TO 50
   12 TETA=3.0+(RHOT-.090)/(.120-.090)
      GO TO 50
   13 TETA=4.0+(RHOT-.120)/(.150-.120)
      GO TO 50
   14 TETA=5.0+(RHOT-.150)/(.175-.150)
      GO TO 50
   15 TETA=6.0+(RHOT-.175)/(.200-.175)
      GO TO 50
   16 TETA=7.0+(RHOT-.200)/(.220-.200)
      GO TO 50
   17 TETA=8.0+(RHOT-.220)/(.250-.220)
      GO TO 50
   18 TETA=9.0+(RHOT-.250)/(.280-.250)
      GO TO 50
   19 TETA=10.0+(RHOT-.280)*5./(.380-.280)
      GO TO 50
   20 TETA=15.0+(RHOT-.380)*5./(.530-.380)
      GO TO 50
   21 TETA=20.0+(RHOT-.530)*5./(.580-.530)
      GO TO 50
   22 TETA=25.0+(RHOT-.580)*5./(.635-.580)
      GO TO 50
   23 TETA=30.0+(RHOT-.635)*5./(.665-.635)
      GO TO 50
   24 TETA=35.0+(RHOT-.665)*5./(.700-.665)
      GO TO 50
   25 TETA=40.0+(RHOT-.700)*5./(.740-.700)
      GO TO 50
   26 TETA=45.0+(RHOT-.740)*5./(.750-.740)
```

```
      GO TO 50
27    TETA=50.0+(RHOT-.750)*5./(.770-.750)
      GO TO 50
28    TETA=55.0+(RHOT-.770)*5./(.780-.770)
      GO TO 50
29    TETA=60.0+(RHOT-.780)*10./(.800-.780)
      GO TO 50
30    TETA=70.0+(RHOT-.800)*10./(.833-.800)
      GO TO 50
31    TETA=80.0+(RHOT-.833)*10./(.860-.833)
      GO TO 50
32    TETA=90.0+(RHOT-.860)*10./(.885-.860)
      GO TO 50
33    TETA=100.+(RHOT-.885)*10./(.950-.885)
      GO TO 50
34    TETA=110.+(RHOT-.950)*10./(.970-.950)
      GO TO 50
35    TETA=120.+(RHOT-.970)*10./(.980-.970)
      GO TO 50
36    TETA=130.+(RHOT-.980)*20./(.990-.980)
      GO TO 50
37    TETA=150.+(RHOT-.990)*15./(.995-.990)
      GO TO 50
38    TETA=165.+(RHOT-.995)*15./(1.00-.995)
50    RETURN
      END
```

RADIATIVE TRANSFER COMPUTER PROGRAM

Code 2

```
C
C       A MONTECARLO PROGRAM WITH DOCUMENTATION.
C       TANK BOUNDARIES AND TOTAL REFLECTION ARE INCLUDED.
C
        COMMON/BLOCK1/XMAX,YMAX,ZMAX,X,Y,Z,T,GAMA,TETA,FI,PI,WT,S,IS,
C
        REAL*8 VALU
        COMMON/SCADAT/ANGL(50),VALU(50)
C
C       READ DATA FOR SCATTERING FUNCTION.
C
        DO 9 I=1,34
        READ(4,11)ANGL(I),VALU(I)
   11   FORMAT(F10.4,E15.5)
    9   CONTINUE
C
C       READ DATA FROM THE INPUT PHOTON DATA FILE.
C
        READ(5,25)MAXNPH,NMAX,IS
   25   FORMAT(3(2X,I12))
        READ(5,30)TETAI,FII
   30   FORMAT(2(5X,F8.3))
        READ(5,35)XMAX,YMAX,ZMAX
   35   FORMAT(3(5X,F8.3))
        READ(5,37)S
   37   FORMAT(F8.3)
        READ(5,24)A400,A500,A600
   24   FORMAT(3(9X,F8.3))
        WRITE(6,26)MAXNPH
   26   FORMAT('0','MAXIMUM NO. OF PHOTONS TO BE TRACED= ',I9)
        WRITE(6,27)NMAX
   27   FORMAT('0','MAXIMUM NO. OF EVENTS FOR EACH PHOTON= ',I12)
        WRITE(6,29)IS
   29   FORMAT('0','INITIAL SEED FOR RANDOM NO. GENERATOR= ',I12)
        WRITE(6,31)TETAI,FII
   31   FORMAT('0','INITIAL TETA IN DEGREES= ',F8.3,'   INITIAL FI IN DE-
       1GRS= ',F8.3)
        WRITE(6,30)XMAX,YMAX,ZMAX
   30   FORMAT('0','TANK DIMENSIONS IN METERS:','  XMAX=',F8.3,
       1'  YMAX=',F8.3,'  ZMAX=',F8.3)
        WRITE(6,38)S
   38   FORMAT('0','SCATTERING COEFFICIENT IN INVERSED METERS= ',F8.3)
        WRITE(6,23)A400,A500,A600
   23   FORMAT('0','ABSORPTION COEFFICIENTS AT 400, 500, 600 NM IN INV.
       1ERS:','  A400=',F8.3,'  A500=',F8.3,'  A600=',F8.3,//////)
        ANW=1.334
C
C       ANW IS THE REFRACTION INDEX OF WATER.
```

```
      PI=3.141592654
      DTRC=PI/180.
      XMAX=XMAX*S
      YMAX=YMAX*S
      ZMAX=ZMAX*S
      TETAI=TETAI*DTRC
      FII=FII*DTRC
      NPH=1
   10 IF(NPH .GT. MAXNPH)GO TO 2000
C
C     NPH IS  THE NO. OF PHOTONS AT A GIVEN TIME.
C     RECORD NO. OF PHOTONS TRACED AND TEST FOR END OF COMPUTATIONS.
C     INITIALIZE THE COORDINATES OF THE PHOTON ENTERING THE MEDIUM.
C
      TETA=TETAI
      FI=FII
      X=0.
      Y=0.
      Z=0.000001
C
C     DECIDE HOW FAR PHOTON TRAVELS BEFORE AN EVENT OCCURS.
C
      CALL RANDNO(IS,RHOD)
      T=-ALOG(RHOD)
      GAMA=T
C
C     T IS THE DISTANCE IN SCATTERING LENGTH UNITS PHOTON TRAVELS TO THE
C     EVENT PHOTON IS AT.
C
      X=X+T*SIN(TETA)*COS(FI)
      Y=Y+T*SIN(TETA)*SIN(FI)
      Z=Z+T*COS(TETA)
      GO TO 150
  100 NPH=NPH+1
C
C     EITHER ABSORPTION HAS OCCURED,OR PHOTON HAS COME OUT OF WATER. THE
C     FORE,START A NEW PHOTON.
C
      GO TO 10
  150 CONTINUE
      KMIN=2
      IF (Z) 400,500,500
  400 XINT=X-Z*TAN(TETA)*COS(FI)
      YINT=Y-Z*TAN(TETA)*SIN(FI)
      DINT=SQRT(XINT**2+YINT**2)
      DDINT=DINT/S
      IF(DDINT .GT. 0.20)GO TO 100
```

```
      IF (RNW*SIN(TETA) .GT. 1.0) GO TO 604
      TETAAR=ARSIN(RNW*SIN(TETA))
      IF(TETAAR .GT. 1.0)GO TO 100
      XINT=XINT/S
      YINT=YINT/S
      DINT=DDINT
      ACT=ABS(COS(TETA))
      TCUT=(ABS(ZR)-ABS(Z))/ACT
      GAMA=GAMA+TCUT
      GAMA=GAMA/S
      WRITE (6,410) DINT,TETAAR
  410 FORMAT(///,2X,'DISTANCE FROM AXIS= ',F8.5,5X,'POLAR ANGLE = ',F8.5)
      WRITE (6,420) FI,XINT,YINT
  420 FORMAT (' ','AZIMUTH ANGLE= ',F8.5,5X,'XINT= ',F8.5,5X,'YINT= ',F8.5)
      WRITE(6,109) GAMA
  109 FORMAT('0','GAMA = ',E12.3)
      WRITE (6,888)J
  888 FORMAT(' ','NO. OF EVENTS=',I8)
      WRITE(6,101)NPH
  101 FORMAT('0','NO. OF PHOTONS TRACED = ',I8)
C
C       CALCULATE PHOTON PROBABILITY WEIGHT.
C
      CALL PHPW(PI,GAMA,DINT,A400,A500,A600)
      WRITE(6,5999)IS
 5999 FORMAT('  RANDOM NUMBER USED  ',I12)
      GO TO 100
  604 KMIN=J+1
      ACT=ABS(COS(TETA))
      TCUT=(ABS(ZR)-ABS(Z))/ACT
      GAMA=GAMA+TCUT
      TETA=PI-TETA
      FI=FI+PI
      IF(FI .GE. 2. PI)FI=FI-2.*PI
      X=XINT
      Y=YINT
      Z=0.000001
      CALL RANDNO(IS,RHOD)
      T=-ALOG(RHOD)
      X=X+T*SIN(TETA) COS(FI)
      Y=Y+T*SIN(TETA) SIN(FI)
      Z=Z+T*COS(TETA)
  500 CALL PSIW(KMIN,NMAX,J,IRTCOD)
      IF(IRTCOD .EQ. 1)GO TO 100
      IF(IRTCOD .EQ. 2)GO TO 400
      GO TO 100
 2000 WRITE (6,5000) IS
 5000 FORMAT (' ','LAST RANDOM NUMBER USED=',I12)
```

```
STOP
END
```

```
      SUBROUTINE PSIJ(KMIN,KMAX,J,IPTCOD)

C     THIS SUBROUTINE WILL BE CALLED ONLY WHEN PHOTON IS STILL IN  'TH'
C     (WHEN Z>0).
C     IT DETERMINES THE COORDINATES OF THE END POINT IN THE 'IN-OUT-TH'
C     SYSTEM BY FIRST ROTATING THE SYSTEM USING ANGLES TETA AND FI.
C     IT GENERATES THE ROTATION MATRIX,WITH THE CONSTRAINT THAT YSTAR-
C     AXIS LIES IN A PLANE PARALLEL TO THE YZ-PLANE.
C     THE ROTATION MATRIX IS DESIGNATED AS AIJ(I=1,3,J=1,3).

      REAL*8 VALU
      COMMON/SCADAT/ANGL(50),VALU(50)
      COMMON/BLOCK1/XMAX,YMAX,ZMAX,X,Y,Z,T,GAMA,TETA,FI,PI,DTR,C,IS,IT
      IPTCOD=0
      DO 1290 J=KMIN,KMAX
      CT=COS(TETA)
      CF=COS(FI)
      CT2=CT*CT
      CF2=CF*CF
      ST=SIN(TETA)
      SF=SIN(FI)
      ST2=ST*ST
      SF2=SF*SF
      SS1=CT2+SF2*ST2
      SS=SQRT(SS1)
      SSO=1./SS
      A11=SQRT(1.-CF2*ST2)
      A12=-SF*CF*ST2*SSO
      A13=-CT*ST*CF*SSO
      A22=CT*SSO
      A23=-SF*ST*SSO
      A31=CF*ST
      A33=CT
      A32=SF*ST

C     ROTATION MATRIX HAS BEEN GENERATED.
C     SCATTERING HAS OCCURED.
C     CALL ANGELS FIP,TETAP TO DISTINGUISH FROM FI,TETA
C     FIP,TETAP ARE DETERMINED IN SYSTEM WITH Z-AXIS PARALLEL TO THE
C     INCIDENT DIRECTION.

      CALL RANDNO(IS,RHOF)
      FIP=2.*PI*RHOF
      CALL RANDNO(IS,RHOT)
      CALL SCATF3(RHOT,TETA)
      TETA=TETA*DTR
      TETAP=TETA
```

PRECEDING PAGE BLANK NOT FILMED

```
C       DETERMINE HOW FAR BEFORE AN EVENT OCCURS,IN THE ROTATED SYSTE .
C
        CALL RANDNO(IS,RHOD)
        T=-ALOG(RHOD)
C
C       CALCULATE COORDINATES OF END POINT IN THE ROTATED SYSTEM.
C
        XSTAR=T*SIN(TETAP)*COS(FIP)
        YSTAR=T*SIN(TETAP)*SIN(FIP)
        ZSTAR=T*COS(TETAP)
C
C       APPLY ROTATION MATRIX TO DETERMINE THE COORDINATES OF THE END
C       POINT IN A SYSTEM PARALLEL TO THE ORIGINAL ONE BUT DISPLACED.
C
        XR=A11*XSTAR+A31*ZSTAR
        YR=A12*XSTAR+A22*YSTAR+A32*ZSTAR
        ZR=A13*XSTAR+A23*YSTAR+A33*ZSTAR
C
C       CALCULATE TETA,AND FI IN THE PRESENT SYSTEM,WHICH IS PARALLEL TO
C       THE ORIGINAL ONE.
C
        FI=ATAN(ABS(YR)/ABS(XR))
        IF (XR .LT. 0.0)GO TO 133
        IF (YR)  333,333,633
333     FI=2.*PI-FI
        GO TO 533
633     FI=FI
        GO TO 533
133     IF (YR)  233,233,433
233     FI=FI+PI
        GO TO 533
433     FI=PI-FI
533     CONTINUE
        XR2=XR*XR
        YR2=YR*YR
        ZR2=ZR*ZR
        DT=XR2+YR2+ZR2
        SQDT=SQRT(DT)
        TETA=ARCOS(ZR/SQDT)
C
C       CALCULATE X,Y,Z OF THE END POINT OF THE PHOTON WITH RESPECT TO
C       THE ORIGINAL AXIS.
C
        X=X+XR
        Y=Y+YR
        X2=X*X
        Y2=Y*Y
        DIS2=X2+Y2
```


C-2

```
      XMAX2=XMAX*XMAX
      YMAX2=YMAX*YMAX
      DIMAX2=XMAX2+YMAX2
      IF(DIS2 .GE. DIMAX2)GO TO 100
      Z=Z+ZR
      IF (Z) 400,400,700
  700 IF(ZMAX-Z)702,702,701
  702 X=X-(Z-ZMAX)*TAN(TETA)*COS(FI)
      Y=Y-(Z-ZMAX)*TAN(TETA)*SIN(FI)
      ACT=ABS(COS(TETA))
      TT=T-(Z-ZMAX)/ACT
      Z=ZMAX
      CALL RANDNO(IS,RHOB)
      IF(RHOB-0.03)704,704,100
C
C     CHECK THREE PERCENT REFLECTION WITH UNIFORM ANGULAR PROBABILITY.
C
  704 CALL RANDNO(IS,RHOBT)
      TETA=0.5*PI*RHOBT+0.5*PI
      CALL RANDNO(IS,RHOBF)
      FI=2.*PI*RHOBF
      CALL RANDNO(IS,RHOD)
      T=-ALOG(RHOD)
      X=X+T*SIN(TETA)*COS(FI)
      Y=Y+T*SIN(TETA)*SIN(FI)
      Z=ZMAX+T*COS(TETA)
      T=T+TT
  701 GAMA=GAMA+T
 1290 CONTINUE
  100 IRTCOD=1
      GO TO 500
  400 IRTCOD=2
  500 RETURN
      END
```

```
      SUBROUTINE SCATR3(RHOT,TETA)
C
C
C     THIS SUBROUTINE DETERMINES ANGLE 'THETA' FROM A GIVEN (ALREADY
C     CALCULATED FROM MIE THEORY) SCATTERING FUNCTION.
C
C
      REAL*8 VALU
      COMMON/SCADAT/ANGL(50),VALU(50)
      DO 10 I=1,33
      IF(RHOT .GE. VALU(I)  .AND.  RHOT .LE. VALU(I+1))GO TO 20
   10 CONTINUE
   20 TETA=ANGL(I)+(ANGL(I+1)-ANGL(I))*(RHOT-VALU(I))/(VALU(I+1)-
     1VALU(I))
      RETURN
      END
```

```
      SUBROUTINE PHPW(PI,GAMA,DINT,A400,A500,A600)
C
C     THIS SUBROUTINE CALCULATES THE PHOTON PROBABILITY WEIGHT FOR GIVEN
C     WAVELENGTHS.
C
      TIR=0.0254
      TIR2=TIR*TIR
      CK=PI*TIR2
      R=0.15
      WRITE(6,860)R
  860 FORMAT('0','BEAM RADIUS IN METERS= ',F8.3)
      R2=R*R
      DINT2=DINT*DINT
      XINT=(R2-TIR2+DINT2)/(2.*DINT)
      XINT2=XINT*XINT
      YINT=SQRT(ABS(R2-XINT2))
      GC1=ATAN(YINT/XINT)
      GC2=ATAN(YINT/(DINT-XINT))
      GC3=PI-ATAN(YINT/(ABS(XINT-DINT)))
      AAA=GC1*R2+GC2*TIR2-DINT*YINT
      BBB=GC1*R2+GC3*TIR2-DINT*YINT
      BIR=R+TIR
      CIR=R-TIR
      IF(DINT .GE. 0.0  .AND.  DINT .LT. CIR)AREA=CK
      IF(DINT .GE. CIR  .AND.  DINT .LT. R)AREA=BBB
      IF(DINT .GE. R  .AND.  DINT .LT. BIR)AREA=AAA
      IF(DINT .GE. BIR)AREA=0.
      E500=EXP(-GAMA*A500)
C
C     PHOTON PROBABILITY WEIGHTS FOR 500 NM.
C
      PPW500=AREA*E500
      WRITE(6,861)PPW500
  861 FORMAT('0','PHOTON PROB. WT. FOR 500 NM= ',F10.6)
      RETURN
      END
```

```
      SUBROUTINE RANDNO(IX,RNUM)
C
C
C     THIS SUBROUTINE GENERATES UNIFORM RANDOM NUMBERS BETWEEN 0 AND 1.
C
C
      IY=IX*65539
      IF(IY) 5,6,6
    5 IY=IY+2147483647+1
    6 RNUM=IY
      RNUM=RNUM*.4656613E-9
      IX=IY
      RETURN
      END
```

FILE
04: SCATR3 DATA A

0.0	0.000000D+00
0.2000	0.253470D+00
0.4000	0.577508D+00
0.6000	0.678157D+00
0.8000	0.724562D+00
1.0000	0.751686D+00
1.2000	0.769829D+00
1.4000	0.782822D+00
1.6000	0.792812D+00
1.8000	0.800586D+00
2.0000	0.806825D+00
10.0000	0.930186D+00
18.0000	0.949330D+00
26.0000	0.963070D+00
34.0000	0.973075D+00
42.0000	0.980206D+00
50.0000	0.985054D+00
58.0000	0.988406D+00
66.0000	0.990774D+00
74.0000	0.992510D+00
82.0000	0.993834D+00
106.0000	0.996693D+00
114.0000	0.997377D+00
122.0000	0.997960D+00
130.0000	0.998464D+00
138.0000	0.998898D+00
146.0000	0.999265D+00
154.0000	0.999559D+00
162.0000	0.999780D+00
170.0000	0.999927D+00
178.2000	0.999997D+00
178.6000	0.999998D+00
179.2000	0.999999D+00
180.0000	0.100000D+01

```
FILE
  05:MFOTON    DATA      A

           12                100              53479
       9.700             0.
       1.217             1.217            2.600
12.000
       4.800             3.200            2.400
```

```
FILE: MFOTON   EXEC      A

GL TXTLIB FORTMOD1
FI 04 DISK SCATR3 DATA A1
FI 05 DISK MFOTON DATA A1
FI 06 PRINTER
LOAD MFOTON
START
```

APPENDIX B

MEASUREMENT OF SCATTERING FUNCTIONS

B.1 Scattering Functions

Scattering is an inherent property of the water which is useful as an optical parameter. Detailed knowledge of the scattering functions, in fact, can yield information about the particle size distribution and the composition.

The scattering function $\sigma(\theta)$ is defined by the relation

$$\sigma(\theta) = \frac{dJ(\theta)}{HdV} \quad (\text{meter}^{-1} \ \text{Str}^{-1}) \tag{1}$$

where $dJ(\theta)$ is an element of radiant intensity scattered in the direction θ from the incident beam by the volume element dV. H is the irradiance received by the sample volume.

B.2 Determination of Volume Scattering Function

Both the sample volume and the small solid angle, within which the radiant intensity is measured, are determined by the optical geometry of the instrument used. The instruments usually use a finite sample volume and collect the energy scattered at angle θ over some solid angle. The equation (1) is then written as

$$\sigma(\theta) = \frac{J(\theta)}{H.V}$$

$$= \frac{J(\theta)}{H.A.\ell}$$

$$= \frac{P(\theta)}{P(O).\Omega.\ell}$$

where

$P(0)$ = the total light flux entering the sample volume

$P(\theta)$ = the light flux entering a small solid angle Ω about the angle θ at which the measurement is made

Ω = the solid angle over which the measurement of $P(\theta)$ is made

ℓ = length of sample volume

A = the projected area of the sample volume V, as seen in the direction of $P(0)$

It is necessary to know either $P(\theta)$ or $P(0)$ in absolute terms. The scattering instruments allow $P(\theta)/P(0)$ to be computed. The length, ℓ, and the solid angle, Ω are determined by the geometry of the instruments.

When a scattering measurement is made using a finite volume of water, an unavoidable error is caused by absorption in the sample volume. If the instrument used had a sample path length that is small relative to the attenuation length of the water, this error is small and is less than the instrument errors. If the measurement is made using a path length that is not small relative to the attenuation length, the results have to be corrected. One such correction applied can be referred in Reference 10.

B.3 Scatterance Meters

The scattering quantities have exact mathematical definitions which dictate the design of the meters to be used. In principle, measurements of scatterance involve irradiation of sample volume by

a beam of light and recording of the light scattered by the volume through various angles.

Several types of scatterance meters have been developed. Typical types are: Fixed angle, Free angle, and Integrating meters. One ground of subdivision is to distinguish in-vitro and in-situ meters.

It is not our intent to describe in detail various scattering meters used by researchers in this area, however, a brief discussion may be warranted regarding the differences between general type and small angle scattering meters. Typical scattering meters used by Scripps Institution of Oceanography[10] are briefed below.

B.3.1 General Angle Scattering Meter

Its purpose is to determine volume scattering function between the limits of $10^{\circ} \leq \theta \leq 170^{\circ}$. It has a projector which rotates about the sample volume from $\theta = 0^{\circ}$ through $0 = 180^{\circ}$. The measurement at $\theta = 0^{\circ}$ indicates total power in the projected beam, while the measurement at 180° records the background ambient light level. The rest of the readings ($10^{\circ} \leq \theta \leq 170^{\circ}$) measure scattered light.

The output of this instrument contains analog voltage signals representing depth, scan angle position and the photometer signal. A continuous trace of photometer signal versus depth at any fixed angle between 10 and 170 degrees and a continuous trace of photometer signal versus scattering angle at a fixed depth are the two methods of data collection using general angle scattering meters.

B.3.2 Small Angle Scattering Meter

Small angle scattering meter (with which the results used in Reference 1 were measured) is essentially that which was modified and used by Morrison.[3] Main problems in low angle scattering meters are; scattering within the instrument and limitations in defining the limits of solid angle of the measurements.

In the low angle scattering meters used in Reference 10, and attempt is made to reduce the instrument's over internal scattering, it is still significant relative to the small angle forward scattering of clear waters.

The instrument has a projector which having a small point source of light, produces a beam of highly collimated light. After traversing the sample path, the light enters a long focal length lens in the receiver and an image of the point source is formed at its focal length. The light which traverses the water and is neither absorbed nor scattered falls within this small image. Light which is scattered arrives at the image plane displaced from the axis at a distance proportional to the angle through which it has been scattered and is the focal length of the receiver lens. The scattered light is allowed to pass through four field stops before reaching the detector. The first field stop is a small hole and the other three field stops are annulus. The inner and outer radii of the annulus determine the angular interval over which the scattered

light is accepted. The solid angle, Ω, in equation (2) is limited by the angles θ_1, θ_2 imposed by the annulus field stops and is calculated, from $\Omega = 2\pi\ (\theta_2^2 - \theta_1^2)$, where θ_1, and θ_2 are in radians.

The value computed for the volume scattering function $\sigma(\theta)$ is an average value for $\sigma(\theta)$ between the angular limits, θ_1, and θ_2, of the solid angle.

APPENDIX C

LISTINGS FOR POLYMIE AND DBMIE ROUTINES USED TO CALCULATE THE VOLUME SCATTERING FUNCTIONS

MAIN

```
C      MAIN PROG POLYMIE(VECTOR)
C      THE FOLLOWING DOUBLE PRECISION INPUTS ARE REQUIRED:
C      RFR=REAL PART OF REFRACTIVE INDEX
C      RFI=IMAGINARY PART OF REFRACTIVE INDEX
C      RADU=UPPERBOUND ON RADIUS(MICRONS)
C      WAVE=WAVELENGTH IN MICRONS
C      A(I)=PARAMETERS FOR DISTRIBUTION ONE
C      B(I)=PARAMETERS FOR DISTIBUTION TWO
C      THETD(J)=VECTOR OF ANGLES FROM 0-90 (COMPLIMENTS ARE ALSO CALC)
C      OTHER INPUTS ARE:
C      JX=NUMBER OF ANGLES FROM 0-90
C      NRAD=NUMBER OF RADII BETWEEN 0-RADU
C      NPARA=NUMBER OF PARAMETERS IN DISTRIBUTION ONE
C      NPARA2=NUMBER OF PARAMETERS IN DISTRIBUTION TWO
C      TWO=LOGICAL VARIABLE TO ENABLE THE USE OF TWO DISTRIBUTIONS
C
C
C      TWO FUNCTION SUBPROGRAMS DIST(RAD,A) AND DIST2(RAD,B) ARE REQUIRED
C      IN ADDITION TO PDBMIE SUBROUTINE
C
C
C      TWO DATA SETS (6 AND 8) ARE USED FOR OUTPUT; NORMALLY 6=PRINTER
C      AND 8=TAPE
C
C
C
C
   10 FORMAT(3D15.5)
   11 FORMAT(2D15.5)
   12 FORMAT(D15.5)
   13 FORMAT(D15.5,I5)
   14 FORMAT(2I5)
   15 FORMAT(L5)
   16 FORMAT(I5)
   17 FORMAT(D15.5)
   20 FORMAT(1H1)
   25 FORMAT(//T10,'ELEMENTS OF THE TRANSFORMATION MATRIX FOR A SPHERE
     1WITH SIZE PARAMETER = ',F15.5)
   30 FORMAT(//T10,'REFRACTIVE INDEX. REAL = ',D15.5,T60,'IMAGINARY',D15
     1.5,//)
   35 FORMAT(T3,'ANGLE',T17,'SIGMA1',T31,'SIGMA2',T46,'SIGMA3',T61,'SIGM
     1A4',T76,'INTENSITY',T91,'POLARIZATION'//)
   40 FORMAT(F10.4,5E15.6,F15.4)
   45 FORMAT(//T10,' EFFICIENCY FACTOR FOR EXTINCTION',E15.6)
   50 FORMAT(//T10,' EFFICIENCY FACTOR FOR SCATTERING',E15.6)
   55 FORMAT(//T10,' EFFICIENCY FACTOR FOR ABSORPTION',E15.6)
   60 FORMAT(//T10,' ASYMMETRY FACTOR',E15.6//)
   70 FORMAT(//T10,' TOTAL TIME FOR THIS CASE IN SECONDS= ',F15.3//)
```

```
  2 FORMAT(//T10,'PROBABILITY FOR THIS SIZE PARAMETER = ',D15.5,//)
  3 FORMAT(//T10,'NORMALIZATION FACTOR FOR THIS SET OF SIZE PARA=',
   1D15.5,//)
    REAL*8 RFR,RFI,X,QEXT,QSCAT,QABS,THETD(100),PQEXT,PQSCAT,PQABS
 80 FORMAT(//T10,'SCATTERING CROSS SECTION',E15.6)
    REAL*8 ELTRIX(4,100,2),ALAM,CON,CTBRQS,AVCSTH,PELTMX(4,100,2)
    REAL*8 PAVCTH,THE(100),PBSCAT
    REAL*4 AIN(100,2),POLR(100,2)
    REAL*4 PAIN(100,2),PPOLR(100,2)
    REAL 4 PAI(100,2),PPOL(100,2)
    REAL*8 PROB2,PNORM2
    REAL 8 PQEX,PQSCA,PQAB,PBSCA,PAVCT,PELTM(4,100,2)
    REAL 8 RADU,DRAD,WAVE,GAMMA,A(20),PROB,B(20)
    LOGICAL WRN,TWO
    WRN=.FALSE.
    CON=3.1415926535897932D+0
    INTEGER NPARA,NPARA2
 90 READ (5,10) RFR,RFI,WAVE
    READ (5,14) JX,NPARA
    READ (5,12) (THETD(I),I=1,JX)
    READ (5,13) RADU,NRAD
  1 FORMAT (D15.5)
    DO 5 I=1,NPARA
    READ (5,1) A(I)
  5 CONTINUE
    READ(5,15) TWO
    DO 95 I=1,JX
 95 THE(I)=THETD(I)
    IF (TWO) GO TO 61
    GO TO 62
 61 READ(5,16) NPARA2
    DO 62 I=1,NPARA2
    READ(5,17) B(I)
 62 CONTINUE
    PQEXT=0.0D0
    PQEX=0.0D0
    PQSCA=0.0D0
    PQAB=0.0D0
    PBSCA=0.0D0
    PAVCT=0.0D0
    PQSCAT=0.0D0
    PQABS=0.0D0
    PBSCAT=0.0D0
    PAVCTH=0.0D0
    DRAD=RADU/NRAD
    DO 1000 J=1,JX
    DO 1000 K=1,2
    DO 999 I=1,4
```

```
      PELTMX(I,J,K)=0.0D0
      PELTM(I,J,K)=0.0D0
  999 CONTINUE
      PAIN(J,K)=0.0D0
      PAI(J,K)=0.0D0
      PPOL(J,K)=0.0D0
      PPOLR(J,K)=0.0D0
 1000 CONTINUE
      RAD=0.0
      PNORM2=0.0D0
      IF (TWO) GO TO 91
      PNORM2=1.0D0
   91 CONTINUE
      PNORM=0.0D0
      TIME1=0.0
      DO 3000 L=1,NRAD
      RAD=RAD+DRAD
      DO 100 J=1,JX
  100 THETD(J)=THE(J)
      X=2.0D0 CON*RAD/WAVE
      PROB=DIST(RAD,A)
      IF (TWO) GO TO 63
      PROB2=0.0D0
      GO TO 64
   63 PROB2=DIST2(RAD,B)
   64 CALL SETCLK
      CALL PDBMIE ( X,RFR,RFI,THETD,JX,QEXT,QSCAT,CTBRQS,ELTRMX,WRN)
      CALL READCL(TIME)
      IF (WRN) GO TO 1001
      PNORM=PNORM+PROB
      PNORM2=PNORM2+PROB2
      TIME1=TIME1+TIME
      QABS=QEXT-QSCAT
      AVCSTH=CTBRQS/QSCAT
      DO 150 K=1,2
      DO 150 J=1,JX
      AIN(J,K)= ELTRMX(1,J,K)+ELTRMX(2,J,K)
      POLR(J,K)= (ELTRMX(2,J,K)-ELTRMX(1,J,K))/AIN(J,K)
      AIN(J,K)= .5*AIN(J,K)
      PAIN(J,K)=AIN(J,K)*PROB+PAIN(J,K)
      PAI(J,K)=AIN(J,K)*PROB2+PAI(J,K)
      PPOL(J,K)=POLR(J,K)*PROB2+PPOL(J,K)
      PPOLR(J,K)=PPOLR(J,K)+POLR(J,K)*PROB
  150 CONTINUE
      DO 2000 I=1,4
      DO 2000 J=1,JX
      DO 2000 K=1,2
      PELTMX(I,J,K)=PELTMX(I,J,K)+ELTRMX(I,J,K)*PROB
```

```
      PELTM(I,J,K)=PELTM(I,J,K)+ELTRMX(I,J,K)*PROB2
 2000 CONTINUE
      WRITE(6,20)
      WRITE(6,25) X
      WRITE(6,30) RFR,RFI
      WRITE(6,35)
      WRITE(6,40) ((THETD(J),(ELTRMX(I,J,1),I=1,4),AIN(J,1),POLR(J,1)),
     1J=1,JX)
C     WRITE(8,40) ((THETD(J),(ELTRMX(I,J,1),I=1,4),AIN(J,1),POLR(J,1)),
C    1J=1,JX)
      DO 200 J=1,JX
      THETD(J)= 180.0D0-THETD(J)
  200 CONTINUE
      JMX=JX-1
      DO 210 J=1,JMX
      JJ=JX-J
      WRITE(6,40)(THETD(JJ),(ELTRMX(I,JJ,2),I=1,4),AIN(JJ,2),POLR(JJ,2))
C     WRITE(8,40)(THETD(JJ),(ELTRMX(I,JJ,2),I=1,4),AIN(JJ,2),POLR(JJ,2))
  210 CONTINUE
      WRITE(6,45) QEXT
      WRITE(6,50) QSCAT
      WRITE(6,55) QABS
      WRITE(6,60) AVCSTH
      WRITE(6,2) PROB
      WRITE(6,2) PROB2
      WRITE(6,20)
      WRITE(6,70) TIME
      PQSCAT=PQSCAT+QSCAT*PROB
      PQSCA=PQSCA+QSCAT*PROB2
      PQEX=PQEX+QEXT*PROB2
      PQAB=PQAB+QABS*PROB2
      PBSCA=PBSCA+QSCAT*(RAD**2)*PROB2
      PAVCT=PAVCT+AVCSTH*PROB2
      PQEXT=PQEXT+QEXT*PROB
      PQABS=PQABS+QABS*PROB
      PBSCAT=PBSCAT+QSCAT*(RAD**2)*PROB
      PAVCTH=PAVCTH+AVCSTH*PROB
 1001 WRN= .FALSE.
 3000 CONTINUE
      DO 4000 J=1,JX
      DO 4000 K=1,2
      DO 4001 I=1,4
      PELTMX(I,J,K)=PELTMX(I,J,K)/PNORM
      PELTM(I,J,K)=PELTM(I,J,K)/PNORM2
 4001 CONTINUE
      PAIN(J,K)=PAIN(J,K)/PNORM
      PAI(J,K)=PAI(J,K)/PNORM2
      PPOL(J,K)=PPOL(J,K)/PNORM2
```

```
      PPOLR(J,K)=PPOLR(J,K)/PNORM
 4000 CONTINUE
C     END FILE 8
      PQSCAT=PQSCAT/PNORM
      PQEXT=PQEXT/PNORM
      PQABS=PQABS/PNORM
      PBSCAT=PBSCAT*CON/PNORM
      PAVCTH=PAVCTH/PNORM
      PQSCA=PQSCA/PNORM2
      PQEX=PQEX/PNORM2
      PQAB=PQAB/PNORM2
      PBSCA=PBSCA*CON/PNORM2
      PAVCT=PAVCT/PNORM2
      DO 6000 J=1,JX
6000  THETD(J)=THE(J)
      WRITE(6,20)
   65 FORMAT(//T10,'ELEMENTS OF TRANFORMATION MATRIX FOR POLYDISPERSION'
     1,//)
      WRITE(6,65)
      WRITE(6,30) RFR,RFI
      WRITE(6,35)
      WRITE(6,40) ((THETD(J),(PELTMX(I,J,1),I=1,4),PAIN(J,1),PPOLR(J,1)
     1),J=1,JX)
C     WRITE(8,40) ((THETD(J),(PELTMX(I,J,1),I=1,4),PAIN(J,1),PPOLR(J,1)
C    1),J=1,JX)
      DO 5000 J=1,JX
      THETD(J)=180.000-THETD(J)
 5000 CONTINUE
      JMX=JX-1
      DO 5001 J=1,JMX
      JJ=JX-J
      WRITE(6,40) (THETD(JJ),(PELTMX(I,JJ,2),I=1,4),PAIN(JJ,2),PPOLR
     1(JJ,2))
C     WRITE(8,40) (THETD(JJ),(PELTMX(I,JJ,2),I=1,4),PAIN(JJ,2),PPOLR
C    1(JJ,2))
 5001 CONTINUE
C     END FILE 8
      WRITE(6,45) PQEXT
      WRITE(6,50) PQSCAT
      WRITE(6,55) PQABS
      WRITE(6,80) PBSCAT
      WRITE(6,60) PAVCTH
      WRITE(6,3) PNORM
      WRITE(6,70) TIME1
      WRITE(6,20)
      DO 5010 J=1,JX
5010  THETD(J)=THE(J)
      IF (TWO) GOTO 5002
```

```
      GO TO 5003
5002  WRITE(6,20)
      WRITE(6,65)
      WRITE(6,30) RFR,RFI
      WRITE(6,35)
      WRITE(6,40) ((THETD(J),(PELTM(I,J,1),I=1,4),PAI(J,1),PPOL(J,1)
     1),J=1,JX)
C     WRITE(8,40) ((THETD(J),(PELTM(I,J,1),I=1,4),PAI(J,1),PPOL(J,1)
C    1),J=1,JX)
      DO 5004 J=1,JX
      THETD(J)=180.0D0-THETD(J)
 5004 CONTINUE
      JMX=JX-1
      DO 5005 J=1,JMX
      JJ=JX-J
      WRITE(6,40) (THETD(JJ),(PELTM(I,JJ,2),I=1,4),PAI(JJ,2),PPOL
     1(JJ,2))
C     WRITE(8,40) (THETD(JJ),(PELTM(I,JJ,2),I=1,4),PAI(JJ,2),PPOL
C    1(JJ,2))
 5005 CONTINUE
C     END FILE 8
      WRITE(6,45) PQEX
      WRITE(6,50) PQSCA
      WRITE(6,55) PQAB
      WRITE(6,80) PBSCA
      WRITE(6,60) PAVCT
      WRITE(6,3)  PNORM2
      WRITE(6,70) TIME1
      WRITE(6,20)
 5003 STOP
      END
```

```
                    PDBMIE

      SUBROUTINE PDBMIE (X,RFR,RFI,THETD,JX,QEXT,QSCAT,CTBRQS,ELTRMX,WRN
     1)
C     RADIATION SCATTERED BY A SPHERE.  THIS SUBROUTINE CARRIES OUT ALL
C     SUBROUTINE FOR COMPUTING THE PARAMETERS OF THE ELECTROMAGNETIC
C     COMPUTATIONS IN SINGLE PRECISION ARITHMETIC.
C     THIS SUBROUTINE COMPUTES THE CAPITAL A FUNCTION BY MAKING USE OF
C     DOWNWARD RECORRENCE RELATIONSHIP.
C     X ) SIZE PARAMETER OF THE SPHERE,( 2 * PI * RADIUS OF THE SPHERE)/
C     WAVELENGTH OF THE INCIDENT RADIATION).
C     RFI  REFRACTIVE INDEX OF THE MATERIAL OF THE SPHERE.  COMPLEX
C     QUANTITY..FORMO (RFR - I * RFI )
C     THETD(J)) ANGLE IN DEGREES BETWEEN THE DIRECTIONS OF THE INCIDENT
C     AND THE SCATTERED RADIATION.  THETD(J) IS - OR  = 90.0.
C     IF THETD(J) SHOULD HAPPEN TO BE GREATER THAN 90.0, ENTER WITH
C     SUPPLEMENTARY VALUEO SEE COMMENTS BELOW ON ELTRMX..
C     JXO TOTAL NUMBER OF THETD FOR WHICH THE COMPUTATION ARE REQUIRDE.
C     JX SHOULD NOT EXCEED 200 UNLESS THE DIMENSIONS STATEMENTS
C     ARE APPROPRIATELY MODIFIED.
C     MAIN PROGRAM SHOULD ALSO HAVE REAL THETD(200),ELTRMX(4,200,2).
C     DEFINITIONS FOR THE FOLLOWING SYMBOLS CAN BE FOUND IN ' LIGHT
C     SCATTERING BY SMALL PARTICLES, H. C. VAN DE HULST, JOHN WILEY +
C     SONS, INC., NEW YORK, 1957 '.
C     QEXT82 EFFIECIENCY FACTOR FOR EXTINCTION, VAN DE HULST, P.14 + 127
C     QSCAT82 FFFIECIENCY FACTOR FOR SCATTERING,VAN DE HULST,P.14 + 127.
C     CTBRQS) AVERAGE(COSINE THETA) * QSCAT,VAN DE HULST, P. 128.
C     ELTRMX(I,J,K)O ELEMENTS OF THE TRANSFORMATION MATRIX F,VAN DE HUL
C     ST,P.34,45 + 125. I = 1) ELEMENT M SUB 2..I = 2)ELEMENT M SUB 1..
C     I = 3O ELEMENT S SUB 21.. I = 40 ELEMENT D SUB 21...
C     ELTRMX(I,J,1) REPRESENTS THE ITH ELEMENT OF THE MATRIX FOR
C     THE ANGLE THETD(J).. ELTRMX(I,J,2) REPRESENTS THE ITH ELEMENT
C     OF THE MATRIX FOR THE ANGLE 180.0 - THETD(J) ..
5     FORMAT(1)X' THE VALUE OF THE SCATTERING ANGLE IS GREATER THAN 9).)
     $ DEGREES.  IT IS ',E15.4)
6     FORMAT(//1)X' PLEASE READ THE COMMENTS'//)
7     FORMAT(//1OX' THE VALUE OF THE ARGUMENT JX IS GREATER THE 100')
8     FORMAT(//1)X'THE UPPER LIMIT FOR ACAP IS NOT ENOUGH.  SUGGEST GET
     1DETAILED OUTPUT AND MODIFY SUBROUTINE'//)
      REAL*8 X,RX,RFR,RFI,QEXT,QSCAT,T(5),TA(4),TB(2),TC(2),TD(2),TE(2),
     2  CTBRQS,ELTRMX(4,100,2),PI(3,100),TAU(3,100),
     3  CSTHT(100),SI2THT(100),THETD(100)
      COMPLEX*16 RF,RRF,RRFX,WM1,FNA,FNB,TC1,TC2,WFN(2),ACAP(8000),
     2  FNAP,FNBP
      LOGICAL WRN
9     FORMAT(//T10,'WARNING,ACCURACY NOT ACHIEVED'//)
C     TA(1)O REAL PART OF WFN(1).. TA(2)O IMAGINARY PART OF WFN(1)..
C     TA(3)O REAL PART OF WFN(2).. TA(4)O IMAGINARY PART OF WFN(2)..
C     TB(1)O REAL PART OF FNA...TB(2)O IMAGINARY PART OF FNA...
C     TC(1)O REAL PART OF FNB...TC(2)O IMAGINARY PART OF FNB...
```

```
C       TD(1)0 REAL PART OF FNAP.. TD(2) IMAGINARY PART OF FNAP...
C       TE(1)0 REAL PART OF FNBP... TE(2)0 IMAGINARY PART OF FNBP...
C       FNAP + FNBP ARE THE PRECEDING VALUES OF FNA + FNB RESPECTIVELY.
        EQUIVALENCE (WFN(1), TA(1)), (FNA, TB(1)), (FNB, TC(1))
        EQUIVALENCE (FNAP, TD(1)), (FNBP, TE(1))
        IF ( JX .LT. 101 ) GO TO 20
        WRITE (6, 7)
        WRITE(6, 6)
        STOP 1
   20   RF=DCMPLX(RFR,-RFI)
        RRF = 1.0D0/RF
        RX = 1.0D0/X
        RRFX = RRF * RX
        T(1)=(X** 2) (RFR**2+RFI**2)
        T(1)=DSQRT(T(1))
        NMX1 = 1.10D0 * T(1)
        IF (NMX1 .LT. 7999)  GO TO 21
        WRITE(6, 8)
        STOP 2
21      NMX2 = T(1)
        IF (NMX1 .GT. 150) GO TO 22
        NMX1 = 150
        NMX2 = 135
   22   ACAP(NMX1 + 1 ) = ( 0.0D0, 0.0D0 )
        DO 23 N = 1, NMX1
        NN = NMX1 - N + 1
        ACAP(NN) = (NN+1) * RRFX - 1.0D0/((NN+1)*RRFX + ACAP(NN+1))
23      CONTINUE
        DO 30 J = 1, JX
        IF ( THETD(J) .LT. 0.0D0 ) THETD(J) = DABS(THETD(J))
        IF ( THETD(J) .GT. 0.0D0 ) GO TO 24
        CSTHT(J) = 1.0D0
        SI2THT(J) = 0.0D0
        GO TO 30
   24   IF ( THETD(J) .GE. 90.0D0 ) GO TO 25
        T(1) = ( 3.1415926535897932D+0 * THETD(J))/180.D0
        CSTHT(J) = DCOS(T(1))
        SI2THT(J) = 1.0D0 - CSTHT(J)**2
        GO TO 30
   25   IF ( THETD(J) .GT. 90.0D0 ) GO TO 28
        CSTHT(J) = 0.0D0
        SI2THT(J) = 1.0D0
        GO TO 30
28      WRITE (6, 5) THETD(J)
        WRITE(6,6)
        STOP 3
30      CONTINUE
        DO 35 J = 1, JX
```

```
      PI(1,J) = 0.0D0
      PI(2,J) = 1.0D0
      TAU(1,J) = 0.0D0
  300 TAU (2, J) = CSTHT(J)
   35 CONTINUE
      T(1) = DCOS(X)
      T(2) = DSIN(X)
      WM1=DCMPLX(T(1),-T(2))
      WFN(1)=DCMPLX(T(2),T(1))
      WFN(2) = RX * WFN(1) - WM1
      TC1 = ACAP(1) * RRF + RX
      TC2 = ACAP(1) * RF + RX
      FNA = (TC1 * TA(3) - TA(1)) / (TC1 * WFN(2) - WFN(1))
      FNB = (TC2 * TA(3) - TA(1)) / (TC2 * WFN(2) - WFN(1))
      FNAP = FNA
      FNBP = FNB
      T(1) = 1.50D0
      TB(1) = T(1) * TB(1)
      TB(2) = T(1) * TB(2)
      TC(1) = T(1) * TC(1)
      TC(2) = T(1) * TC(2)
      DO 60 J =1,JX
      ELTRMX(1,J,1) = TB(1)   PI(2,J) + TC(1) * TAU(2,J)
      ELTRMX(2,J,1) = TB(2) * PI(2,J) +TC(2) * TAU(2,J)
      ELTRMX(3,J,1) = TC(1) *PI(2,J) +  TB(1) * TAU(2,J)
      ELTRMX(4,J,1) = TC(2) * PI(2,J) + TB(2) * TAU(2,J)
      ELTRMX(1,J,2) = TB(1) * PI(2,J) - TC(1) * TAU(2,J)
      ELTRMX(2,J,2) = TB(2) * PI(2,J) - TC(2) * TAU(2,J)
      ELTRMX(3,J,2) = TC(1) * PI(2,J) -TB(1) * TAU(2,J)
      ELTRMX(4,J,2) = TC(2) * PI(2,J) - TB(2) * TAU(2,J)
   60 CONTINUE
      QEXT = 2.0D0 * ( TB(1) + TC(1))
      QSCAT =(TB(1)**2 + TB(2)**2 + TC(1)**2 + TC(2)**2)/0.75D0
      CTBRQS = 0.0D0
      N = 2
   65 T(1) = 2 * N - 1
      T(2) = N - 1
      T(3) = 2 * N + 1
      DO70J=1,JX
      PI(3,J)=(T(1)*PI(2,J)*CSTHT(J)-N*PI(1,J))/T(2)
      TAU(3,J)=CSTHT(J)*(PI(3,J)-PI(1,J))-T(1)*SI2THT(J)*PI(2,J)+TAU(1,J
     1)
   70 CONTINUE
      WM1 = WFN(1)
      WFN(1) = WFN(2)
      WFN(2) = T(1) * RX * WFN(1) - WM1
      TC1 = ACAP(N) * RRF + N * RX
      TC2 = ACAP(N) * RF + N * RX
```

```
      FNA = (TC1 *TA(3) - TA(1)) / (TC1 * WFN(2) - WFN(1))
      FNB = (TC2 * TA(3) - TA(1)) / (TC2 * WFN(2) - WFN(1))
      T(5) = N
      T(4) = T(1) / (T(5) * T(2))
      T(2) = (T(2)*(T(5) + 1.0D0))/T(5)
      CTBRQS = CTBRQS + T(2) * (TD(1) * TB(1) + TD(2) * TB(2) + TE(1) *
     $TC(1) + TE(2) * TC(2)) + T(4) * (TD(1) * TE(1) + TD(2)   TE(2))
      QEXT = QEXT + T(3) * (TB(1) + TC(1))
      T(4) = TB(1)** 2 + TB(2)**2 + TC(1)**2 + TC(2)**2
      QSCAT = QSCAT + T(3) * T(4)
      T(2) = N * (N + 1)
      T(1) = T(3) / T(2)
      K = (N / 2) * 2
      DO 80 J = 1, JX
      ELTRMX(1,J,1)=ELTRMX(1,J,1)+T(1)*(TB(1)*PI(3,J)+TC(1)*TAU(3,J))
      ELTRMX(2,J,1)=ELTRMX(2,J,1)+T(1)*(TB(2)*PI(3,J)+TC(2)*TAU(3,J))
      ELTRMX(3,J,1)=ELTRMX(3,J,1)+T(1)*(TC(1)*PI(3,J)+TB(1)*TAU(3,J))
      ELTRMX(4,J,1)=ELTRMX(4,J,1)+T(1)*(TC(2)*PI(3,J)+TB(2)*TAU(3,J))
      IF(K.EQ.N) GO TO 75
      ELTRMX(1,J,2)=ELTRMX(1,J,2)+T(1)*(TB(1)*PI(3,J)-TC(1)*TAU(3,J))
      ELTRMX(2,J,2)=ELTRMX(2,J,2)+T(1)*(TB(2)*PI(3,J)-TC(2)*TAU(3,J))
      ELTRMX(3,J,2)=ELTRMX(3,J,2)+T(1)*(TC(1)*PI(3,J)-TB(1) TAU(3,J))
      ELTRMX(4,J,2)=ELTRMX(4,J,2)+T(1)*(TC(2)*PI(3,J)-TB(2) TAU(3,J))
      GOTO80
   75 ELTRMX(1,J,2)=ELTRMX(1,J,2)+T(1)*(-TB(1)*PI(3,J)+TC(1)*TAU(3,J))
      ELTRMX(2,J,2)=ELTRMX(2,J,2)+T(1)*(-TB(2)*PI(3,J)+TC(2)*TAU(3,J))
      ELTRMX(3,J,2)=ELTRMX(3,J,2)+T(1)*(-TC(1)*PI(3,J)+TB(1)*TAU(3,J))
      ELTRMX(4,J,2)=ELTRMX(4,J,2)+T(1)*(-TC(2)*PI(3,J)+TB(2)*TAU(3,J))
   80 CONTINUE
      IF( T(4) .LT. 1.0D-14 ) GO TO 100
      N = N + 1
      DO 90 J = 1, JX
      PI(1, J) = PI(2, J)
      PI(2, J) = PI(3, J)
      TAU(1, J) = TAU(2, J)
      TAU(2, J) = TAU(3, J)
   90 CONTINUE
      FNAP = FNA
      FNBP = FNB
      IF (N .LE. NMX2) GO TO 65
      WRITE(6, 9)
      WRN = .TRUE.
      RETURN
  100 DO120J=1,JX
      DO120K=1,2
      DO115I=1,4
      T(I)=ELTRMX(I,J,K)
  115 CONTINUE
```

```
      ELTRMX(2,J,K) = T(1)**2 + T(2)**2
      ELTRMX(1,J,K) = T(3)**2 + T(4)**2
      ELTRMX(3,J,K) = T(1)*T(3) + T(2)*T(4)
      ELTRMX(4,J,K) = T(2)*T(3) - T(4)*T(1)
120   CONTINUE
      T(1) = 2.0D0 * RX**2
      QEXT = QEXT * T(1)
      QSCAT = QSCAT * T(1)
      CTBRQS = 2.0D0 * CTBRQS * T(1)
      RETURN
      END
```

DIST

```
FUNCTION DIST(RAD,A)
REAL*8 A(20),RAD
REAL*8 DIST,B,C
B=-A(3)
C=RAD**A(4)
C=B*C
DIST=A(1)*(RAD**A(2))*DEXP(C)
RETURN
END
```

DIST2

```
FUNCTION DIST2(RAD,B)
REAL*8 B(20),RAD
REAL*8 DIST2,A
A=-(B(2)+1)
DIST2=B(1)*B(2)*(RAD**A)
RETURN
END
```

APPENDIX D

PROGRAM LISTING FOR CURFIT ROUTINE USED TO FIT THE THEORETICAL SIZE DISTRIBUTIONS TO THE EMPERICAL DATA

MAIN

```
C SUBROUTINE CURFIT
C
C MAKES A LEAST SQUARES FIT TO A NON-LINEAR FUNCTION
C
C DESCRIPTION OF PARAMETERS
C  X       -ARRAY OF IND. VARIABLE DATA POINTS
C  Y       -ARRAY OF DEP. VARIABLE DATA POINTS
C  SIGMAY  -ARRAY OF STANDARD DEVIATIONS FOR Y DATA POINTS
C  NPTS    -NUMBER OF DATA POINTS
C  NTERMS  -NUMBER OF PARAMETERS
C  MODE    -DETERMINES WEIGHTING FOR LEAST SQUARES FIT
C              +1(INSTRUMENTAL)W(I)=1./SIGMAY(I)**2
C               0(NO WEIGHTING)W(I)=1.
C              -1(STATISTICAL) W(I)=1./Y(I)
C  A       -ARRAY OF PARAMETERS
C  DELTAA  -ARRAY OF INCREMENTS FOR PARAMETERS
C  FLAMDA  -PROPORTION OF GRADIENT SEARCH INCLUDED
C  YFIT    -ARRAY OF CALCULATED VALUES OF Y
C  CHISQR  -REDUCED CHI SQUARE FOR FIT
C
C SUBROUTINES AND FUNCTION SUBPROGRAMS REQUIRED
C   FUNCTN(X,I,A)
C      EVALUATES THE FITTING FUNCTION FOR THE ITH TERM
C   SSP ROUTINE DSINV
C      INVERTS CURVATURE MATRIX
C
C COMMENTS
C   DATA FORMAT
C      NPTS,NTERMS,MODE(3I5)
C      X(I),Y(I),(SIGMAY(I)),(2(3)E12.6)
      DIMENSION X(100),Y(100),SIGMAY(100),A(20),DELTAA(20),SIGMAA(20),
     1YFIT(100),YFITI(100)
      LOGICAL GRAD,CUR,GRID
   21 FORMAT(3L5)
      READ(5,21) GRAD,CLR,GRID
      READ(5,1) NPTS,NTERMS,MODE
    1 FORMAT(3I5)
      IF (MODE) 2,2,4
    2 READ(5,3) (X(I),Y(I),I=1,NPTS)
    3 FORMAT(2E12.6)
      GO TO 6
    4 READ(5,5) (X(I),Y(I),SIGMAY(I),I=1,NPTS)
    5 FORMAT(3E12.6)
    6 READ(5,7) (A(J),DELTAA(J),J=1,NTERMS)
    7 FORMAT(2E12.6)
      ISUM=0
      CHISQ1=1.0
   14 FLAMDA=.001
```

```
      IF(CUR) GO TO 22
      IF(GRID) GO TO 23
      CALL GRADLS(X,Y,SIGMAY,NPTS,NTERMS,MODE,A,DELTAA,
     1YFIT,CHISQR)
      GO TO 24
22     CALL CURFIT(X,Y,SIGMAY,NPTS,NTERMS,MODE,A,DELTAA,SIGMAA,FLAMDA,
     1YFIT,CHISQR)
      GO TO 24
  23 CALL GRIDLS(X,Y,SIGMAY,NPTS,NTERMS,MODE,A,DELTAA,
     1SIGMAA,YFIT,CHISQR)
      GO TO 24
  24 PRINT 8, (A(J),J=1,NTERMS)
   8 FORMAT(' ',E12.6)
      PRINT 9,CHISQR
   9 FORMAT(' ','CHISQR=',1X,E12.6,/)
      IF (CHISQ1-CHISQR) 12,13,12
  12 CHISQ1=CHISQR
      ISUM=ISUM+1
      IF (ISUM-10) 14,13,13
  13 DO 11 I=1,NPTS
  11 YFITI(I)=1./YFIT(I)
      PRINT 10
  10 FORMAT(' ',13X,'IND.VAR.',12X,'DEP.VAR.',11X,'INV.DEP.VAR.',/)
      PRINT 15,(X(I),YFIT(I),YFITI(I),I=1,NPTS)
  15 FORMAT(' ',10X,E12.6,8X,E12.6,8X,E12.6)
      STOP
      END
```

CURFIT

```
      SUBROUTINE CURFIT(X,Y,SIGMAY,NPTS,NTERMS,MODE,A
     1,DELTAA,SIGMAA,FLAMDA,YFIT,CHISQR)
      DOUBLE PRECISION ARRAY
      DIMENSION X(100),Y(100),SIGMAY(100),A(20),DELTAA(20),SIGMAA(20),
     1YFIT(100),WEIGHT(100),ALPHA(20,20),BETA(20),DERIV(20),ARRAY(20,
     120),B(20)
   11 NFREE=NPTS-NTERMS
      IF (NFREE) 13,13,20
   13 CHISQR=0.
      GO TO 110
C EVALUATE WEIGHTS
   20 DO 30 I=1,NPTS
   21 IF (MODE) 22,27,29
   22 IF (Y(I)) 25,27,23
   23 WEIGHT(I)=1./Y(I)
      GO TO 30
   25 WEIGHT(I)=1./(-Y(I))
      GO TO 30
   27 WEIGHT(I)=1.
      GO TO 30
   29 WEIGHT(I)=1./SIGMAY(I)**2
   30 CONTINUE
C EVALUATE ALPHA AND BETA MATRICES
   31 DO 34 J=1,NTERMS
      BETA(J)=0.
      DO 34 K=1,J
   34 ALPHA(J,K)=0.
   41 DO 50 I=1,NPTS
      CALL FDERIV(X,I,A,DELTAA,NTERMS,DERIV)
      DO 46 J=1,NTERMS
      BETA(J)=BETA(J)+WEIGHT(I)*(Y(I)-FUNCTN(X,I,A))*DERIV(J)
      DO 46 K=1,J
   46 ALPHA(J,K)=ALPHA(J,K)+WEIGHT(I)*DERIV(J)*DERIV(K)
   50 CONTINUE
   51 DO 53 J=1,NTERMS
      DO 53 K=1,J
   53 ALPHA(K,J)=ALPHA(J,K)
C EVALUATE CHISQR AT STARTING POINT
   61 DO 62 I=1,NPTS
   62 YFIT(I)=FUNCTN(X,I,A)
   63 CHISQ1=FCHISQ(Y,SIGMAY,NPTS,NFREE,MODE,YFIT)
C INVERT CURVATURE MATRIX TO FIND NEW PARAMETERS
   71 DO 74 J=1,NTERMS
   72 DO 73 K=1,NTERMS
   73 ARRAY(J,K)=ALPHA(J,K)/SQRT(ALPHA(J,J)*ALPHA(K,K))
   74 ARRAY(J,J)=1.+FLAMDA
   80 CALL MATINV(ARRAY,NTERMS,1)
   81 DO 84 J=1,NTERMS
```

```
      B(J)=A(J)
      DO 84 K=1,NTERMS
   84 B(J)=B(J)+BETA(K)*ARRAY(J,K)/SQRT(ALPHA(J,J)*ALPHA(K,K))
C  IF CHI SQUARE INCREASED,INCREASE FLAMDA
   91 DO 92 I=1,NPTS
   92 YFIT(I)=FUNCTN(X,I,B)
   93 CHISQR=FCHISQ(Y,SIGMAY,NPTS,NFREE,MODE,YFIT)
      IF (CHISQ1-CHISQR) 95,101,101
   95 FLAMDA=10.*FLAMDA
      GO TO 71
  101 DO 103 J=1,NTERMS
  103 A(J)=B(J)
      FLAMDA=FLAMDA/10.
  110 RETURN
      END
```

FDERIV

```
      SUBROUTINE FDERIV(X,I,A,DELTAA,NTERMS,DERIV)
      DIMENSION X(100),A(20),DELTAA(20),DERIV(20)
11    DO 18 J=1,NTERMS
      AJ=A(J)
      DELTA=DELTAA(J)
      A(J)=AJ+DELTA
      YFIT=FUNCTN(X,I,A)
      A(J)=AJ-DELTA
      DERIV(J)=(YFIT-FUNCTN(X,I,A))/(2.*DELTA)
18    A(J)=AJ
      RETURN
      END
```

MATINV

```
      SUBROUTINE MATINV(ARRAY,NTERMS,MCODE)
      DOUBLE PRECISION ARRAY,B
      DIMENSION ARRAY(20,20),B(210)
      DO 1 I=1,NTERMS
      DO 1 J=1,NTERMS
      CALL LOC(I,J,IJ,NTERMS,NTERMS,MCODE)
    1 B(IJ)=ARRAY(I,J)
      EPS=1.0E-16
      CALL DSINV(B,NTERMS,EPS,IER)
      IF (IER) 2,4,3
    2 PRINT 10
   10 FORMAT(' ','NO RESULT',/)
      GO TO 4
    3 PRINT 11
   11 FORMAT(' ','WARNING',/)
    4 DO 5 I=1,NTERMS
      DO 5 J=1,NTERMS
      CALL LOC(I,J,IJ,NTERMS,NTERMS,MCODE)
    5 ARRAY(I,J)=B(IJ)
      RETURN
      END
```

FCHISQ

```
      FUNCTION FCHISQ(Y,SIGMAY,NPTS,NFREE,MODE,YFIT)
      DIMENSION Y(100),SIGMAY(100),YFIT(100)
      SUM=0.
      DO 5 I=1,NPTS
      IF(MODE) 1,2,3
    1 W=1./Y(I)
      GO TO 4
    2 W=1.
      GO TO 4
    3 W=1./(SIGMAY(I)**2)
    4 SUM=(Y(I)-YFIT(I))*(Y(I)-YFIT(I))*W
    5 CONTINUE
      FCHISQ=SUM/NFREE
      RETURN
      END
```

```
C
C     ..................................................................
C
C        SUBROUTINE DSINV
C
C        PURPOSE
C           INVERT A GIVEN SYMMETRIC POSITIVE DEFINITE MATRIX
C
C        USAGE
C           CALL DSINV(A,N,EPS,IER)
C
C        DESCRIPTION OF PARAMETERS
C           A       - DOUBLE PRECISION UPPER TRIANGULAR PART OF GIVEN
C                     SYMMETRIC POSITIVE DEFINITE N BY N COEFFICIENT
C                     MATRIX.
C                     ON RETURN A CONTAINS THE RESULTANT UPPER
C                     TRIANGULAR MATRIX IN DOUBLE PRECISION.
C           N       - THE NUMBER OF ROWS (COLUMNS) IN GIVEN MATRIX.
C           EPS     - SINGLE PRECISION INPUT CONSTANT WHICH IS USED
C                     AS RELATIVE TOLERANCE FOR TEST ON LOSS OF
C                     SIGNIFICANCE.
C           IER     - RESULTING ERROR PARAMETER CODED AS FOLLOWS
C                     IER=0  - NO ERROR
C                     IER=-1 - NO RESULT BECAUSE OF WRONG INPUT PARAME-
C                              TER N OR BECAUSE SOME RADICAND IS NON-
C                              POSITIVE (MATRIX A IS NOT POSITIVE
C                              DEFINITE, POSSIBLY DUE TO LOSS OF SIGNI-
C                              FICANCE)
C                     IER=K  - WARNING WHICH INDICATES LOSS OF SIGNIFI-
C                              CANCE. THE RADICAND FORMED AT FACTORIZA-
C                              TION STEP K+1 WAS STILL POSITIVE BUT NO
C                              LONGER GREATER THAN ABS(EPS*A(K+1,K+1)).
C
C        REMARKS
C           THE UPPER TRIANGULAR PART OF GIVEN MATRIX IS ASSUMED TO BE
C           STORED COLUMNWISE IN N*(N+1)/2 SUCCESSIVE STORAGE LOCATIONS.
C           IN THE SAME STORAGE LOCATIONS THE RESULTING UPPER TRIANGU-
C           LAR MATRIX IS STORED COLUMNWISE TOO.
C           THE PROCEDURE GIVES RESULTS IF N IS GREATER THAN 0 AND ALL
C           CALCULATED RADICANDS ARE POSITIVE.
C
C        SUBROUTINES AND FUNCTION SUBPROGRAMS REQUIRED
C           DMFSD
C
C        METHOD
C           SOLUTION IS DONE USING FACTORIZATION BY SUBROUTINE DMFSD.
C
C     ..................................................................
```

```
C
      SUBROUTINE DSINV(A,N,EPS,IER)
C
C
      DIMENSION A(210)
      DOUBLE PRECISION A,DIN,WORK
C
C        FACTORIZE GIVEN MATRIX BY MEANS OF SUBROUTINE DMFSD
C        A = TRANSPOSE(T) * T
      CALL DMFSD(A,N,EPS,IER)
      IF(IER) 9,1,1
C
C        INVERT UPPER TRIANGULAR MATRIX T
C        PREPARE INVERSION-LOOP
    1 IPIV=N*(N+1)/2
      IND=IPIV
C
C        INITIALIZE INVERSION-LOOP
      DO 6 I=1,N
      DIN=1.D0/A(IPIV)
      A(IPIV)=DIN
      MIN=N
      KEND=I-1
      LANF=N-KEND
      IF(KEND) 5,5,2
    2 J=IND
C
C        INITIALIZE ROW-LOOP
      DO 4 K=1,KEND
      WORK=0.D0
      MIN=MIN-1
      LHOR=IPIV
      LVER=J
C
C        START INNER LOOP
      DO 3 L=LANF,MIN
      LVER=LVER+1
      LHOR=LHOR+L
    3 WORK=WORK+A(LVER)*A(LHOR)
C        END OF INNER LOOP
C
      A(J)=-WORK*DIN
    4 J=J-MIN
C        END OF ROW-LOOP
C
    5 IPIV=IPIV-MIN
    6 IND=IND-1
C        END OF INVERSION-LOOP
```

```
C
C          CALCULATE INVERSE(A) BY MEANS OF INVERSE(T)
C          INVERSE(A) = INVERSE(T) * TRANSPOSE(INVERSE(T))
C          INITIALIZE MULTIPLICATION-LOOP
        DO 8 I=1,N
        IPIV=IPIV+I
        J=IPIV
C
C          INITIALIZE ROW-LOOP
        DO 8 K=I,N
        WORK=0.D0
        LHOR=J
C
C          START INNER LOOP
        DO 7 L=K,N
        LVER=LHOR+K-I
        WORK=WORK+A(LHOR)*A(LVER)
    7   LHOR=LHOR+L
C          END OF INNER LOOP
C
        A(J)=WORK
    8   J=J+K
C          END OF ROW- AND MULTIPLICATION-LOOP
C
    9   RETURN
        END
```

```
C
C     ..................................................................
C
C        SUBROUTINE DMFSD
C
C        PURPOSE
C           FACTOR A GIVEN SYMMETRIC POSITIVE DEFINITE MATRIX
C
C        USAGE
C           CALL DMFSD(A,N,EPS,IER)
C
C        DESCRIPTION OF PARAMETERS
C           A      - DOUBLE PRECISION UPPER TRIANGULAR PART OF GIVEN
C                    SYMMETRIC POSITIVE DEFINITE N BY N COEFFICIENT
C                    MATRIX.
C                    ON RETURN A CONTAINS THE RESULTANT UPPER
C                    TRIANGULAR MATRIX IN DOUBLE PRECISION.
C           N      - THE NUMBER OF ROWS (COLUMNS) IN GIVEN MATRIX.
C           EPS    - SINGLE PRECISION INPUT CONSTANT WHICH IS USED
C                    AS RELATIVE TOLERANCE FOR TEST ON LOSS OF
C                    SIGNIFICANCE.
C           IER    - RESULTING ERROR PARAMETER CODED AS FOLLOWS
C                    IER=0  - NO ERROR
C                    IER=-1 - NO RESULT BECAUSE OF WRONG INPUT PARAME-
C                             TER N OR BECAUSE SOME RADICAND IS NON-
C                             POSITIVE (MATRIX A IS NOT POSITIVE
C                             DEFINITE, POSSIBLY DUE TO LOSS OF SIGNI-
C                             FICANCE)
C                    IER=K  - WARNING WHICH INDICATES LOSS OF SIGNIFI-
C                             CANCE. THE RADICAND FORMED AT FACTORIZA-
C                             TION STEP K+1 WAS STILL POSITIVE BUT NO
C                             LONGER GREATER THAN ABS(EPS*A(K+1,K+1)).
C
C        REMARKS
C           THE UPPER TRIANGULAR PART OF GIVEN MATRIX IS ASSUMED TO BE
C           STORED COLUMNWISE IN N*(N+1)/2 SUCCESSIVE STORAGE LOCATIONS.
C           IN THE SAME STORAGE LOCATIONS THE RESULTING UPPER TRIANGU-
C           LAR MATRIX IS STORED COLUMNWISE TOO.
C           THE PROCEDURE GIVES RESULTS IF N IS GREATER THAN 0 AND ALL
C           CALCULATED RADICANDS ARE POSITIVE.
C           THE PRODUCT OF RETURNED DIAGONAL TERMS IS EQUAL TO THE
C           SQUARE-ROOT OF THE DETERMINANT OF THE GIVEN MATRIX.
C
C        SUBROUTINES AND FUNCTION SUBPROGRAMS REQUIRED
C           NONE
C
C        METHOD
C           SOLUTION IS DONE USING THE SQUARE-ROOT METHOD OF CHOLESKY.
```

```
C            THE GIVEN MATRIX IS REPRESENTED AS PRODUCT OF TWO TRIANGULAR
C            MATRICES, WHERE THE LEFT HAND FACTOR IS THE TRANSPOSE OF
C            THE RETURNED RIGHT HAND FACTOR.
C
C     ..................................................................
C
      SUBROUTINE DMFSD(A,N,EPS,IER)
C
C
      DIMENSION A(210)
      DOUBLE PRECISION DPIV,DSUM,A
C
C        TEST ON WRONG INPUT PARAMETER N
      IF(N-1) 12,1,1
    1 IER=0
C
C        INITIALIZE DIAGONAL-LOOP
      KPIV=0
      DO 11 K=1,N
      KPIV=KPIV+K
      IND=KPIV
      LEND=K-1
C
C        CALCULATE TOLERANCE
      TOL=ABS(EPS SNGL(A(KPIV)))
C
C        START FACTORIZATION-LOOP OVER K-TH ROW
      DO 11 I=K,N
      DSUM=0.D0
      IF(LEND) 2,4,2
C
C        START INNER LOOP
    2 DO 3 L=1,LEND
      LANF=KPIV-L
      LIND=IND-L
    3 DSUM=DSUM+A(LANF)*A(LIND)
C        END OF INNER LOOP
C
C        TRANSFORM ELEMENT A(IND)
    4 DSUM=A(IND)-DSUM
      IF(I-K) 10,5,10
C
C        TEST FOR NEGATIVE PIVOT ELEMENT AND FOR LOSS OF SIGNIFICANCE
    5 IF(SNGL(DSUM)-TOL) 6,6,9
    6 IF(DSUM) 12,12,7
    7 IF(IER) 8,8,9
    8 IER=K-1
C
```

```
C         COMPUTE PIVOT ELEMENT
    9  DPIV=DSQRT(DSUM)
       A(KPIV)=DPIV
       DPIV=1.DO/DPIV
       GO TO 11
C
C         CALCULATE TERMS IN ROW
   10  A(IND)=DSUM*DPIV
   11  IND=IND+I
C         END OF DIAGONAL-LOOP
C
       RETURN
   12  IER=-1
       RETURN
       END
```

APPENDIX E

RELATIONSHIP BETWEEN EXTINCTION, SCATTERING, AND ABSORPTION COEFFICIENTS AND THE MIE PARAMETERS

The extinction (α), scattering (s), and absorption (a) coefficients for suspended particulates can be calculated using the Mie formalism. Using the Mie parameters, $a_n(x,m)$ and $b_n(x,m)$ of equations (3-7) the extinction coefficient is given by:

$$\alpha = \frac{\lambda^2}{2\pi}\int \sum_{n=1}^{\infty} (2n+1) \left\{ \mathrm{Re}(a_n(x,m)) + \mathrm{Re}(b_n(x,m)) \right\} n(r)dr \quad \text{(E-1)}$$

where n(r) is the particle size distribution function and $x = 2\pi r/\lambda$. The expression for the scattering coefficient is:

$$s = \frac{\lambda^2}{2\pi}\int \sum_{n=1}^{\infty} (2n+1) \left\{ \left| a_n(x,m) \right|^2 + \left| b_n(x,m) \right|^2 \right\} n(r)dr \quad \text{(E-2)}$$

The absorption coefficient is the difference between α and s, thus

$$a = \frac{\lambda^2}{2\pi}\int \sum_{n=1}^{\infty} (2n+1) \left\{ \mathrm{Re}(a_n(x,m)) + \mathrm{Re}(b_n(x,m)) - \left| a_n(x,m) \right|^2 - \left| b_n(x,m) \right|^2 \right\} n(r)\, dr. \quad \text{(E-3)}$$

The values for α, s, and a used in the Monte Carlo routine were not calculated in this way because the values explicitly depend on the concentration through n(r). Instead α, s, and a were chosen to correspond to physically observed values.

The absorption coefficient depends on the imaginary part of the index of refraction, but in a non-trivial way. If Im(m) = 0 then it can be shown[25] that

$$\left| a_n(x,m) - \tfrac{1}{2} \right|^2 = \tfrac{1}{4}$$
$$\left| b_n(x,m) - \tfrac{1}{2} \right|^2 = \tfrac{1}{4} \; . \qquad \text{(E-4)}$$

Expanding equation (E-4) leads to

$$\left[\mathrm{Re}(a_n(x,m))\right]^2 - \mathrm{Re}(a_n(x,m)) + \left[\mathrm{Im}(a_n(x,m))\right]^2 + \tfrac{1}{4} = \tfrac{1}{4}$$

or

$$\mathrm{Re}(a_n(x,m)) = \left[\mathrm{Re}(a_n(x,m))\right]^2 + \left[\mathrm{Im}(a_n(x,m))\right]^2$$
$$= \left| a_n(x,m) \right|^2 \qquad \text{(E-5)}$$

with a similar result holding for $b_n(x,m)$. Using these results in equation (E-3) leads to a=o. Thus if the imaginary part of the index of refraction is zero the absorption coefficient is also zero.

If $\mathrm{Im}(m) \neq 0$ then[25]

$$\left| a_n(x,m) - \tfrac{1}{2} \right|^2 < \tfrac{1}{4}$$
$$\left| b_n(x,m) - \tfrac{1}{2} \right|^2 < \tfrac{1}{4} \qquad \text{(E-6)}$$

Which, after expansion, leads to

$$\mathrm{Re}(a_n(x,m)) > \left| a\ (x,m) \right|^2$$
$$\mathrm{Re}(b_n(x,m)) > \left| b\ (x,m) \right|^2, \qquad \text{(E-7)}$$

so that, by equation (E-3), a>o for a non-zero imaginary component in the index of refraction.

REFERENCES

1. A.H. Ghovanlou, "Analytical Model for Remote Sensing of Water Turbidity," The MITRE Corporation, MTR-7290, September, 1976.

2. A.H. Ghovanlou, "Radiative Transfer Model for Remote Sensing of Suspended Sediments in Water," The MITRE Corporation, MTR-7433, March, 1977.

3. R.E. Morrison, "Studies of the Optical Properties of Seawater at Argus Island in the North Atlantic and in Long Island and Block Island Sounds," Ph.D. Thesis, New York University, 1967.

4. S.Q. Duntley, "Light in the Sea," J. Opt. Soc. America, Vol. 53, No. 2, February 1963.

5. G. Kullenberg, Rep Inst, Fys, Oceanog., 5, 16. Kobenhauns Universitet., 1969.

6. N.G. Jerlov, Medd. Oceanog. Inst. Goteborg, 30, 1961.

7. J.E. Tyler, Limm. and Oceanog., 6, 1961.

8. G. Kullenberg and O. Berg, Rep. Inst. Fys. Oceanog., 19, 40, Kobenhavns Universitet, 1972.

9. G. Kullenberg, Deep Sea Res., 15, 1968.

10. T.J. Petzold, "Volume Scattering Functions for Selected Ocean Waters," AD-753474, Scripps Institution of Oceanography, October 1972.

11. H.R. Gordon, O.B. Brown, and M.M. Jacobs, "Computed Relationship between the Inherent and Apparent Optical Properties of a Flat Homogeneous Ocean," Applied Optics, Vol. 14, No. 2, February 1975.

12. Elgin A. Dunnington, "Biological Effects of Stress on Commercial Fisheries," In: William T. Mason and Kevin C. Flynn (eds.), The Potomac Estuary Bilogical Resources: Trends and Options Interstate Commission on the Potomac River Basin, Bethesda, MD, April 1976, pp 110-112.

REFERENCES (Concluded)

13. M. Born, E. Wolf, "Principles of Optics," Fifth edition, Pergamou Press, (1975), p. 633.

14. M. Kerker, "The Scattering of Light," Academic Press, (1969), Chapters 3 and 4.

15. J.A. Stratton, "Electromagnetic Theory," McGraw-Hill Book Co., Inc. (1941), p. 563.

16. D. Deirmendjian, "Electromagnetic Scattering on Spherical Polydispersions," American Elsevier Publishing Co., Inc., (1969).

17. J.V. Dave, "Subroutines for Computing the Parameters of the Electromagnetic Radiation Scattered by a Sphere, " IBM Report No. 320-3237, May 1968.

18. G. Mie, Annid, Physik (4), Vol. 25 (1908), p. 377.

19. P. Debye, Annid, Physik (4), Vol. 30 (1909), p. 57.

20. R.S. Chapman, "Particle Size and X-Ray Analysis of Feldspar Calvert, Ball, and Jordon Soils," NASA TM X-73941, February 1977.

21. "Handbook of Chemistry and Physics," Chemical Rubber Publishing Co., (1960), p. 1510.

22. G.W. Grams, et.al., "Complex Index of Refraction of Airborne Soil Particles," Journal of Applied Meteorology, Vol. 13, June 1974, p. 459.

23. N.G. Jerlov, E.S. Nielsen, eds., "Optical Aspects of Oceanography," Academic Press, (1974), p. 152.

24. D.K. Todd, "The Water Encyclopedia," Water Information Center, (1970), p. 86.

25. D. Deirmendjian, "Electromagnetic Scattering on Spherical Polydispersions," American Elsevier Publishing Co., Inc., (1969), p. 24.

DISTRIBUTION LIST

D-10
C.A. Zraket

D-12
H. Benington
C. Grandy
A. Tachmindji

D-40
S. Blum
W. Sievers

D-41
S. Lewis

W-50
R. Greeley
R. Ouellette
Westpark Storage*

W-51
L. Gsellman
R. Pikul
T. Wright

W-52
G. Bennington
D. Blake
E. Friedman
N. Gadsby
A. Ghovanlou
S. Goldstein
W. Jacobsen
A. Johnson
K. Rebibo
M. Scholl
E. Ward

W-54
G. Erskine
J. Golden
S. Lubore

W-55
A. Challis**
N. Coates
E. Sharp
J. Stone

W-56
M. Bracken
L. Thomas

W-50 Library

METREK Library

Technical Center
(2)

NASA/Langley
Research Center
(100)

*To be sent to Westpark Storage for distribution by Dr. Ouellette

**Send to Jean Reynolds